Investigation of Fluid Flow in a Torque Converter's Stator Using Computational Fluid Dynamics Methods.

by

Shoab Ahmed Talukder

A THESIS

Submitted to the
University of Technology, Sydney.

For the degree of
Master of Engineering (Research)
2014

CERTIFICATE OF AUTHORSHIP/ORIGINALITY

I certify that the work in this thesis has not previously been submitted for a degree nor has it been submitted as part of requirements for a degree except as fully acknowledged within the text.

I also certify that the thesis has been written by me. Any help that I have received in my research work and the preparation of the thesis itself has been acknowledged. In addition, I certify that all information sources and literature used are indicated in the thesis.

Production Note:
Signature removed prior to publication.

Shoab Ahmed Talukder

23/07/2014

ABSTRACT

An automotive torque converter is a widely used hydro-mechanical device for transferring engine power to the transmission in the modern automotive industries. The typical three-dimensional geometrical structures of the stator, pump and turbine made this torque converter very complex. The goal of this study is to gain a sound understanding of the complex three-dimensional fluid flow inside the stator. This study was performed using Computational Fluid Dynamics software. For the sake of gaining a sound understanding, all three elements of the torque converter were included in the simulation. The geometry for the torque converter used was a donation from Dr Mahesh Athavale (Manager, CFDRC). However, the construction of the geometry was thoroughly studied to gain a comprehensive understanding of the construction as well as making the necessary changes. The performance of the torque converter was compared with existing data. This was undertaken for the validation of the work. Then the fluid flow was studied for a changed stator blade number. Thus the variation of performance can easily be noticed with the change in the geometrical structure. The effect of pseudo plastic fluid and dilatant fluid was also studied in order to determine the performance characteristics. All these investigations would lead to a clearer realization of the fluid flow inside the stator and thus help to increase the performance of the torque converter. Out of this research studies on torque converter two publications have been produced.

1. IMECE2011-65078: Effects of Number of Stator Blades on the Performance of a Torque Converter, which was published by the ASME conference 2011, held on November 11-17, 2011, Denver, Colorado, USA.

2. 18th AFMC-2012: Numerical Study of Performance of a Torque Converter Employing a Power-Law Fluid, which was published by the AFMC on its 18th conference, held on December 3-7, 2012, Launceston, Tasmania, Australia.

ACKNOWLEDGMENTS

I would like to thank a number of people whose effort and support allowed me to reach this stage in my career. My supervisor, Dr Phuoc Huynh, and co-supervisor, Dr Peter Watterson, gave me continuous support and helped in every possible manner. Without their proper guidance, advice, assistance, encouragement and ideas this thesis wouldn't have been completed. I shall be ever thankful to Dr Mahesh Athavale (Manager, CFDRC), who's donation helped considerably to overcome the difficulties that we were facing. I also would like to take the opportunity to thank all the CFDRC customer support crews, who helped us with tips and professional advice and led us to this completion.

I would like to thank my wife Tahmina, son Zarif, my parents and my younger brother Dr. Jonayed and sister Annie for their tremendous amount of mental support over the years and that they continue to give to this day. I would like to take the opportunity to thank Matt Gaston and Peter Brady for their help and support. I also would like to thank the Director of Research Programs and all research administration Officers, for their patient support throughout my candidature.

And I also would like to thank my friends for all that they have done for me. Above all I would like to mention my gratefulness to almighty for his kindness and blessings.

TABLE OF CONTENTS

A THESIS i
ABSTRACT ii
ACKNOWLEDGMENTS iii
CHAPTER 1: INTRODUCTION 1
1.1 Engineering significance 2
1.2 Problem Statement 3
1.3 Torque Converter Description, Principles and Function 4
1.4 History and Review of Previous Torque Converter Studies 7
1.5 Computational Research 10
CHAPTER 2: CFD FACILITIES 12
2.1 Computational Fluid Dynamics 12
2.2 Specifications of the torque converter 13
2.3 Construction of the geometry 14
CHAPTER 3: SIMULATION PROCEDURE 19
3.1. Configuring the program for simulation 19
3.1.1. Problem Type (PT) 20
3.1.2. Model Option (MO) 20
3.1.3. Volume Condition (VC) 21
3.1.4. Boundary Condition (BC) 22
3.1.5. Additional Input for Mixing-plane 23
3.1.6. Initial Condition (IC) 23
3.1.7. Solver Control (SC) 24
3.1.8. Output (out) 25
3.1.9. Run (Run) 25
CHAPTER 4: FLUID FLOW INVESTIGATION. 28
4.1 Angle measurement: 28
4.1.1 Validation and verification 29
4.2 Effect of a different number of stator blades on the Torque Converter's performance 43
4.2.1 Geometric construction procedure for changing the stator blade number 43
4.2.2 Performance comparison with the change of numbers of stator blades. 46
4.3 Performance Investigation of a Torque Converter Using Non-Newtonian Fluids 57
CHAPTER 5: CONCLUSIONS 67
Summary and Conclusions 67
CHAPTER 6: RECOMMENDATIONS FOR FUTURE WORK 70
BIBLIOGRAPHY 71
My publications 79

LIST OF FIGURES

Figure 1: Cross-sectional view of a typical torque converter (Lui, Y. PhD thesis, 2001). 3
Figure 2: Torque converter fluid flow path (Liu, Y. PhD thesis, 2001). 5
Figure 3 : Dimensions of the Torque converter (in millimetres) (TKN=Thickness of the blade)....17
Figure 4: The frame of the stator blade in the Geom. 19
Figure 5: Stator blade after grid generation and surface shading....20
Figure 6: Stator blade (primary position of the construction of the channel with grid). 20
Figure 7: Stator channel after revolution and deletion. 21
Figure 8: Complete stator channel with grid generation. 22
Figure 9: IJK co-ordinates reorientation. 23
Figure 10: CFD─ACE (U) working window. 24
Figure 11: Sample of a Residual plotter. 32
Figure 12: Angle Measurement. 34
Figure 13: Inlet, Mid-chord and Exit plane of a stator. 37
Figure 14: Torque ratio and efficiency curve for 2350 rpm at different speed ratios. 38
Figure 15: Capacity factor curve for 2350 rpm at different speed ratios. 39
Figure 16: Efficiency and torque ratio vs. speed ratio curve plotted from simulations at 313K. 40
Figure 17: "Numerical Investigation of the Pump Flow in an Automotive Torque Converter" (SAE Tech paper series 1999-01-1056). 41
Figure 18: Fluid flow at the stator pressure side near the stator blade for 2350 rpm at 0.065 SR. 43
Figure 19: Fluid flow at the stator suction side near the stator blade for 2350 rpm at 0.065 SR. 44
Figure 20 : Fluid flow at the stator mid-plane for 2350 rpm at 0.065 SR. 45
Figure 21 : Fluid flow at the stator outlet for 2350 rpm at 0.065 SR. 45
Figure 22: Efficiency comparison for different temperatures. 46
Figure 23: Fluid flow in the stator inlet at 313K. 47
Figure 24: Fluid flow in the stator outlet at 313K. 47
Figure 25: Fluid flow in the stator inlet at 373K. 48
Figure 26: Fluid flow in the stator outlet at 373K. 48
Figure 27 : Stator blade without face and block. 52
Figure 28 : Stator channel with shaded stator blade and face formed in one side of the channel. 53
Figure 29 : 13─blade stator channel with one side extension. 54
Figure 30 : 13─blade stator channel with the indication of increased dimension. 54
Figure 31 : Stator with 13 blades. 55
Figure 32: Efficiency comparison between the torque converters with 13, 18, 19 and 16 stator blades. 56

Figure 34 : Axial flow at the 19─blade stator inlet at 0.2 speed ratio with 1000 rpm pump speed. 48
Figure 35 : Axial flow at the mid─plane of the 19─blade stator at 0.2 speed ratio with 1000 rpm pump speed. 49
Figure 36 : Axial flow at the outlet of the 19─blade stator at 0.2 speed ratio with 1000 rpm pump speed. 49
Figure 37 : Axial flow plotted with pressure contour at the pressure side of the 19─blade stator for 1000 rpm pump speed at 0.2 speed ratio. 50
Figure 38 : Axial flow plotted with pressure contour at the suction side of the 19─blade stator for 1000 rpm pump speed at 0.2 speed ratio. 50
Figure 39 : Axial flow at the 13─blade stator inlet at 0.2 speed ratio with 1000 rpm pump speed. 51
Figure 40 : Axial flow at the mid─plane of the 13─blade stator at 0.2 speed ratio with 1000 rpm pump speed. 51
Figure 41 : Axial flow at the outlet of the 13─blade stator at 0.2 speed ratio with 1000 rpm pump speed. 52
Figure 42 : Axial flow plotted with pressure contour at the pressure side of the blade, of the 13─blade stator for 1000 rpm pump speed at 0.2 speed ratio. 52
Figure 43 : Axial flow plotted with pressure contour at the suction side of the blade, of the 13─blade stator for 1000 rpm pump speed at 0.2 speed ratio. 53
Figure 44: Pressure contour with axial flow, very close to the suction side of the 18─blade stator wall for 1000 rpm pump speed at 0.2 speed ratio. 53
Figure 45 : Pressure contour with axial flow, very close to the pressure side of the 18─blade stator wall for 1000 rpm pump speed at 0.2 speed ratio. 54
Figure 46: Turbine efficiency vs. power law index graph at 313K temperature. 59
Figure 47: Turbine torque ratio vs. power law index graph at 313K temperature. 59
Figure 48: Turbine efficiency & torque ratio vs. power law index graph at 373K temperature. 60
Figure 49: Efficiency curve comparison for temperature 313K and 373K. 60
Figure 50: Fluid flow in the pressure side at the inlet plane of the stator at 313K. 61
Figure 51: Flow in the suction side at the inlet plane of the stator at 313K. 62
Figure 52: Velocity vectors with pressure contour in the pressure side and suction side at the inlet plane of the stator at 313K. 63
Figure 53: Fluid flow in the pressure side and suction side at the outlet plane of the stator at 313K. 64
Figure 54: Fluid flow at the inlet of the stator for temperature 373K. 65
Figure 55: Fluid flow at the stator outlet for temperature 373K. 65

LIST OF TABLES

1. Specification of Torque Converter. …… Page 18
2. Specifications for the simulating Torque Converter…… Page 36
3. Specifications of the TC used in SAE paper series 1999-01-1056, by Shin, Chang and Mahesh. ……...……..Page 36
4. The comparison table for torque ratio between the study simulation result and Shin, Chang, Athavale (1999) result (for the impeller speed of 2350rpm) at different speed ratio. ……...…….... Page 38
5. The comparison table for efficiency between the study simulation result and Shin, Chang, Athavale (1999) result (for the impeller speed of 2350rpm) at different speed ratio. …….…….. Page 39
6. Presentation of Speed Ratio and Torque Ratio in a table form from Figure 17;(SAE-1999-01-1056). ……...……..…Page 41
7. Presentation of Speed Ratio and Torque Ratio in a table form for the impeller speed of 2000, achieved from our simulation. …… Page 42
8. Presentation of the difference between the study simulation data and data extracted from the graph (Figure 17). ……. Page 42

CHAPTER 1: INTRODUCTION

The main focus of this thesis is to provide a sound understanding of the three-dimensional fluid flow inside a torque converter. This will help to develop a more efficient torque converter, which will result in vehicles with better fuel economy. Fuel economy is important, both because the world's natural resources are limited and because environmental pollution has already reached an unacceptable level.

Minimum pollution levels can only be achieved through greater efficiency in technology, transport, industry and all other related areas. A higher efficiency torque converter can help achieve minimal pollution. As billions of torque converters are used every day all over the world, the slightest improvement in efficiency will result in a significant contribution. This will be an enhancement of fuel economy, and will enable a decrease in operating cost and pollution. In order to increase the efficiency of the torque converter it is essential to know the three-dimensional closed loop fluid flows.

Different structural arrangements can cause variations to the fluid flow inside the torque converter. The structural arrangements could be on the basis of the blade numbers, blade angles, tip-bending, and size of the components of the torque converter or other governing factors. This is why it is very important to know the flow characteristics. The long narrow passage with curved and varying cross-sectional shape causes the fluid flow to be very complex in this turbo-machine.

This complex three-dimensional fluid flow is dominated by rotational speed, secondary flows, viscous effects and separation. The fluid flow is also dependent on the performance parameters, such as speed ratio, torque ratio, capacity factor,

and K factor. In order to obtain a more efficient torque converter, a detailed understanding of the fluid flow is essential. To achieve that goal all these aspects must be taken into consideration. Due to these complexities and several of the governing factors, the numerical studies became very complex and subsequently very few of them have been reported (SAE-1999-01-1056). This study is undertaking a numerical analysis of the torque converter's internal fluid flow using CFD (Computational Fluid Dynamics) software.

CFD is high-tech digital simulation software. It has the capability of designing a prototype according to the user's instruction. It then digitally simulates the prototype and shows the probable result, as it takes into account the physics of the material according to the user's instructions. For the given data and conditions provided the simulation gives probable results.

1.1 Engineering significance

A torque converter is a complex hydrodynamic turbo-machine. The closed-loop multi-component structure makes it complex. It is commonly used in automatic transmission vehicles including cars, buses, trucks, locomotives, tanks etc., to serve the purpose of transmitting the power and torque from the engine to the transmission. It is used for numerous reasons. The torque converter can multiply the engine torque up to an approximate factor of two, under required circumstances. It also acts as an engine torsional disturbance damper and shock load damper. It provides a smooth speed ratio change from the engine to the transmission. Even to engage gas turbines, a torque converter is often used as a soft clutch.

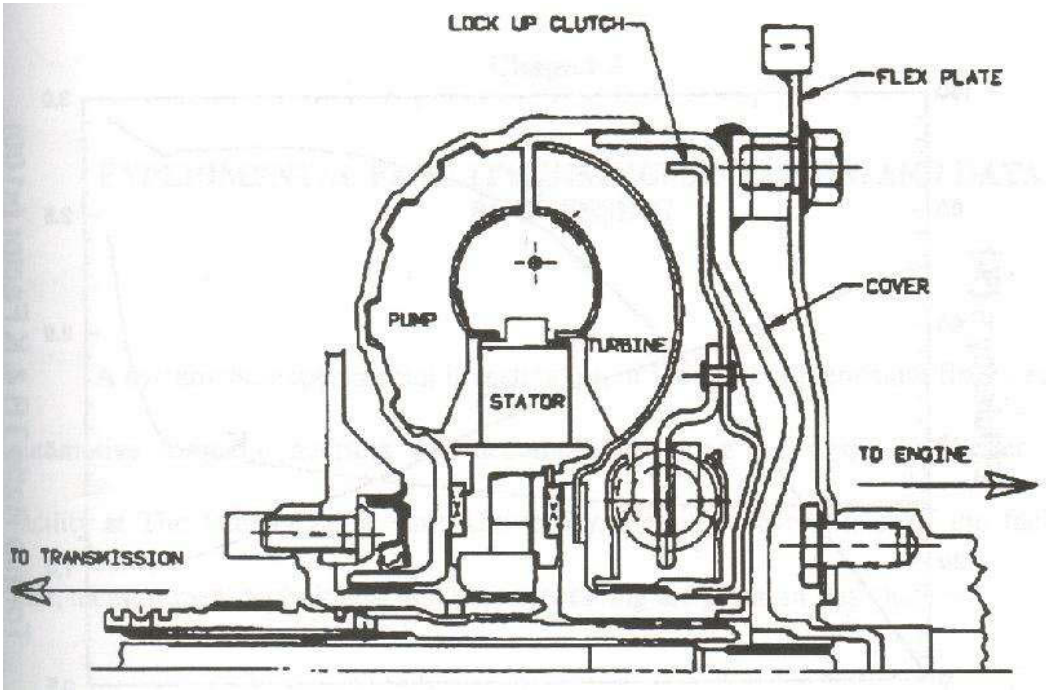

Figure 1: Cross-sectional view of a typical torque converter (Lui, Y. PhD thesis, 2001).

A typical torque converter has three major components, as shown in Figure 1: (1) a pump, which is attached directly to the cover of the torque converter and connected to the engine shaft; (2) a turbine, which sits freely inside the casing and provides power to the transmission shaft; (3) a stator, which is attached to the transmission housing through a one-way clutch. As a working fluid the torque converter uses pressurised transmission oil. The engine rotates the pump, and the pump imputes angular momentum to the fluid as it rotates. The fluid ejected by the pump enters the turbine channels. The angular momentum is then extracted by the turbine as it revolves, and this provides the torque transfer between the pump and the turbine. The torque drives the transmission shaft connected to the turbine. The stator is placed in between the turbine exit and the inlet of the pump. The function of the stator ideally is to redirect the fluid to obtain a zero flow incidence into the pump at a certain designed speed ratio. It also acts as a torque reactor at a low speed ratio, providing the torque amplification, thus differentiating the torque converter from the conventional fluid coupling. The pump and the turbine rotate at different speeds. Depending

on the particular operating conditions and application, the stator is either locked or allowed to float freely.

1.2 Problem Statement

The objective of this study is to visualise and understand the three-dimensional fluid flow inside the stator of the torque converter using Computational Fluid Dynamics software. As the torque converter is a complex closed-loop system, all three components are taken into account, with the aim of a realistic result.

As this is simulation software, it needs specific input data to simulate the situation. The most difficult part of the simulation is to have an adequate converged result. The residual plotter helps us to determine the convergence. An adequate convergence requires perfect meshing of the grids and optimum boundary condition settings. The closed-loop complex structures make this simulation a time-consuming and tedious job.

The result of the simulation provides numerous data. Calculating those output data, torque ratio, efficiency, capacity factor etc can be obtained. The result can then be compared to the existing data, derived from previous experiments or research works. If the comparison between the simulation data and previous research data is satisfactory, then the investigation can proceed.

The number of the stator blades can be changed in the torque converter. The stator blade angle can be changed. The fluid in the torque converter can be changed and the torque converter performance can be monitored. This can lead to suggestions for improved efficiency.

1.3 Torque Converter Description, Principles and Function

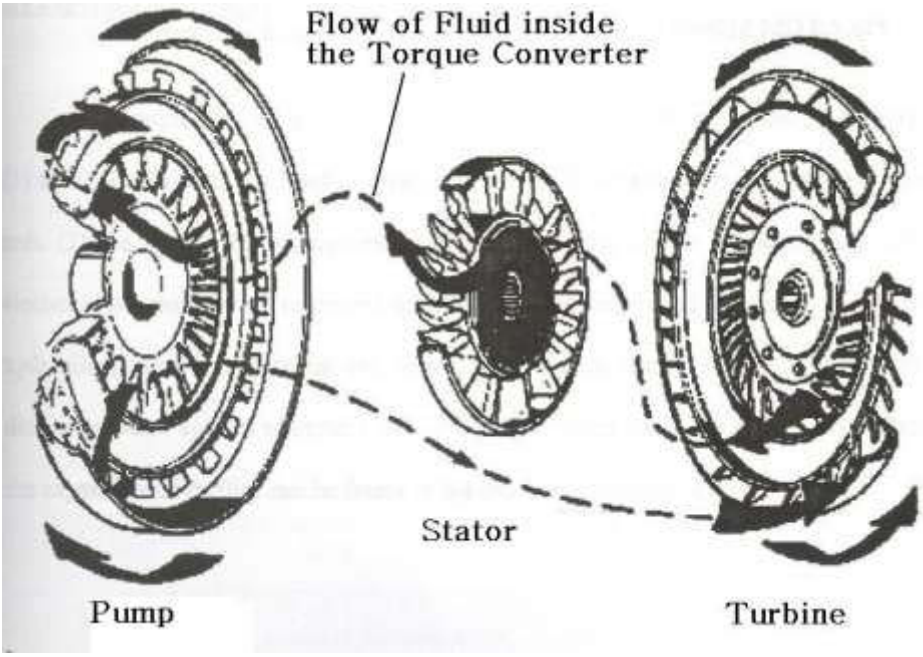

Figure 2: Torque converter fluid flow path (Liu, Y. PhD thesis, 2001).

The recirculating fluid flow path of an automotive torque converter assembly is shown in Figure 2. The blade numbers vary from manufacturer to manufacturer. There are 25 to 35 blades in both the pump and the turbine and around 20 airfoil-like blades in the torque converter stator.

The operational interpretation of a torque converter is very similar to the centrifugal pump. For the pump of the torque converter: (i) the flow enters the pump axially through the inlet and is turned outward in the radial direction by the guide vanes, (ii) the flow is accelerated by the radial pump blades in the radial and tangential directions, and in this manner the kinetic and potential (pressure) energy are passed on into the flow, and (iii) the flow is turned and exits in the axial direction from the pump (Brun 1996).

For the turbine of the torque converter: (i) the high energy flow from the pump enters axially and is turned toward the inward radial direction, the flow also has tangential velocities, (ii) the pressure on the blades (flow energy) is absorbed by the turbine blades and the flow energy (pressure on the blade) is converted into turbine rotation, and (iii) the flow is made to exit the turbine in the axial direction. The function of the stator is to redirect the flow from the turbine exit to the inlet of the pump. The flow at the turbine exit has a strong negative tangential velocity (opposite to the pump rotation). The stator causes the flow to have a zero or positive tangential incidence in to the pump. Due to the closed-loop interaction of the pump, turbine, and stator, the flow field in the torque converter is highly three-dimensional, unsteady and turbulent (Brun 1996).

The functions of the torque converter and the conventional fluid coupling have many similar aspects. That is to say both have mixed-flow pumps and turbines and both provide smooth torque transmission. As the operating parameters defined for the fluid coupling are the same as for the torque converter, thus the parameters directly apply to it. The key performance parameters include speed ratio, torque ratio, input capacity factor, K factor. K factor is defined as pump speed (rpm) over the square root of the pump torque (Brun 1996, Dong 1998).

The speed ratio (SR), for a fluid coupling (and torque converter) is generally defined as:

$$SR=\omega_t / \omega_{p,} \qquad (1.1)$$

Where,

ω_t = turbine angular speed; ω_p = pump angular speed.

And torque ratio (TR), is defined as:

$$TR= \tau_t / \tau_p \qquad (1.2)$$

Where, τ_t Torque of the turbine, τ_p Torque of the pump.

The efficiency of the torque converter is:

$$\varepsilon = P_t / P_{p.} = (\omega_t / \omega_p) . (\tau_t / \tau_p) = SR . TR \qquad (1.3)$$

Where P_t =output turbine shaft power, P_p = input pump shaft power.

For a conventional fluid coupling consisting of a pump and a turbine,

neglecting the mechanical losses

$$\tau_t = \tau_p$$

That is, the output torque always has to be equal to the input torque (TR=1). If equation (1.3) is rewritten with TR=1, it gives ε = SR.

K factor (Also known as capacity factor) is defined as:

$$\mathbf{K = N/\sqrt{T}.}$$

K= K factor(Capacity factor).

Units are radians/second/√(newton-meters) i.e. (rad/s/(N*m)^0.5)

Where N= pump speed (rpm) and T= pump Torque

And in another way, capacity factor is defined as:

$$C = 1/ K^2$$

C = Capacity factor.

Units are newton-meters/(radians/second)^2 i.e. (N*m/(rad/s)^2)

When it comes down to choosing capacity factor, preference of units are the governing constituent. This study chose capacity factor $C=1/K^2$. This produced unit 10^{-6}kg m/rpm^2. This was in order to validate the findings with the existing result of Shin's paper(SAE-1999-01-1056), that was published using the unit 10^{-6}kg m/rpm^2.

Consequently, efficiency is a linear function of speed ratio for a conventional fluid coupling, reaching unity at SR=1 (in reality due to bearing losses, actual couplings' maximum efficiencies are approximately 98%).

Unlike the conventional fluid pump, in the automotive torque converter, there is an additional element introduced to the flow. It is called the stator, also known as the reactor. It allows the multiplication of the torque, which significantly changes the performance of the torque converter from a conventional fluid coupling. Neglecting the mechanical losses, a torque balance for a torque converter is:

$$\tau_p = \tau_s + \tau_t \quad \text{i.e. } \tau_p - \tau_t = \tau_s$$

Where τ_s is the torque for the stator. Thus, in a torque converter, output torque can be higher than the input torque when the stator produces negative (counter rotation) torque. This is when the torque multiplication occurs (Brun 1996).

Many torque converters are equipped with a one-way clutch for the stator, to achieve high efficiency at a high speed ratio. The stator is mechanically decoupled from the fixed frame and hence allowed to rotate freely at the point when ε = SR (coupling point). As the stator cannot effectively exert torque, the torque converter is no better than a hydraulic coupling above the coupling point (Brun 1996).

1.4 History and Review of Previous Torque Converter Studies

The torque converter was first designed and fabricated by Dr Hermann Foettinger and Dr Bauer at Vulcan shipyards in Hamburg, between 1903 and 1907. It was built to serve as a speed reduction gear between the engine (steam turbine) and the ship's propeller. That model was powered by steam turbines, and introduced a new type of transmission. Passenger cars first experienced the torque converter in 1938 as a fluid coupling. Since then it has become very popular and millions of torque converter are produced each year, as most of the current vehicles use torque converters for automatic transmission (Brun 1996).

The theory of one-dimensional analysis for the torque converter was first done by Spannhake in 1949. He assumed that the torque converter fluid flow follows a mean flow path with a uniform through-flow velocity. In order to analyse the flow in all three elements, he applied torque and energy conservation principles. He divided the losses into two categories, frictional loss and incidence loss. In 1953 Ziebart found out that the interaction effects between the turbine and the stator became very distinct when the gap between the elements was at a minimum. He applied photographic techniques and a large water table to visualise flow phenomena in different blade cascades of the original Foettinger torque converter (Dong 1998).

The one-dimensional analysis method for different configurations of a torque converter was improved in 1955 by Ishihara to forecast the torque converter performance characteristics. He developed a method of calculating the losses, efficiency, and torque ratio of a torque converter from the geometric and operational model. A correlation for a friction loss coefficient that agrees with the performance data at the design condition was also derived by Ishihara. The water-table test facility (similar to Ziebart, 1953) developed by Upton (1962) aimed to visualise flow phenomena in different blade cascades. A number of blade profiles were developed by Upton, some of which are still in use. His test facility was widely used for the early development of GM torque converters (Brun 1996).

Jandasek (1962) presented the design method in detail for the single-stage three-element torque converter. It consisted of a comprehensive collection of data defining the relationship between blade angles, converter capacity, converter slip and road load, efficiency, torque ratio, radii, relationship of torque and speed of torque converter and mass flow. He also discovered that the stall torque ratio depends greatly on the pump exit angle and the act of the stator is not efficient at the designed speed ratio (Dong 1998).

Ishihara and Emori (1966) developed a method to describe the non-steady dynamics within the torque converter. They mentioned that the steady state vibrational characteristics were adequate for the analysis of non-steady operating conditions of the torque converter (Brun 1996).

Mercure (1979) used a two dimensional Euler code in order to visualise a fluid flow through a three-component torque converter, and to develop an optimum design of the stator. His study, however, was preliminary. Anderson (1982) developed a streamlined curvature method to calculate the flow field inside a torque converter. He came up with a conclusion that one-dimensional flow theory was good enough to calculate performance characteristics, but multidimensional flow codes are necessary to predict internal flow patterns (Brun 1996).

Numazawa et al. (1983) developed a liquid-resin film method to visualise the torque converter blade's flow patterns and end wall surfaces. They used this technique to study the effect of axial length on the flow field. Their study concluded with a smoother flow and higher efficiency torque converter (Brun 1996).

Adrian and Fister (1983, 1985) experimented on an industrial torque converter using a two-dimensional laser Doppler velocimeter to measure the flow inside. The arrangement of the elements of the torque converter was different from the conventional ones (radial exit of the mixed-flow pump, turbine with radial flow, and radial flow stator). According to the data, they concluded that the stator flow

is highly three-dimensional in the entire range of operations, and strong wake phenomena exist at the pump exit (Dong 1998).

Bahr et al. (1990) used a Plexiglas torque converter and measured the flow with a one component laser Doppler velocimeter. The rotor speed was reduced due to the nature of the material used. They measured at two different speed ratios and learned that the instantaneous turbine and impeller blades had a strong effect on the average velocity field in the stator. They did not find any noticeable flow separation at the 0.065 speed ratio. There was also no trace of the flow separation at the 0.8 speed ratio. They found that the flow rate and torque distribution varied considerably a lot from the conventional one dimensional flow theory. They also stated that the torque is very poorly distributed near the core and therefore should be redesigned for a more uniform flow and less separation (Dong 1998).

Kubo et al. (1991) experimented with a steady state five-hole probe method to measure static pressure, total pressure in the gap region and three velocity components. The study was carried out concerning the gap region of a torque converter under the range of speed ratio of 0 to 0.8. 3 points for pump exit, 3 points for turbine exit and 16 points for stator exit were measured. The deviation angle, the difference between the flow and blade angles were used to improve the performance prediction of torque converters (Brun 1996).

As an extension for the Bahr's laser velocimeter measurement, Gruver (1992) measured three components of velocity in the pump manipulating the Bahr's torque converter. He used speed ratios of 0.065 and 0.08. Velocities were calculated at inlet, mid-cord and exit planes. For both the speed ratios, the through flow distribution was fairly three-dimensional. Except for the core, the flow was well distributed near the shell and the mid-span region. It was found out that about one third of the pump passage (near the core) was not active. Through velocity was found to be either very small or negative in this region. The mid-cord and the exit planes produced strong secondary flows for both the speed ratio conditions. The most alarming characteristic of the flow field was that the secondary flow circulated counter clockwise at the mid-cord plane and

transformed to clockwise at the exit plane. It was also noticed that the relative stator blade positions have a strong effect on the flow field at the pump inlet (Dong 1998).

As a continuation of Bahr's and Gruver's laser velocimeter measurements, Brun (1996) used a plexiglass torque converter installed in an oil bath of matching index of refraction (for good optical laser access) to study the velocity field. He emphasised the 0.065 and 0.8 speed ratios (close to coupling speed) out of a wide range of operating conditions. In the stator, a small low velocity wake/separation region was observed on the pressure side in the first half of the passage and on the suction side in the second half of the passage (Dong 1998a).

Yu dong (1998) has carried out an experimental investigation in order to get a clearer understanding of the fluid flow field inside the torque converter. A high-frequency response five-hole probe was developed for his study on unsteady flow measurement. He reported a strong secondary flow at the pump mid-cord. He also mentioned about the flow concentration on the pressure side of the pump blade. He also mentioned high losses due to the wake flow in the core-suction corner (Dong 1998).

Lui, Y. (2001) performed an experimental investigation of the three dimensional flow field inside automotive torque converter. He used a high-frequency response five-hole probe developed by Dong, Marathe, and Lakshminarayana. He stated flow separation near the suction surface at the turbine mid-cord. At the peak efficiency condition, he observer flow separation near the pump core/suction side corner (Liu 2001).

1.5 Computational Research

In this new era of computing, the capability of Computational Fluid Dynamics (CFD) is being extensively acknowledged. For the analysing and understanding of fluid flow behaviour in the torque converter, researchers all over the world are already experiencing the advantage of using CFD. With the revolutionary progress of computational competence, CFD is expected to provide all the required analysis in an efficient manner (Liu 2001).

Abe At al. (1991) obtained a very strong three-dimensional and secondary flow by computing the internal flow field of a torque converter using a steady interaction technique and a third-order upwind scheme (Liu 2001).

Schulz, Greim and Volgmann (1996) utilised a numerical method for the three-dimensional fluid flow-field in a torque converter, using steady or unsteady incompressible viscous flow to calculate the flow field. A vectorisable code was used to achieve an optimal performance on a modern vector computer. For a wide range of operational conditions, the flow at the stator outlet was reported to be uniform. The interaction of the stator with the pump and the turbine showed some unsteady behaviour, but it was reasonably negligible (Liu 2001).

By et al. (1995b) computed the flow field in the pump of a torque converter using his modified Navier-Stokes code. They concluded that the inlet velocity profile strongly affects the total pressure loss and that the nature of the secondary flow field strongly depends on the pump rotation (Liu 2001).

Marathe and Lakshminarayana (1996) utilized a two-dimensional, steady, incompressible Navier-Stokes code to get the mid-span flow field of the stator. For the designed condition the, calculated midspan flow was accurate, but the off-design condition was not particularly accurate (Liu 2001).

Tsujita and Mizuki (1996) experimented with a three-dimensional, incompressible, turbulent flow in the pump of an automotive torque converter. They tried at three different speed ratios: 0.02, 0.4 and 0.8 keeping the same inlet boundary condition. The K-ε model was used for turbulence. The computed result was satisfactory compared to the experimental results (Liu 2001).

In keeping with the growing use of CFD software, Cigarini and Jonnavihula (1995) simulated a three-dimensional fluid flow for an automotive torque converter using the STAR-CD. They applied the steady interaction technique implemented in that fluid dynamic program. The computed performance characteristics agreed well with the experimental ones.

In order to improve the torque converter's efficiency, Ejiri and Kubo (1998, 1999) carried out a viscous calculation using STAR-CD, and modified the torque converter. The computational result was reasonably close to the actual flow pattern. Continuing with their research, they also concluded that for the maximum overall torque converter efficiency, there is an optimum value for turbine bias angle and the contraction ratio of the pump passage (Liu 2001).

Seunghan Yang, Sehyun Shin and Incheol Bae (1999) carried out a computational flow analysis on a torque converter. They compared it with an experimental result and found their analysis to be satisfactory. In their paper they described the mixing-plane (Sehyun shin 1999).

The increasing pressure for pollution control and constant demand for higher fuel economic vehicle has lead Sehyun Shin, Hyukjae chang and Mahesh Athavale to investigate the flow field in an automotive torque converter. In 1999 they have performed a numerical analysis, in order to achieve a detailed incompressible, three dimensional, turbulent and viscous flow field within the pump of an automotive torque converter. They have used a modified Navier-Stoke flow code for the computation of the torque converter flow along with mixing plane and K─ε turbulence models. Their numerical analysis showed remarkable similarity with the experimental performance data in terms of torque ratio, efficiency and

input capacity factor. They rely on their numerical analysis more than the one-dimensional analysis to predict the performance of a torque converter (Sehyun shin 1999).

CHAPTER 2: CFD FACILITIES

2.1 Computational Fluid Dynamics

The Computational Fluid Dynamics (CFD) computer program used here is called CFD─ACE+ of the CFDRC and ESI group. This is a multi-physics computational analysis program. This program was used to predict the temperature and velocity of the fluid flow inside a torque converter. Hence it presents the three dimensional fluid flow in different temperature and velocity. A standard package for the CFD─ACU+ includes the following applications.

CFD─GEOM – This is used for the construction of the geometrical structure of the given problem and grid generation. The smart NURBS library of Geom covers a wide array of CAD creation capabilities. It has both structured and unstructured grid generation potential. It is a very good tool for 3-D geometry construction, covering a wide range of drawing aspects.

CFD─ACUE-GUI – Stands for the graphical user interface. This is where the Solver set up the problem in order to run, by putting in necessary conditions and data. CFD─ACUE-GUI has some limitations for each of the modules. The flow module is designed for incompressible flows and the pressure-based method used by CFD ACE has limitations for supersonic flows.

CFD─ACE Solver – This is the solver that performs the computation for the given problem, according to the provided conditions and data. This is an advanced polyhedral solver.

CFD─VIEW – This is a post processor. It is for visualising and investigating the result given by the solver. (CFD User Manual)

PC Workstation:

- Microsoft Windows XP, Professional version 2002, Service Pac 3
- Processor-Intel® Core™ 2 Duo CPU, E8400 @ 3.00 GHz.
- Internal Memory- 3.25 GB of RAM
- Hard Drive- at least 20 GB
- Mouse-3 button
- Graphics card 3D graphics card with at least 256 Mb Memory

2.2 Specifications of the torque converter

Before the geometrical construction, all the dimensions of the torque converter were measured. The specification of the torque converter, that is going to be constructed for the simulation, is mention below.

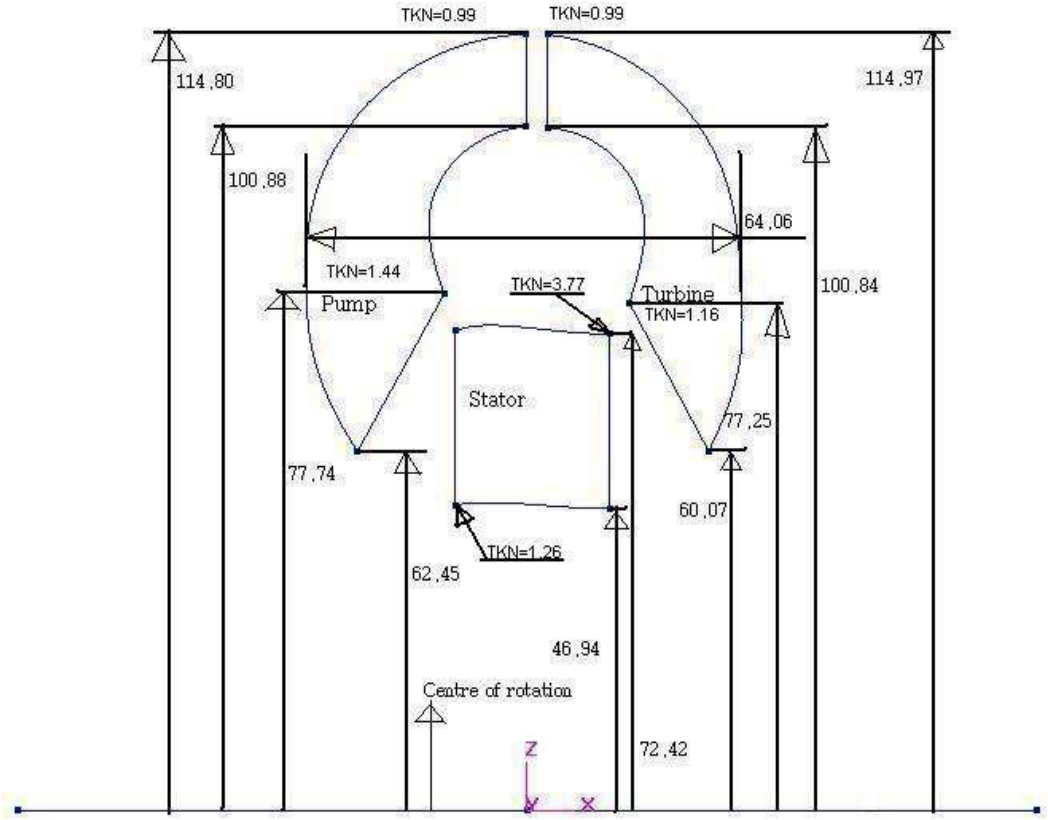

Figure 3 : Dimensions of the Torque converter (in millimetres) (TKN=Thickness of the blade).

The above mentioned figure is a two dimensional picture of the torque converter, presenting the dimensions of all the three components. The torque converter has three different types of channels, Pump channel, turbine channel and stator channel. These channels are of different geometrical structure due to the difference of their job definition. At the inlet fluid gets in almost radially, so the inlet of the pump is almost radial. However at the exit, the fluid flow leaves the pump channel at an angle with the axis of rotation, due to the centrifugal force caused by the spinning of the torque converter. For that reason the exit of the pump has necessary bending so that it releases the flow at an angle that is easy to catch for the turbine. And due to that, the inlet of the turbine has an inlet angle to catch the flowing fluid and a different angle at exit, so that the reactor or stator can guide the fluid easily. For the stator, the blunted inlet helps the mixed flow to enter smoothly. Next the fluid is redirected to the pump inlet. Even the cross sectional area differs from inlet to exit for each of the components of the torque converter. All these complexities in the geometrical assembly make the torque

converter a very complex three dimensional structure. The specifications for the torque converter are as following.

Element	Inlet angle Deg	Exit angle Deg	Number of blades
Pump	-16.30 ^{o}	-4.75 ^{o}	29
Turbine	33 ^{o}	-66.75 ^{o}	31
Stator	16.60 ^{o}	65.65 ^{o}	16

Table 1: Specification of Torque Converter.

The construction procedures of the torque converter with the CFD─GEOM are mentioned in the following section. The torque converter was structured keeping the x axis as the axis of rotation.

2.3 Construction of the geometry

CFD─GEOM has the facility for drawing almost any given physical structure. The geometrical structure and grid generation for the torque converter has been performed by CFD─GEOM software. Although this study has used the geometry corrected and donated by Dr Mahesh Athavale (Manager, CFDRC) for the simulation, the primary torque converter has been constructed independently. The geometry was able to go through the simulation after fine tuning.

Primarily to draw the frame, it was firstly important to determine the three-dimensional co-ordinates for the given structure. Once the co-ordinates of the structure were determined, then the points were placed according to the available co-ordinates, using the point creation tool button at the Geometry tab.

Using the curve creation and line creation tool button, the frame of the stator blade was then shaped. The geometry construction was carried out in such a manner that the grid generation and viewing of different parts becomes progressively easier.

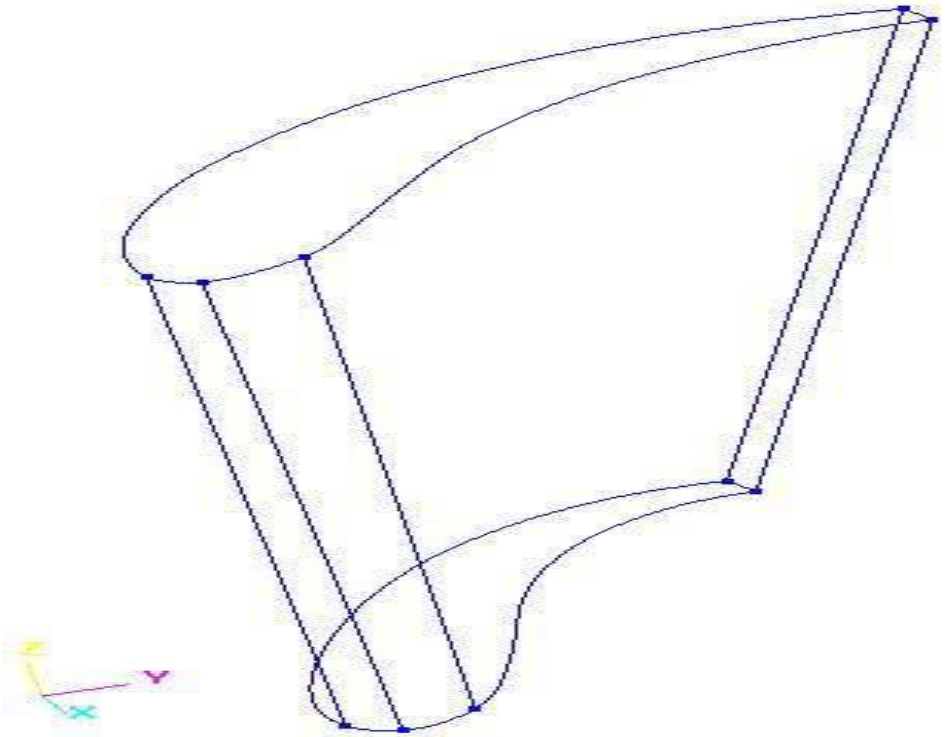

Figure 4: The frame of the stator blade in the Geom.

After structuring all three blades (stator, pump and turbine) the grid generation was performed for the structure. The structured grid generation on the defined model was chosen. Subsequently the structured face was also created. Because it contained a high number of grids, it was relatively logical to construct the structured grid across the system. The stator blade has been shaded so that it could be easily seen through the complex grid structure of the stator channel.

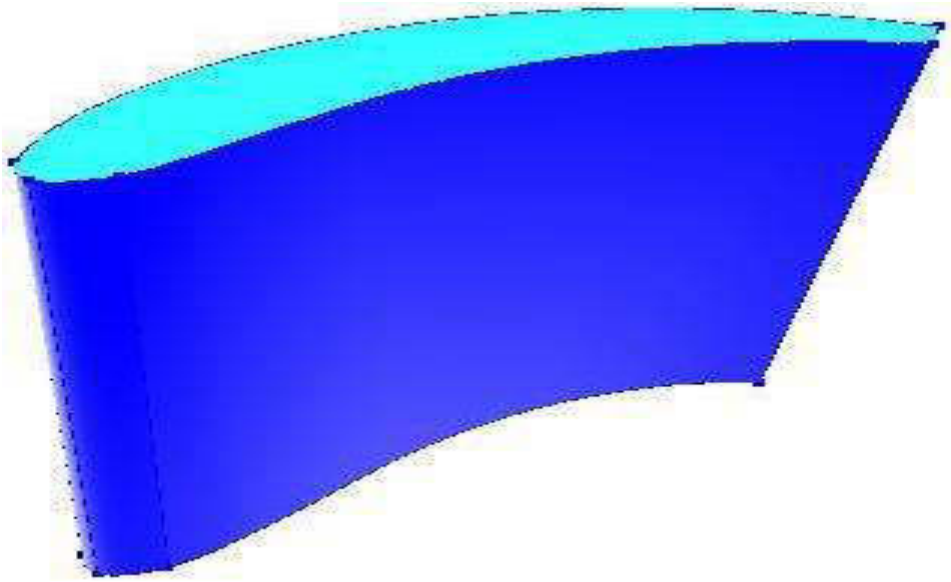

Figure 5: Stator blade after grid generation and surface shading.

The concept was to build a channel through which fluid will pass. The basic idea behind the channel construction was to set the stator blade in the middle of the channel, so that the blade of the stator stays in the middle of the flow and the flow pattern can easily be visualised. For that the channel was split up at approximately its mid point. Then one side of the channel was constructed according to the co-ordinates of the split points.

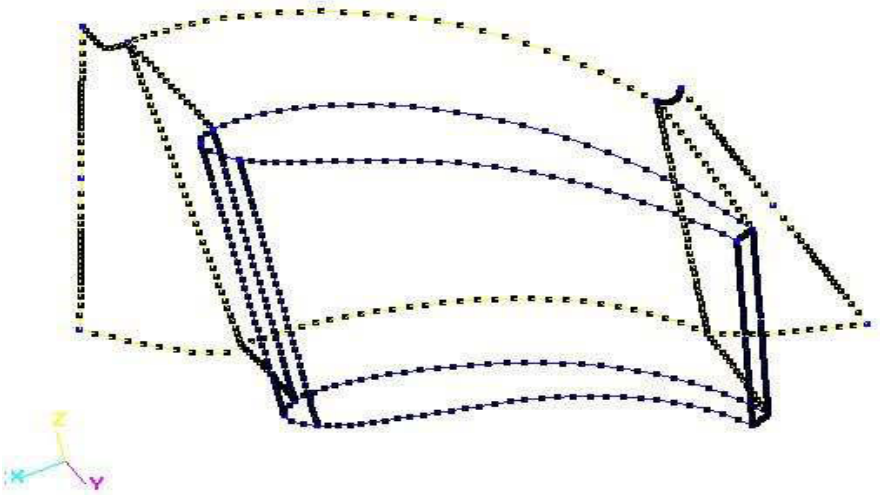

Figure 6: Stator blade (primary position of the construction of the channel with grid).

The other side was constructed similarly. The plan was to create a channel and placing the blunted stator blade in the middle of the flow, and both the sides of

the channel would be defined as cyclic BC, as in the geometry, the sides of the channels are recurring.

The mixing plane extension was also constructed at the same time. As the stator, pump and turbine have different numbers of blades, there would be mixing of flows within the channels at their exits and inlets. This had several limitations. One of the limitations was, “The grid in the circumferential direction should be circular and radii of the corresponding grid lines should match exactly.” (CFD─ACE (U) User Manual:- Chapter 13. “Mixing Plane”). By manipulating the revolution tool, the condition of the mixing plane was satisfied.

The structure was then set ready for revolution. The face of the back was selected (Figure. 7) and the following parameters were set for a revolution angle -22.5 with the revolution axis “X” for a 16-bade stator. Later on the newly created block was deleted and new grids were created. The revolution was carried out because the channel sides have to be rotationally symmetric, and the block was deleted because it is important to obtain different separate blocks for the pressure side and suction side of the stator and separately for the mixing plane.

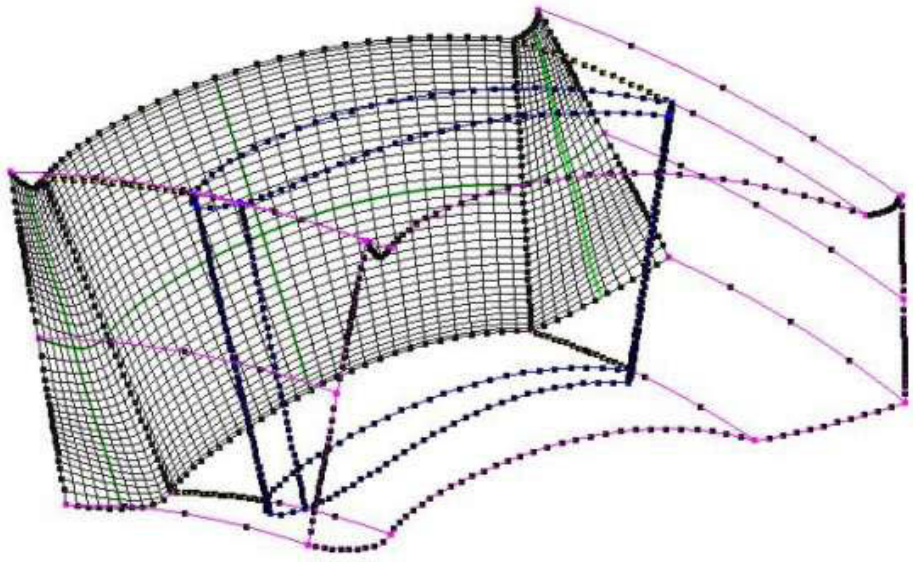

Figure 7: Stator channel after revolution and deletion.

After re-gridding and re-blocking, the stator channel was completed.

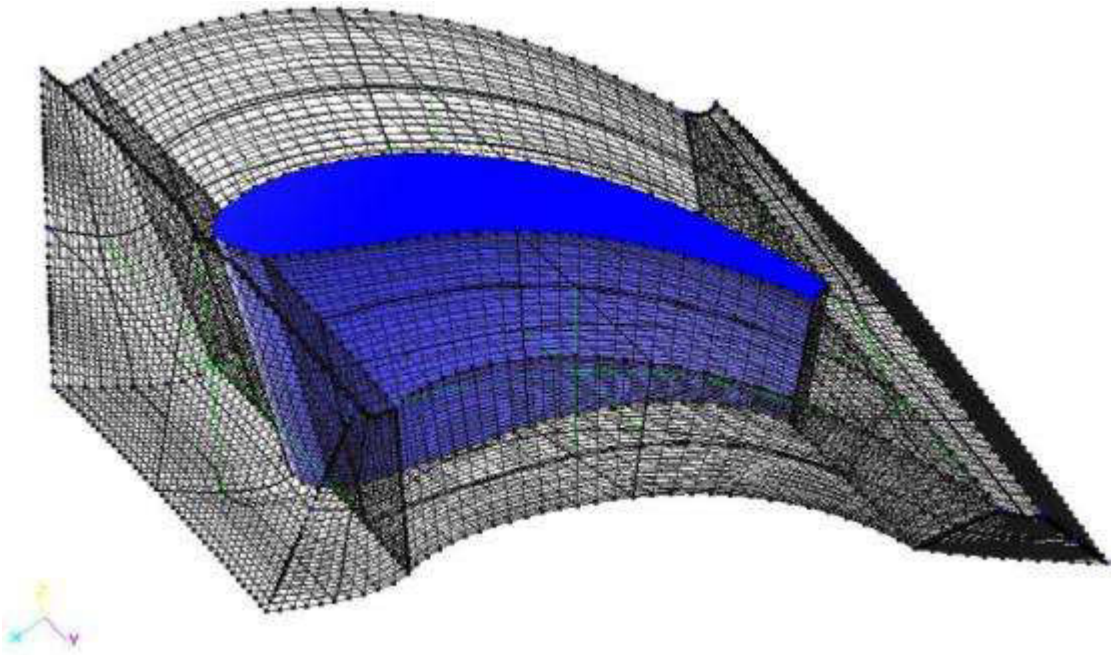

Figure 8: Complete stator channel with grid generation.

The torque converter consists of three components in a closed loop fluid circuit. For a better understanding of the fluid flow, all three components were added to the simulation.

The construction of the pump and the turbine was similar to that of the construction of the stator, the only difference relating to the blade geometry. The stator blade had a blunted inlet which had to be modelled accurately (cast iron is usually used for stator blades). However, the blades of the pump and turbine were considered as fabricated plane sheets of metal (as in practice, it is commonly used these days). The rest of the procedure was similar to that for the Stator. A structured 3-D block was then created from the grid structure.

After structuring the geometry, block reorientation had to be carried out. As the simulation would pass the information according to the orientation of the block co-ordinates, it had to be oriented in the same manner for all the parts of the torque converter. For example, if the “i” co-ordinate represents the flow direction, then all three parts of the turbine and their extended mixing plane must

contain the same co-ordinate, and the other co-ordinates (j, k) must also follow the similar positions.

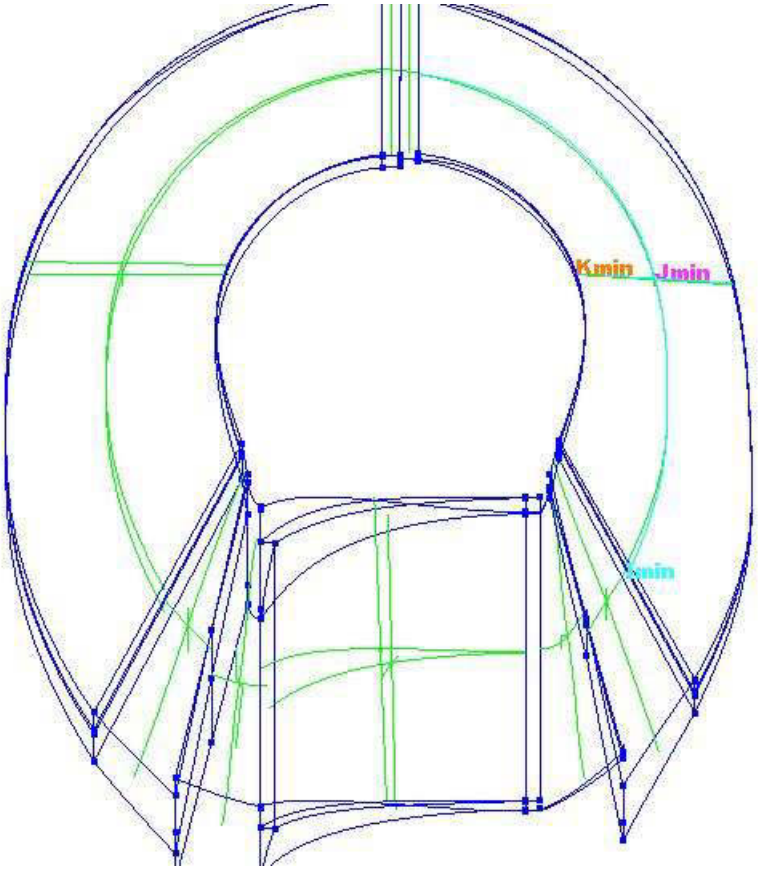

Figure 9: IJK co-ordinates reorientation.

After completing the reorientation, the geometric construction of the torque converter was completed. So far the file was being saved as NAME.GEOM, a file that was meant for the geometrical structure construction.

The simulation was performed in DTF format which was CFD─ACE Graphical User Interface. The subject was saved as NAME.DTF file and readied for the simulation settings.

CHAPTER 3: SIMULATION PROCEDURE

3.1. Configuring the program for simulation

The geometry that was drawn with the CFD─GEOM has already been saved as NAME.DTF. The DTF extension referred to the CFD─ACE (U) program. That indicated that the Geom file was ready for simulation configuration. The structure was visible in the viewer window as below.

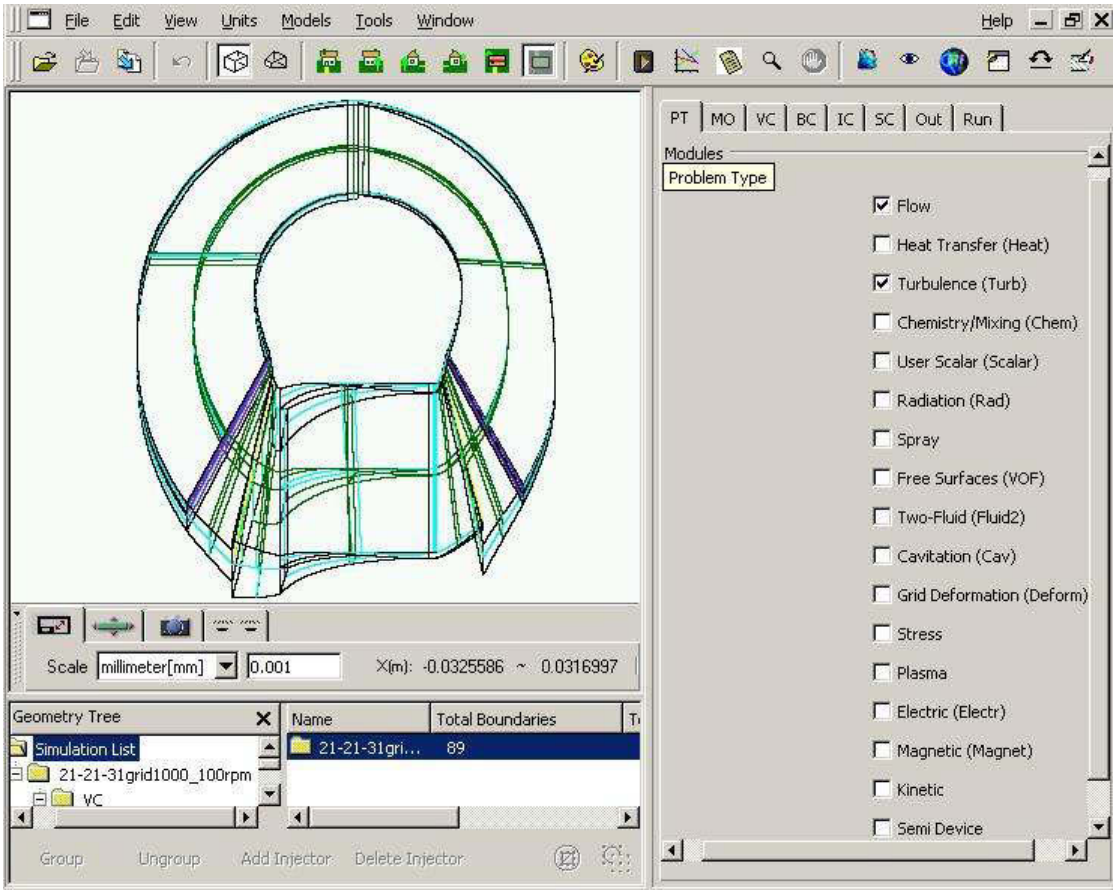

Figure 10: CFD─ACE (U) working window.

The first requirement was providing the entity bar with the required scale for the geometry. For this computational experiment the scale was set to mm

(millimetres). It is very important to notify this scaling according to the geometry construction (CFD Manual).

In order to configure the simulation, the physical and numerical settings had to be made in the control panel (CFD User manual). The eight distinct panels of the control panel are described below in brief.

3.1.1. Problem Type (PT)

The Problem Type panel is the first among the control panels. The Flow module and the Turbulence (Turb) module are the ones worked on for the given problem.

3.1.2. Model Option (MO)

There were three tabs available for the given Flow and Turbulent problem. The Shared tab enables the writing of a name for the simulation and selection of the transient condition. Specifically for this simulation, the time dependence was set to steady, as multiple rotating reference frames had rendered the problem steady. And for that the rotational reference had been set as frame rotation (VC based). The rotational speeds were then specified individually in the Volume condition control panel. The reference pressure was set at 100000 Pa under the 'Flow' tab of MO.

For the Turbulent model, K-ε (K-Epsilon) was chosen for the present Torque converter problem. The model adopted in CFD─ACE+ is based on Launder and Spalding (1974) (CFD User manual- turbulence module). It was set under the Turbulence tab.

Turbulent kinetec energy $\boldsymbol{k}$ was assumed 1.08 m^2/s^2 and dissipation rate $\boldsymbol{\varepsilon}$ was assumed to be 10.3 m^2/s^3 at the inlet and the outlet. The kinetic turbulent energy is

$$k = \frac{1}{2}\left(u'^2 + v'^2 + w'^2\right),$$

Where: u', v', w' are fluctuations of velocity in x, y and z axes respectively, [m/s].

Backflow dissipation rate could be derived as following:

$$D = \frac{C_{\mu}^{0.75}\,\kappa^{1.5}}{\kappa \cdot L}$$ Where, $C_{\mu} = 0.09$ (turbulence model constant) and $\kappa = 0.4$ (Karman Constant) are constants and L = reasonable length scale in [m] (CFD ACE Tutorial- Turbulent flow over a Backward-Facing Step).

3.1.3. Volume Condition (VC)

The Volume Condition allows the material properties and source terms to be set on a volume by volume basis. For this particular simulation, properties and rotation options were utilised in the Volume Condition panel.

Under the VC Setting mode the selected fluid for the torque converter simulation was engine oil. The desired oil type was not available in the database, so the Density and the Dynamic viscosity were set externally as user inputs. As the particular problem was not set as temperature dependent (Isothermal condition), density and fluid kinematic viscosity were set as constant.

For the rotation option there were three types of settings. One was that the pump had a rotational speed of 1000 rpm. As the "X" axis was the axis of rotation, the angular rotational vector was set at -6000 deg/s in W_x only. The (-) minus sign appeared for the conventionally chosen right hand rule direction along the axis of rotation of the pump.

The stator had no rotational frame. It was simulated as stationary for that particular speed ratio.

The turbine's rotational frame speed was set at a speed ratio of 0.60, that is 600 rpm. As the X-axis was the axis of rotation and the angular rotational vector was set at -3600 deg/s in W_x only. To get the angular rotation the following formula was used: deg/s= rpm/60 × 360. The (-) minus sign stood for the rotational direction only.

3.1.4. Boundary Condition (BC)

This control panel allows the boundary conditions to be set for each of the boundary patches. Each of the structured faces was a separate boundary condition. The BC Setting had four modes; General, Cyclic, Thin wall, Arbitrary interface. Those used in this experiment were General mode, which allows the computational boundary conditions to be set, and the cyclic mode, which sets up the cyclic BC pairs. A name was allocated to every patch for the convenience of the user for picking up the patches during the simulation set up and from the output file.

The type for each of the BC patches needed to be declared in the BC type section. Inlet, Outlet, Wall, Rotating Wall, Symmetry, Interface, Thin Wall, Cyclic were the options for the BC type. For the pump and turbine, the BC type was rotating wall and the setting was similar to the VC control panel. The Boundary Condition type for the Stator was Wall. All X, Y & Z-directional velocities for the wall were set to zero.

The cyclic boundary condition, also known as the periodic boundary condition, was used in rotating mechanical machines which produce revolving periodic flow and heat transfer fields (CFD user manual-cyclic BC).

As the geometric construction of the blades was periodic and only one blade for each of the elements was constructed with a plane of periodicity set up halfway between adjacent blades, the Cyclic Boundary Condition was applied at those planes of periodicity (Shin, Chang & Athavale, 1999).

Those interfaces act as a communicator in between two adjacent blocks. They transfer the data of flow, heat and also other information. Therefore they did not require any data inputs from the users.

The torque converter has three components, pump, turbine and stator. All three components have inlets and outlets and they were defined in the Boundary condition type. The mixing plane was used because a different rotational domain

was present. As the mixing plane was in operation, the inlets and outlets for all three components had special names under this condition. All the inlets were named as “Mixpdn” meaning mixing plane down-stream (inlet), and the outlets were named as “mixpup”, meaning Mixing Plane up-stream (outlet). Each had specific numbers and the mixing plane identified them by those numbers.

The mixing plane between pump and turbine was numbered as 1. Accordingly, the upstream for that plane was “Mixpup_1” and this was the pump outlet. The downstream for that plane was “Mixpdn_1”, which was the inlet to the turbine. Consequently the plane in between turbine and stator was number 2 and the plane in between Stator and Pump was number 3.

3.1.5. Additional Input for Mixing-plane

There is an additional data file requirement for the mixing-plane application. That data file is basically a text file named as axis.dat, containing six lines of obligatory information. This file must be present in the directory from which the simulation will run. The file contains six lines of data as listed below:

1.0 0.0 0.0

0.0 0.0 0.0

1 -0.024 0.0137 0.054

10.0

1

0.25 1.00

Three real numbers in the first line determine the direction cosines of the axis of rotation. The second line contains the x0, y0, z0 coordinates of a point on the axis of rotation. The first parameter in the third line is a flag to set the mixing plane working. The remaining three numbers contain approximate coordinates of a point in the flow field. The fourth line contains the value of velocity to initialise the flow. The fifth line is an integer variable that specifies the frequency of the updating and data transfer across the mixing-plane interfaces. The sixth line

states the linear relaxation to be used for the mixing plane, for pressure and velocity respectively.

3.1.6. Initial Condition (IC)

The initial condition control panel allowed the user to set some initial values for the simulation. That could be achieved either by the all-volume method which would have made the same change for all the available volumes. Another method was the volume by volume method that can be used for setting different values for each individual volume. Those methods also provided the option to select the result as an initial condition from a previous simulation or to put a constant IC for the desired volumes. For this experiment all the initial conditions were set to default values except for the turbulence. The values for turbulence were kept the same as that in the BC Turbulence setting.

3.1.7. Solver Control (SC)

The Solver Control enabled the user to specify the numerical aspects of the solution and to select the solver output options (CFD user manual- Solver Control).

The Iteration tab had the following options. One was the number of maximum iterations to be performed by the Solver. The convergence criterion was the minimum value for the decrease of residual values for each variable. The simulation would stop automatically if any of those clauses were satisfied.

The spatial tab represents the spatial differencing scheme and controls the spatial accuracy of the simulation (CDF User Manual–SC). Different schemes of accuracy could be assigned for different variables with the help of this control panel.

The solvers allowed use of the desired linear equation solver, in order to solve the algebraic equations for each dependent variable. There were two types of solvers: CGS+Pre stands for conjugate-gradient-squared plus preconditioning

solver and AMG for Algebraic Multigrid Solver. As those solvers detect their own convergence, sweeps or convergence criterion could be fixed by the user.

Relaxation was available for both solver variables and auxiliary variables. The values of relaxation for solver variables were set below 1, though more than 1 was allowed. However, for auxiliary variables, between the relaxations must be within 0 to 1, (CFD User Manual -relaxation).

The “Limits” panel enables the user to assign a minimum and maximum value for any of the variables listed. Solutions must be checked as to whether any particular variable hits the given limits or not. If it does, then the convergence could be artificial and the result might not be feasible (CFD user Manual – Limits).

In the Advanced tab of the solver control, Buffer output and Higher Accuracy were common for all types of problems. Buffer output options allowed writing the output file only when the internal buffers were full. Commonly, users avoid this unless the program takes a long time for a higher number of iterations or time steps. In that case users choose the option to cut down the turnaround time consumed by the output writing.

The higher accuracy option was added to version 2004 in an experimental form. It was meant to give a higher accuracy result for the same given grid, but that will take a considerably longer time and it also contained some unresolved problems.

3.1.8. Output (out)

Output Control Plane allows the user to select when or how frequently s/he would like to obtain the results at the solver output. The print option is used to get the required report written in the output file. Diagnostics were used to monitor the performance of the linear equation solvers. This would be printed

after the specified iteration frequency. The summary reports for the required variables could also be printed in the output if this was checked for printing.

The Graphic option enables the user to select their desired output result for particular variables. That gives users the freedom to choose the specific outputs and avoid the unwanted variables, which is time-consuming both in the writing of the output files and sorting the variables results. This option was located in the Output Control panel. The Monitor tab allows the user to print out the solution variables in one or more locations. CFD ACE + has a built-in monitor point plotter to perform this task (CFD user manual- Flow Module).

3.1.9. Run (Run)

Parallel Run provides a number of output files. This basically enables the user to control the CFD ACE solver and monitor the simulation while it is in progress.

Submit to solver is the option that initiates the CFD─ACE-Solver for the current simulation. It provides the user with an option to change the name of the simulation if any unsaved changes have been made. Otherwise it initiates the simulation.

Parametric Run with Sim Manager and Optimisation Run with Sim Manager save the DTF file and launches it under parametric Wizard and Optimisation Wizard mode respectively. Appropriate settings are necessary for running the simulation.

The Residual plotter plots the absolute residuals for each variable that is being solved.

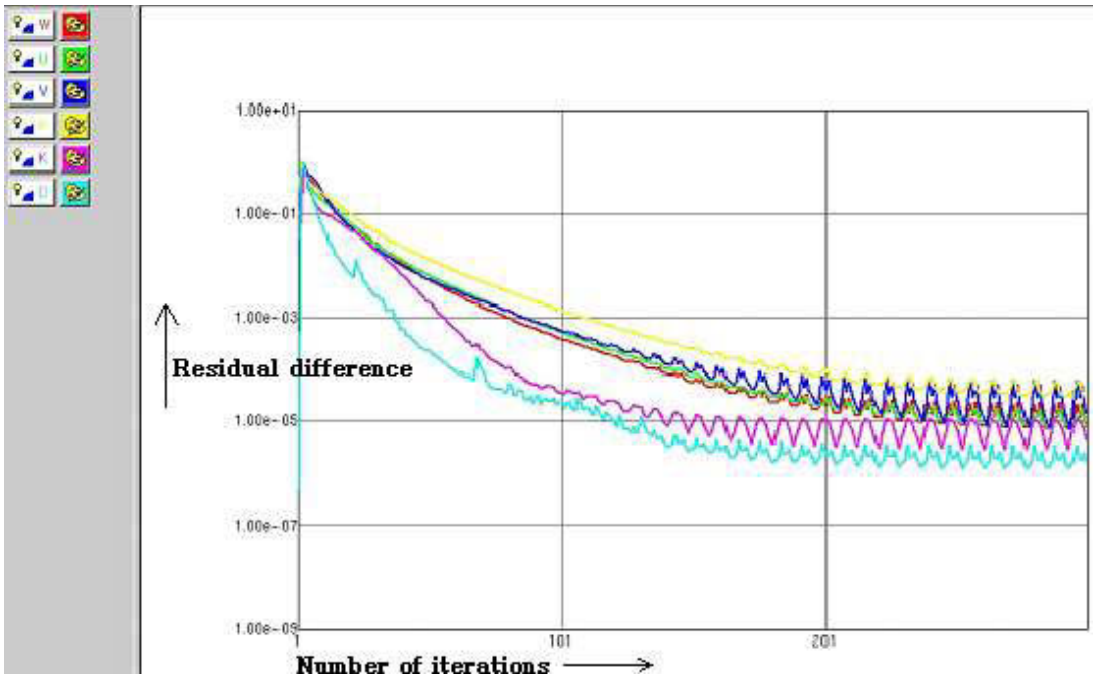

Figure 11: Sample of a Residual plotter.

In the normalised condition (by hitting the 'Nor' on the residual plotter), a drop of 3 to 4 orders of magnitude in each individual variable's residual is considered as acceptable for a good solution.

The View output tab allows the output file to be viewed. It contains the output data as per the instruction in the output control panel. Commonly users ask for this to be printed out at the end of the simulation.

The Plot Monitor Point enables the monitor plotter while the simulation is in progress. It acts similarly to the residual plotter.

The Save and Continue are meant to instruct the solver to save the simulation data, up to that particular iteration and then continue to run the simulation, while the Save and Stop tab save the data and cease the simulation procedure immediately. The Stop option terminates the simulation immediately.

The data provided above are only intended to be examples. For the sake of different simulation conditions, data were subjected to change. The actual simulation could contain more or less activating options than mentioned above.

In this research, there was a mixing plane mismatch for a considerable time period while running the simulation. This mismatch could cause divergence and provide unrealistic results. This was the main reason for using the structure donated by DR Mahesh Athavale and we are extremely grateful to him for his kind donation. Some necessary changes were carried out in the geometry and configuration of the simulation for the respective modification of the torque converter structure.

CHAPTER 4: FLUID FLOW INVESTIGATION.

4.1 Angle measurement:

The model of the torque converter was measured very carefully in order to get the blade angle. This measurement was done with the help of CFD-GEOM. CFD-GEOM has tools to measure angles. As blades of each of the components were symmetrical to each other, one blade of each component was measured. In the measuring method used, the plane containing the axis of rotation was the zero reference and the point of tangency was placed on the blade mean camberline. The 'X' axis was used as the axis of rotation.

According to the assembly of the three components (pump, turbine and stator), the position of the blades varied from each other. So for convenience, a new line at the point of tangency was created, which was parallel to the axis of rotation. The angle was measured from that newly drawn line. This was done for both inlet and outlet of every blade's angle measurement. The following figure is given for better understanding of the measurement procedure.

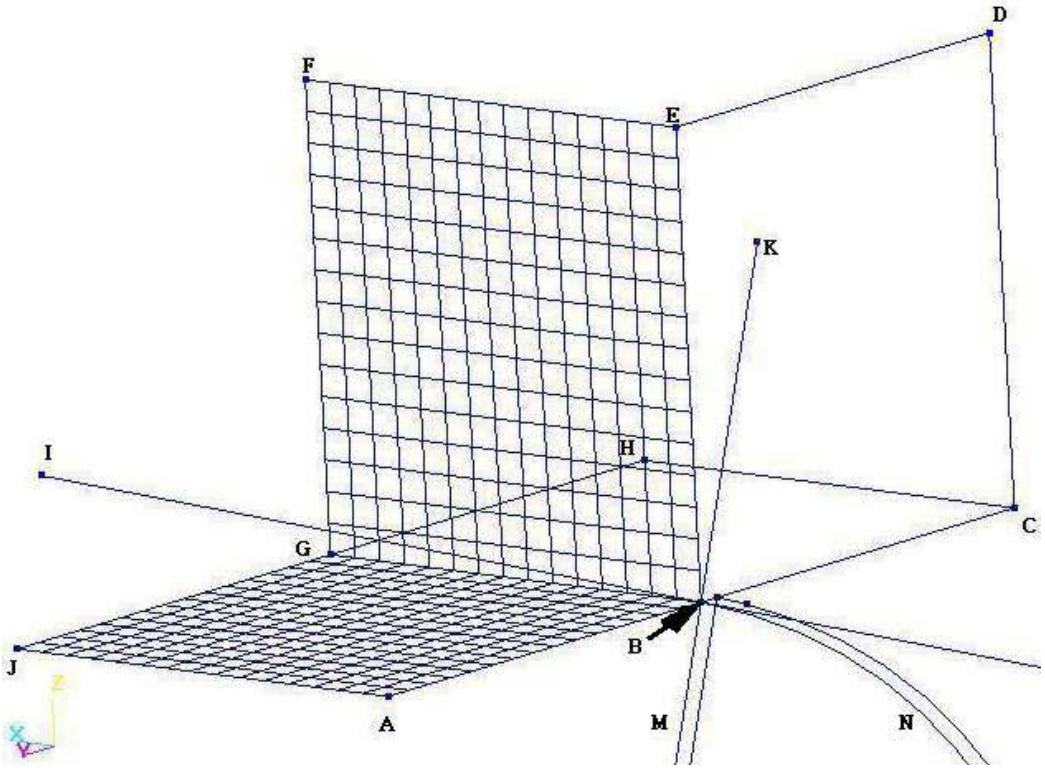

Figure 12: Angle Measurement.

This figure mentioned above was taken from the outlet of the pump while angle measurement was in progress and illustrates the line and planes that were drawn. ‘BMN’ is considered as a segment of the pump blade at outlet. ‘B’ is the point of tangency. ‘BI’ is the tangential extension of the camberline of the pump blade at its outlet. ‘BG’ is the line parallel to the axis of rotation (X axis). ‘BA’ is parallel to the Y axis and ‘BE’ is parallel to the Z axis. Here X axis (axis of rotation) is the datum for the measurement of angle.

‘BI’ is the tangential extension of the blade camberline at the point of tangency ‘B’ and ‘BK’ is the extension line of the edge of the blade (blade face). The angle of the blade is determined by the angle formed between the tangent of the blade camberline at the point of tangency and the axis of rotation. The line ‘BI’ itself is the tangential extension of the blade camberline at point of tangency ‘B’ and the line ‘BG’ is representing the axis of rotation as mentioned earlier. As this structure is highly three-dimensional, there remains a good chance of error, if the angle between ‘BI’ and ‘BJ’ is measured directly with the help of the CFD-GEOM provided angle measurement facility. The existence of the third dimension i.e. ‘Y’ axis, may cause diversion in angle measurement. This was tested with the change of ‘Y’ axis value for the same pair of lines and the measured value of angle between them had changed. This occurred due to the three dimensional existence. To stay away from this complication the choice was made to have a projection of the ‘BI’ on BC-BG plane. Then the angle between the projected line and ‘BG’ (axis of rotation) was measured while they were in the same plane. Thus at first, the angle from three−dimension to two−dimension was converted and then the angle between them was measured while they were in the same plane. That is how the measurement was done using a two−dimensional environment. This same strategy was followed for the measurement of all the angles of all the components of the torque converter.

4.1.1 Validation and verification

The torque converter used for the simulation was 230 mm in diameter. It had 16 stator blades, 29 pump blades and 31 turbine blades. All the specifications for the torque converter used in the simulation are provided below.

Element	Inlet angle Deg	Exit angle Deg	Number of blades
Pump	-16.30 ^{o}	-4.75 ^{o}	29
Turbine	33 ^{o}	-66.75 ^{o}	31
Stator	16.60 ^{o}	65.65 ^{o}	16

Table 2: Specifications for the simulating Torque Converter.

This is very close to the specification provided in the SAE paper series 1999-01-1056, by Shin, Chang and Mahesh, except for the turbine inlet and exit angle. The specifications of the torque converter for the SAE paper series 1999-01-1056, by Shin, Chang and Mahesh, are provided below.

Element	Inlet angle	Exit angle	Number of blades
Pump	-16.5	-6.0	29
Turbine	49.5	-57.5	31
Stator	16.5	72.0	16

Table 3: Specifications of the TC used in SAE paper series 1999-01-1056, by Shin, Chang and Mahesh.

The pump and turbine have blades of uniform thickness and the stator has varying thickness and camber and twist. Each of the blades of the stator, turbine and pump has the exact repeating structure respectively.

Consequently, one blade from each of the components was constructed with the plane of periodicity located at the mid section between neighbouring blades. For those planes of periodicity, cyclic boundary conditions were used. The pump channel, along with the blade, was set as a rotating wall in CFD ─ACE with a speed of 1000, 2000 and 2350 rpm. The turbine was also set as a rotating wall with varying speed ratios for each of the pump speeds. The wall boundary condition was applied to the stator blades.

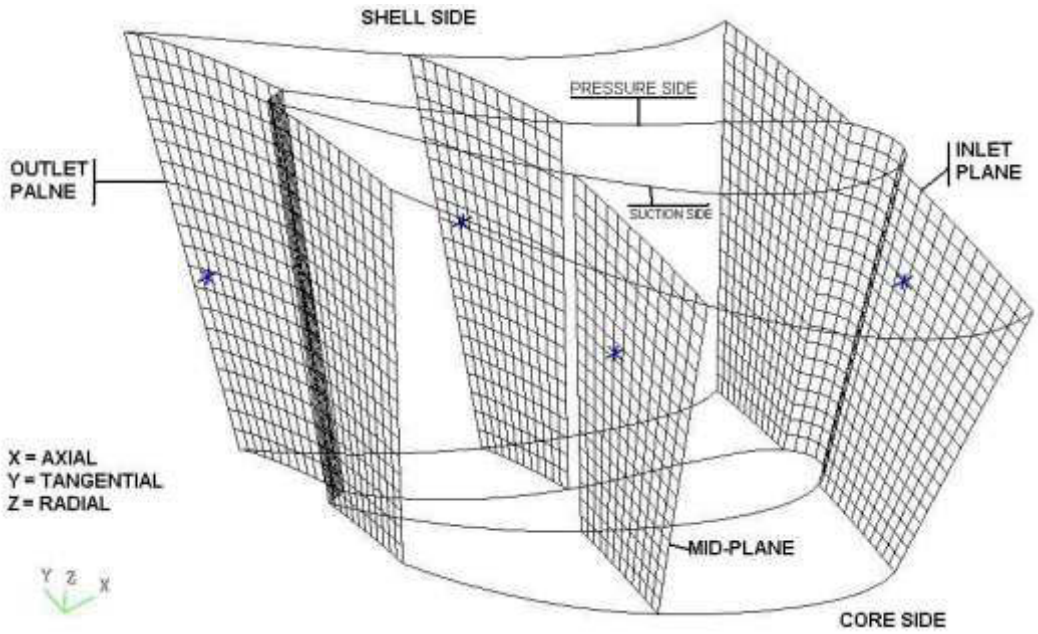

Figure 13: Inlet, Mid-chord and Exit plane of a stator.

All the components were given the grid structure which contains 38 × 21 × 22 grid stations. Thirty eight grids were applied in the streamwise direction (inlet to exit that is direction of the flow), 21 grids were applied for pitchwise (suction to pressure) and another 22 were applied for the spanwise (shell to core) direction. The simulation was set up for 1000 iterations, for 1000, 2000 and 2350 rpm impeller speed with 0.1, 0.2, 0.4, 0.6 and 0.8 speed ratios for each of them. The total of all residuals was reduced up to four orders of magnitude for each of the variables, within 600 iterations for all the simulations for 2350 rpm pump speed. For 1000 and 2000 rpm it was close to three orders of magnitude for each of the variables.

The results were then plotted to compare with Shin and Mahesh's work (SAE-1999-01-1056), discussed as following.

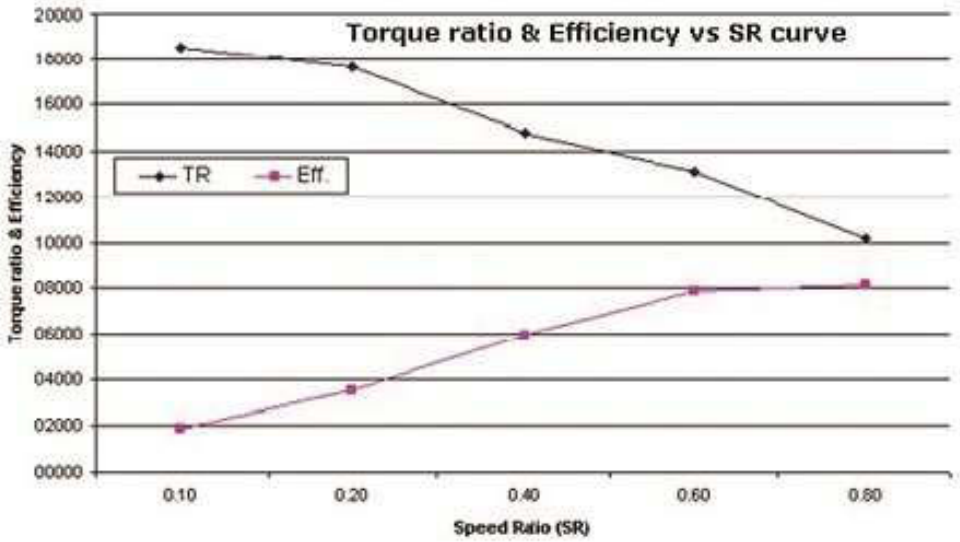

Figure 14: Torque ratio and efficiency curve for 2350 rpm at different speed ratios.

For better comparison the simulation for the impeller speed of 2350 rpm with different speed ratios was run. The torque ratio and efficiency for the simulation output data and the approximate values taken from the Shin, Chang, Athavale (1999) {numerical ones} graph (figure 16) are presented below.

Speed ratio	**0.1**	**0.2**	**0.4**	**0.6**	**0.8**
Torque ratio for 2350 rpm of pump speed [taken from our simulation]	**1.85**	**1.76**	**1.48**	**1.31**	**1.01**
Torque ratio (approx) [taken from Shin, Chang, Athavale (1999)]	**1.9**	**1.7**	**1.5**	**1.4**	**1.05**

Table 4: The comparison table for torque ratio between the study simulation result and Shin, Chang, Athavale (1999) result (for the impeller speed of 2350rpm) at different speed ratio.

Speed ratio	0.1	0.2	0.4	0.6	0.8
Efficiency (%) for 2350 rpm of pump speed [taken from our simulation]	18.5	35.23	59.35	78.88	81.11
Efficiency in (%) (Approx) for 2350 rpm [taken from Shin, Chang, Athavale (1999)]	20-21	38-39	64-65	78-79	80-81

Table 5: The comparison table for efficiency between the study simulation result and Shin, Chang, Athavale (1999) result (for the impeller speed of 2350rpm) at different speed ratio.

These data give the impression that the data for both simulations are very similar, except for the efficiency value for the speed ratio 0.4.

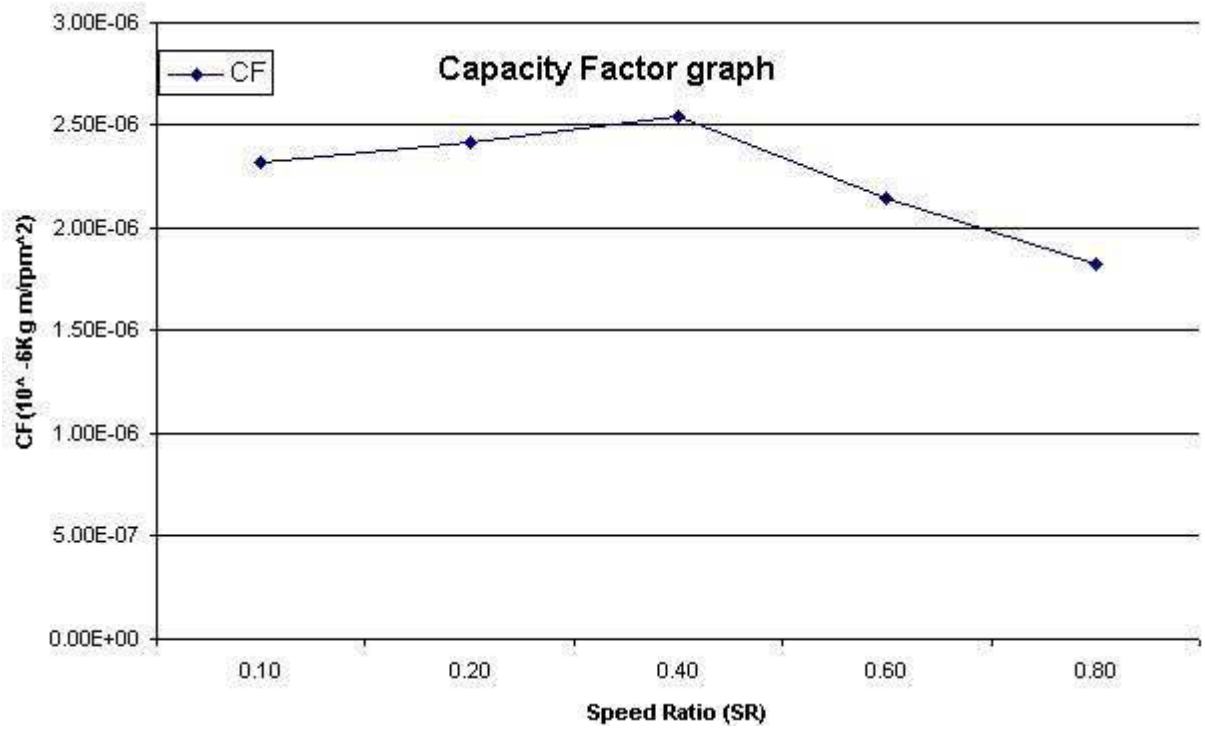

Figure 15: Capacity factor curve for 2350 rpm at different speed ratios.

The pattern of the capacity factor using the data of the study 2350 rpm simulation is also very close to the capacity factor curve plotted in Figure 15, except for the

value for the 0.4 speed ratio. In addition, the capacity factor for the study simulation shows slightly higher values regarding the graph of our reference (figure 17). The slight difference between the study simulation and the reference numerical result could be due to the influence of the fluid property difference and angle variation. Considering this, it could be said that this study work agrees well with the reference work. For more convenience the data for 2000 rpm pump speed at varying speed ratios is presented.

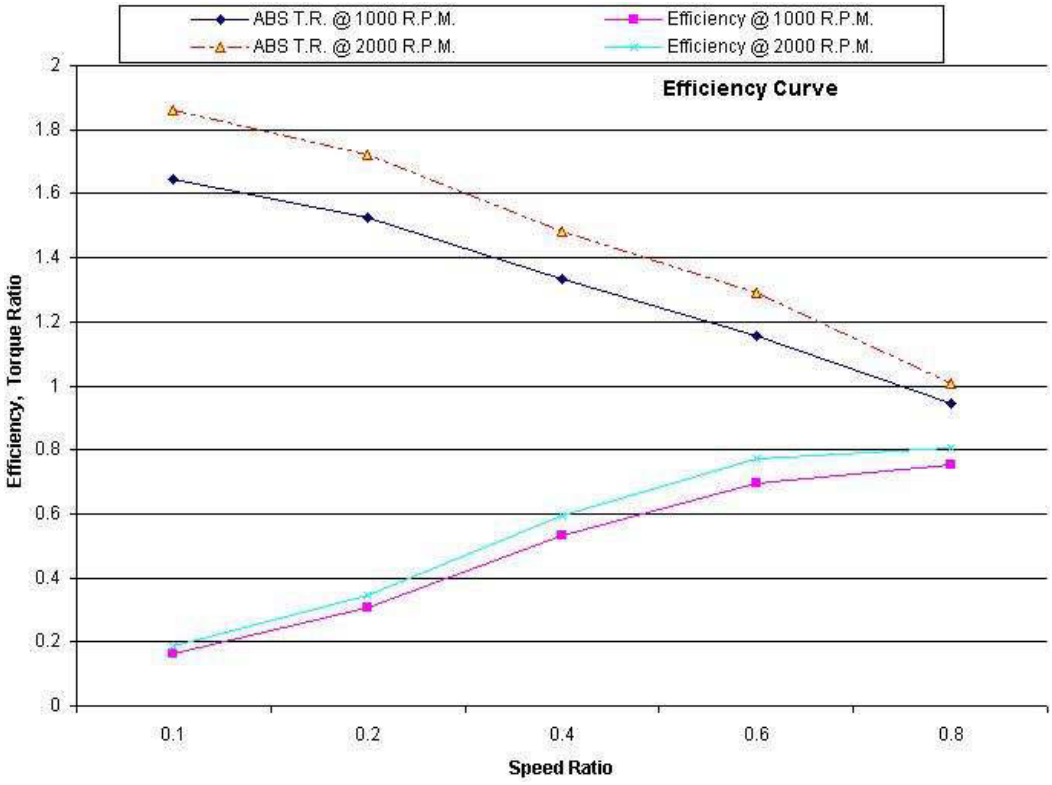

Figure 16: Efficiency and torque ratio vs. speed ratio curve plotted from simulations at 313K.

An attempt wasmade to compare the graph in figure 16 with the study efficiency and torque ratio (T.R.) vs. speed ratio graph for 1000 and 2000 rpm at different speed ratios.

The comparison in Figure 16 shows that the torque ratio (T.R.) for 2000 rpm pump speed is higher than that of 1000 rpm, and that eventually efficiency also

increases. This indicates that torque ratio and efficiency increase over the range of impeller speed.

The Shin, Chang and Athavale's comparison chart (SAE-1999-01-1056) is presented below so that the graphs (figure 14, 15 & 16) may be compared with each other. It should be mentioned here that the following curves represent 2350 rpm at different speed ratios.

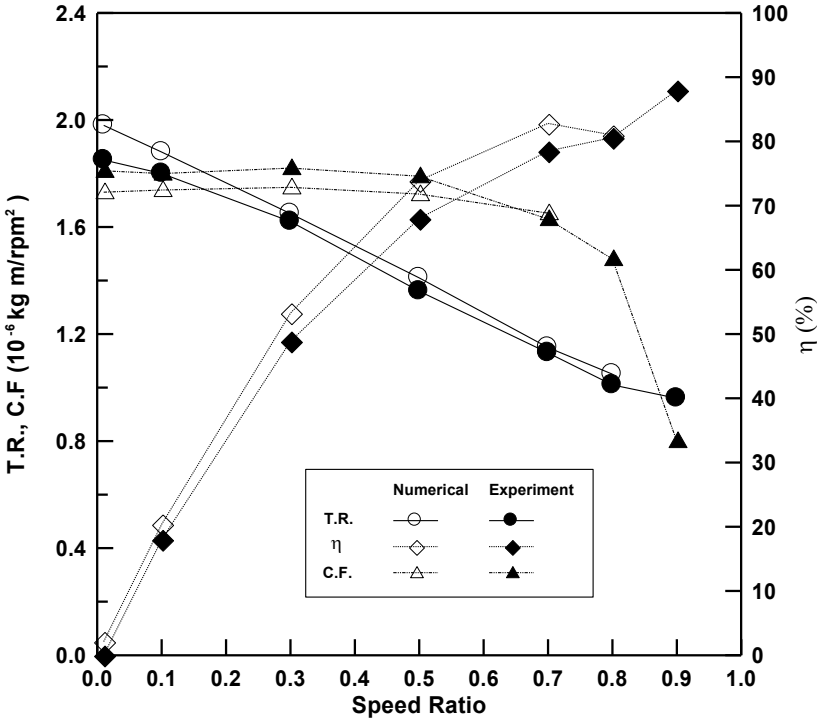

Figure 17: "Numerical Investigation of the Pump Flow in an Automotive Torque Converter" (SAE Tech paper series 1999-01-1056).

Although the curves from the Shin paper (SAE-1999-01-1056) are for 2350 rpm and this comparison is with the curves for 2000 rpm, a comparison is still useful, as there is only 350 rpm of difference which is sufficiently small and that is why similar curves should be obtained.

If the reference diagram (Figure 17; (SAE-1999-01-1056)) is examined, the torque ratios for 2350 rpm at different speed ratios are approximately as follow:

Speed ratio	**0.1**	**0.2**	**0.4**	**0.6**	**0.8**
T.R. (approx)	**1.9**	**1.7**	**1.5**	**1.4**	**1.05**

Table 6: Presentation of Speed Ratio and Torque Ratio in a table form from Figure 17;(SAE-1999-01-1056).

On the other hand, the study simulation provides the following data for the impeller speed of 2000 rpm, at different speed ratios.

Speed ratio	**0.1**	**0.2**	**0.4**	**0.6**	**0.8**
T.R. (approx)	**1.86**	**1.72**	**1.48**	**1.29**	**1.01**

Table 7: Presentation of Speed Ratio and Torque Ratio in a table form for the impeller speed of 2000, achieved from our simulation.

Though the above mentioned two sets of data do not match exactly, they demonstrate close similarity with each other, considering the 350 rpm difference between them. The difference is under 4% except for 8.5% at speed ratio 0.6.

the study efficiency curves for 2000 rpm impeller speed also demonstrated a pattern similar to Shin's efficiency curve and the experimental curve, mentioned in the SAE Tech paper series 1999-01-1056. The table below will assist in seeing the closeness of the two sets of data. The data for SAE Tech paper series 1999-01-1056 is taken from the graph itself and for that graph the closest approximate values are provided in the following table.

Speed ratio	**0.1**	**0.2**	**0.4**	**0.6**	**0.8**
Efficiency (%) (approx) for 2350 rpm (figure 16).	**20-21**	**38-39**	**64-65**	**78-79**	**80-81**
Efficiency (%) (approx) for 2000 rpm (figure 15).	**18.63**	**34.44**	**59.36**	**77.45**	**80.45**
Difference (%)	**1.37-2.37 %**	**3.56-4.56%**	**4.64–5.64%**	**0.55-1.55%**	**-0.45 – 0.15**

Table 8: Presentation of the difference between the study simulation data and data extracted from the graph (Figure 17).

The highest difference in efficiency between Shin's work and the study simulation for 2000 rpm pump speed, as mentioned above, is 5.64%. Therefore, considering the angle difference, it can be seen that this work is well validated by these comparisons with the SAE Tech paper series 1999-01-1056.

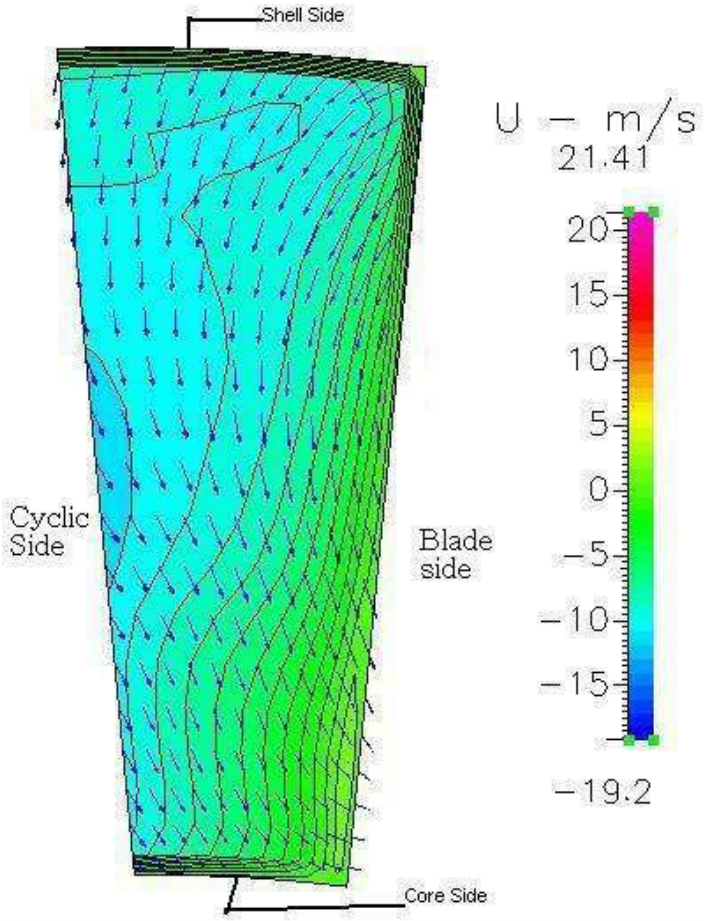

The estimation of flow at the stator inlet is performed on the basis of the velocity vector and pressure data provided by the simulation. This simulation was carried out for 2350 rpm of impeller speed at a speed ratio (SR) of 0.065. This figure represents the velocity vector plot with the pressure contour of the fluid flow, inflowing to the stator of the torque converter.

Figure 18: Fluid flow at the stator pressure side near the stator blade for 2350 rpm at 0.065 SR.

There was no sign of flow separation in this region. As shown in Figure 18, a minor deviation in the flow was observed near the stator blade of the stator pressure side but no circulating flow was found. The maximum value of the through-flow was found to be 9 m/s and the minimum was 1 m/s.

There was no sign of flow separation in this suction side of the stator, which is reasonable. A slight variation in the flow is also recognised near the stator blade. Not all the figures were taken at the same colour map, and the numbers of contours were rearranged in order to obtain better visibility. This explains why the colour and number of contours may vary from one to another.

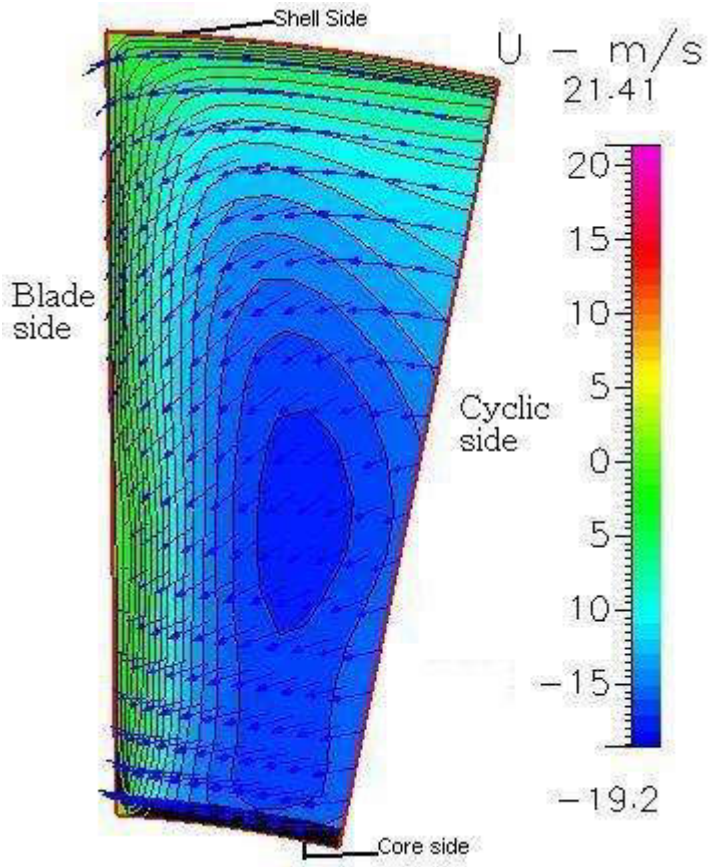

Figure 19: Fluid flow at the stator suction side near the stator blade for 2350 rpm at 0.065 SR.

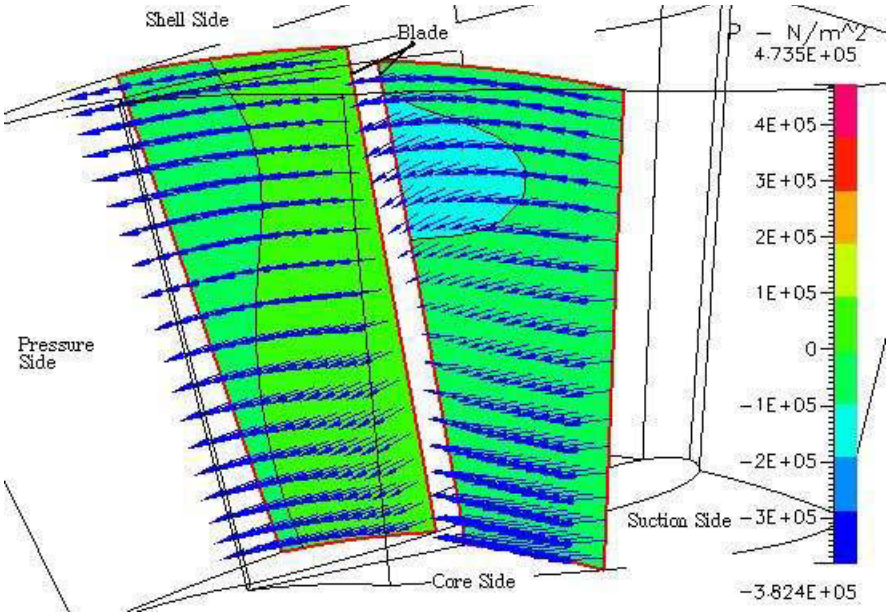

Figure 20 : Fluid flow at the stator mid-plane for 2350 rpm at 0.065 SR.

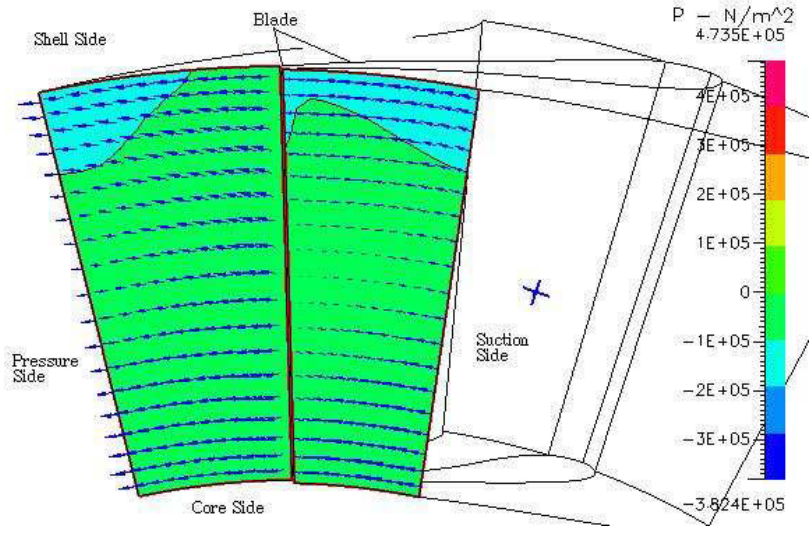

Figure 21 : Fluid flow at the stator outlet for 2350 rpm at 0.065 SR.

Figure 19 shows the fluid flow at the mid plane. The suction side shows a lower pressure than the pressure side, and a small deviation in the fluid flow near the suction side is visible. For the outlet (Figure 20), uniform flow is observed with a relatively lower fluid velocity at the suction side near the blade.

A comparison was also made of the efficiency of the torque converter for the same impeller speed for two different temperatures. Only two temperatures were used in the comparison, one being 313K and the 373K. The comparison for 1000 rpm impeller speed shows that the torque converter is more efficient at a higher speed ratio for a higher temperature, but at a low speed ratio it remained almost the same. So it can be said that at low speed ratio, the effect of temperature is not particularly significant. The comparison chart is presented below.

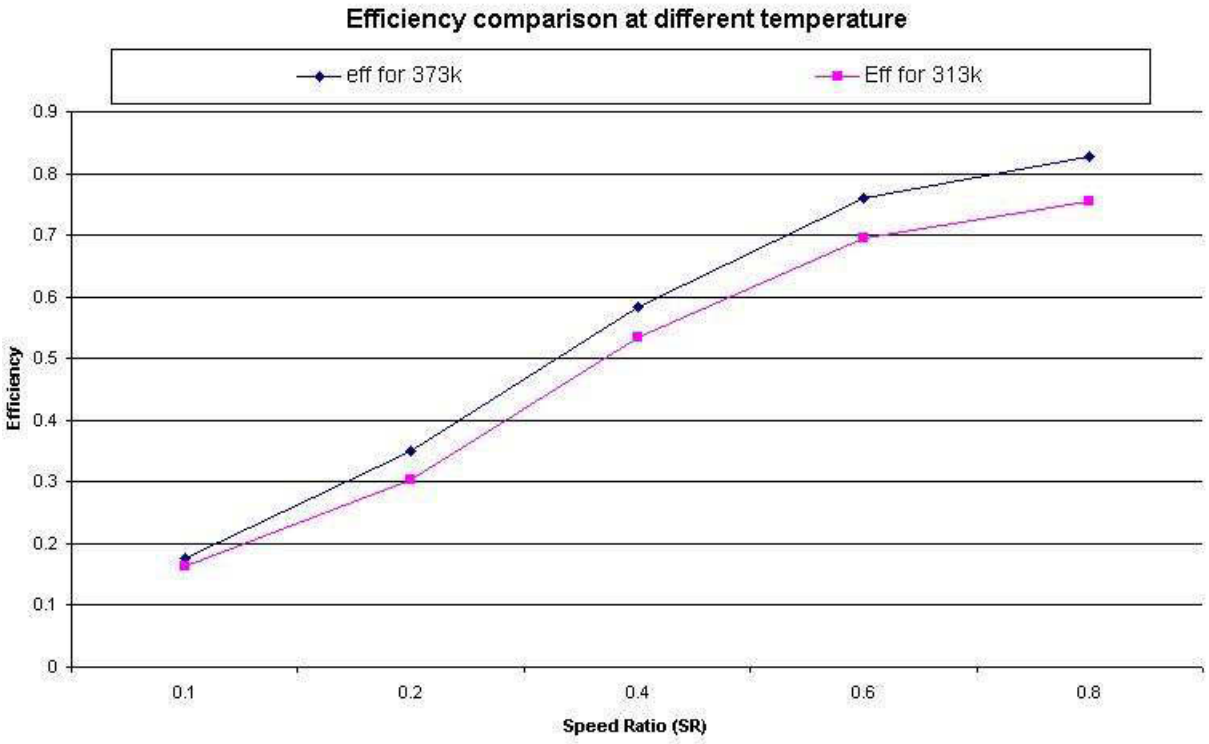

Figure 22: Efficiency comparison for different temperatures.

The following figures are for the impeller speed 1000 at 0.6 speed ratio.

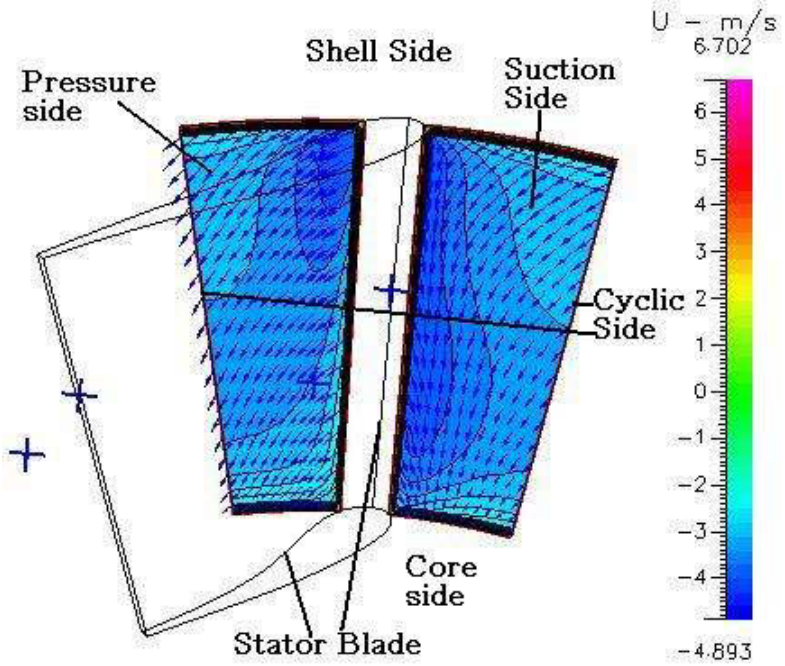

Figure 23: Fluid flow in the stator inlet at 313K.

The pressure contour with velocity vector plot indicates the existence of a deviated flow path for 313K of temperature, but there is no circulating flow was found.

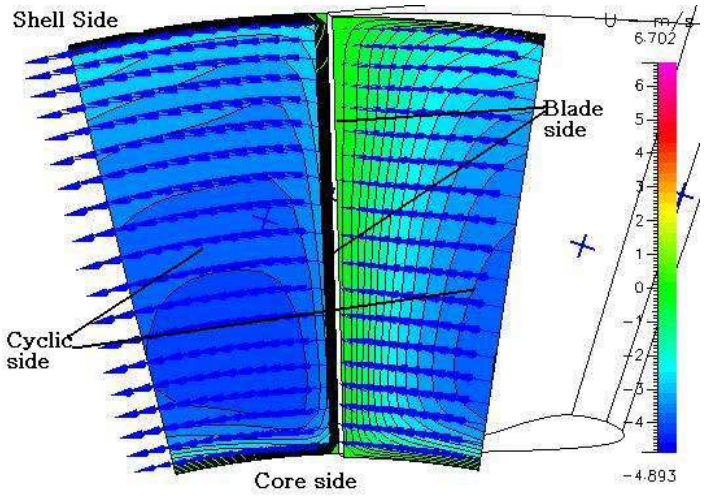

Figure 24: Fluid flow in the stator outlet at 313K.

Flow at the outlet seems to have uniform through-flow. This result has been obtained according to the simulation for 313K at a pump speed of 1000 rpm and 0.6 speed ratio.

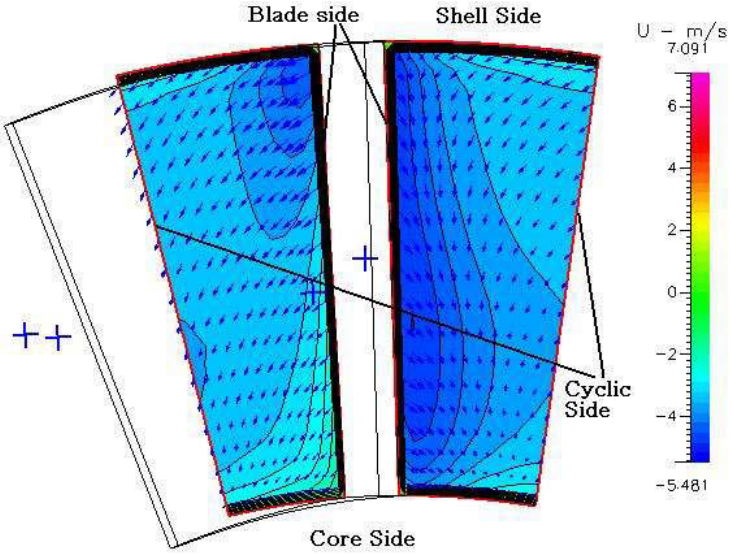

Figure 25: Fluid flow in the stator inlet at 373K.

The velocity vector plot with pressure contour indicates some directional deviation in the flow at the inlet, but there was no trace of circulating fluid.

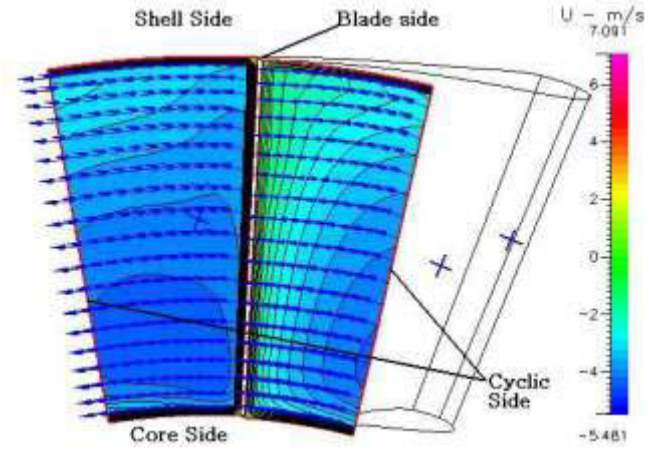

Figure 26: Fluid flow in the stator outlet at 373K.

The simulation at 373K for the pump speed of 1000 rpm and 600 rpm turbine speed indicates that the fluid flow at the stator outlet is quite uniform.

The difference between a fine converged result and an insufficient converged result can be presented as follows. In this thesis the degree of convergence is mentioned repeatedly. What is meant by a degree of convergence is that the value of the residuals in the residual plotter dropped down from 1.00E+00 to 1.00E-01 i.e. one degree of convergence; or 1.00E-00 to 1.00E-02 i.e. two degrees of convergence. what is being considered is a result as a fine converged

one, when it reaches at least four degree of convergence reflecting in the residual plotter, for all the parameters individually.

Different parameters converge at a different rate. So, in the residual plotter, all of them do not reach the same level of convergence at the same time. What is being considered here are the values of the same simulation as an insufficient converged result which was allowed to converge at a level of two degree of convergence only. what is being shown is a sample calculation to express the approximate result difference between the fine converged results and the insufficient converged results. The results were taken from identical simulation configuration. The only difference in the configuration was the change of number of iterations. Other than that, all the specifications of both the simulations were unchanged.

For this sampling, the idea was taken from a simulation where the pumps were rotating at 2350 rpm, and turbines were set at 0.6 speed ratio, i.e. 1410 rpm. The simulation was first run for 1000 iterations and necessary data was taken from the output of the simulation. Then the iteration under the solver control panel was changed from 1000 iterations to 50 iterations. Then the simulation ran for 50 iterations. The required data from the simulation output was then extracted. Out of the extracted data, calculation were done of the torque ratio and efficiency for 1000 iterations and 50 iterations separately. A distinction will be drawn between the fine converged results and the insufficient converged results using the following “Relative change” formula.

Relative change in percentage (U) $= | (U^{\Delta} - U^{*}) / U^{*} | \times 100$.

U = Relative change in value.

U^{Δ} = (Value for insufficient converged result).

U^{*} = Value for fine converged result.

To demonstrate the difference between a fine converged result and an insufficient converged result, a sample of the relative change in result will be presented. For this sampling we have chosen data from above mentioned simulation.

For the fine converged result, torque ratio was found to be 1.2298 and efficiency was 73.7897%; and for the insufficient converged result, torque ratio was found 1.1871 and efficiency was 71.2240%. According to the relative change formula, for torque ratio the results are:

Relative change of torque ratio (in percentage) = | (1.1871 – 1.2298) / 1.2298 | × 100

= 5.25 %.

And Relative change of efficiency (in percentage) = | (71.2240-73.7897)/ 73.7897 | × 100

= 3.48 %

It reflects that the insufficient converged result differs from the fine converged result by 3.48% to 5.25% approximately. In relation to this sampling, it can be said that the data mentioned in this thesis from insufficient converged results are significant. It is just that four or more degree of convergence will provide better result. The above comparison reflects that the difference between them will not cause a high variation in the result.

The difference between this work and the work of Shin, Chang, Athavale (1999) was very little. This validated the simulation results of this study against an existing research. two papers have been accepted and published in two different conferences. IMECE2011-65078: Effects of Number of Stator Blades on the Performance of a Torque Converter was published in the ASME conference 2011 and Numerical Study of Performance of a Torque Converter Employing a Power-Law Fluid was published in the 18th Australasian Fluid Mechanics Conference (AFMC) 2012.

4.2 Effect of a different number of stator blades on the Torque Converter's performance.

A number of test simulations were run for a torque converter with different stator blade numbers. These simulations were undertaken in order to examine the change of the performance with the change of the number of the stator blades; turbine and pump blade numbers were retained at 31 and 29 respectively. The stator blade numbers were changed from 16 blades to 13, 18 and 19 blades.

For this test, the geometry of the torque converter was re-shaped as the number of blades was changed, but the angle of the stator inlet and outlet were kept the same. Pump blades and turbine blades construction were untouched during this remodelling. This would change the effective flow area through the stator and would provide change in guidance to the flow, which would have an influence on the efficiency.

4.2.1 Geometric construction procedure for changing the stator blade number.

The following demonstrates the construction procedure for changing the stator blade number from 16 to 13 without changing the blade shape. For better visibility and for avoiding complexity, pump and turbine parts were blanked during the re-construction.

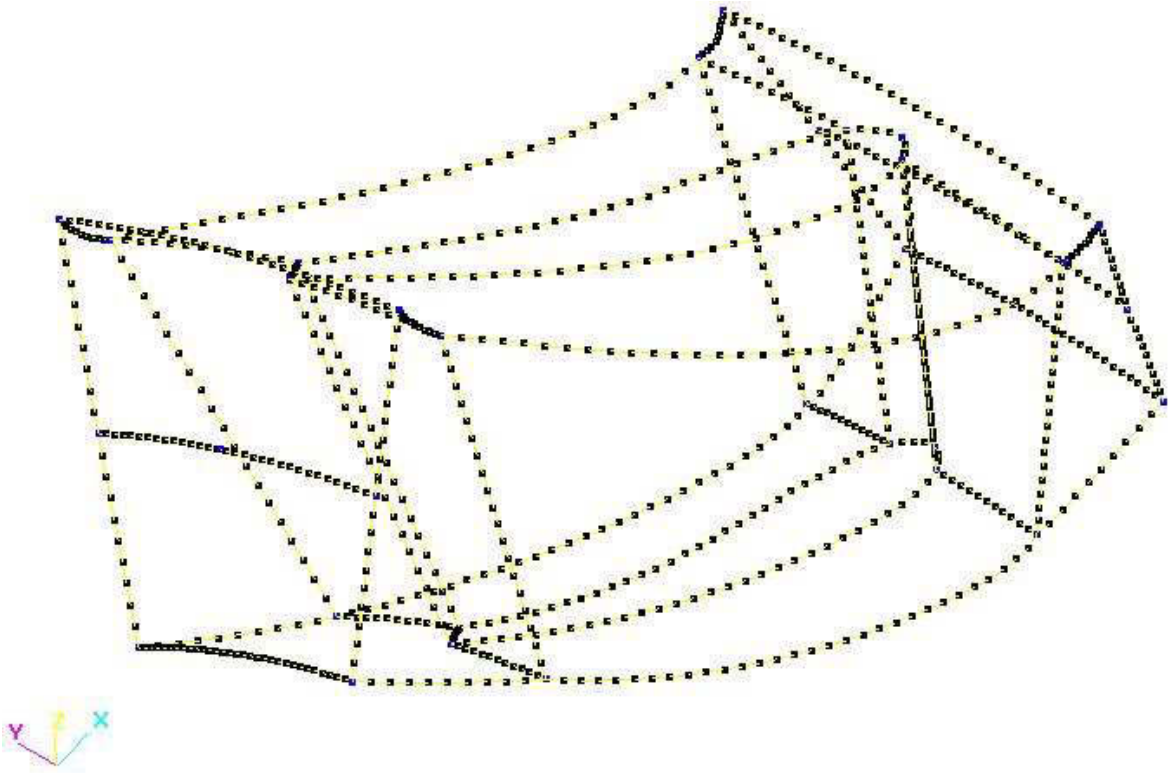

Figure 27 : Stator blade without face and block.

First the blocks for the stator were deleted followed by the deletion of the faces of the stator. One side of the stator channel along with the upstream and down stream mixing planes were then re-faced using the face creation option in the CFD─-GEOM. The face creation option under the grid tab was turned on, and the desired grid was selected with the left mouse click and activated for face creation by clicking the middle mouse button. Following this procedure all the faces were created. Figure 27 shows the stator channel after one side face creation.

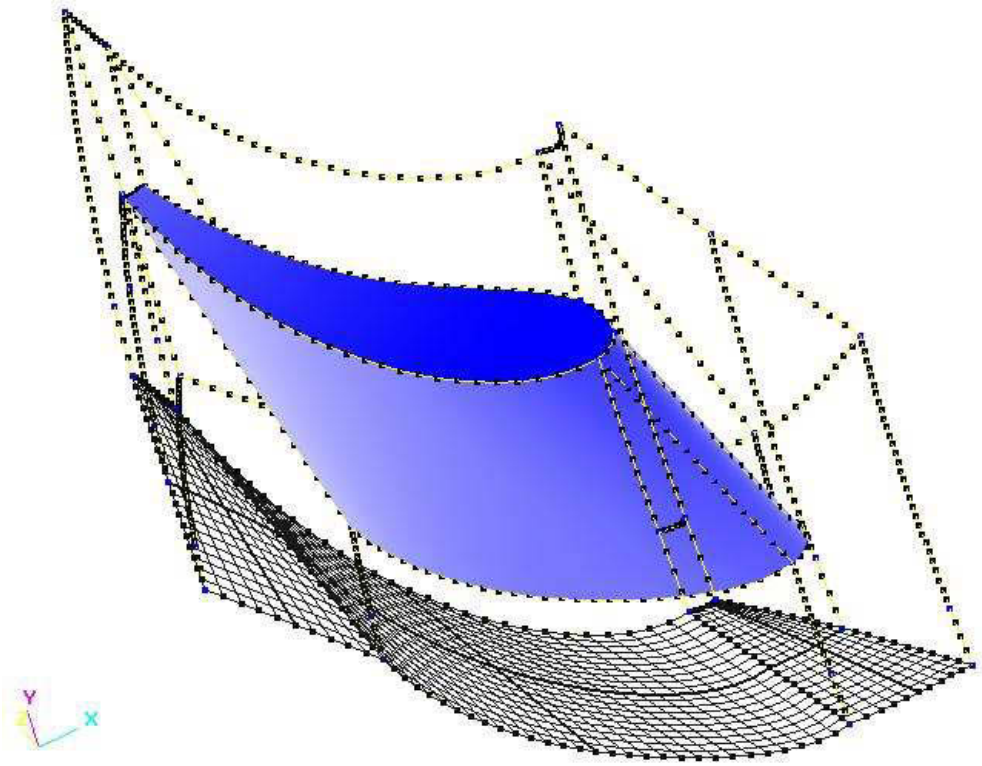

Figure 28 : Stator channel with shaded stator blade and face formed in one side of the channel.

Two sides of the channel have to be rotationally symmetric. For that panning was used to create the sides using the rotation tool. While re-structuring the channel from 16 stator blade to 13 stator blades, the channel will get bigger. The stator has been designed consisting of 16 stator blades which segregate the 360 degrees of a circle into 16 segments, resulting in 16 equal dimensions of channels. Each solitary channel of the stator spans an angle of 22.5 deg with respect to the centre. To produce a 13 blade stator, the angle will be 27.6923 deg. The difference is 5.1923 deg. In order to keep the stator blade in the middle of the channel, the extension in each side will be 2.5962 deg. In order to get the rotationally symmetric condition satisfied and keep the stator blade in the middle of the channel, the face with respect to “X” axis was rotated at 25.0961 deg.

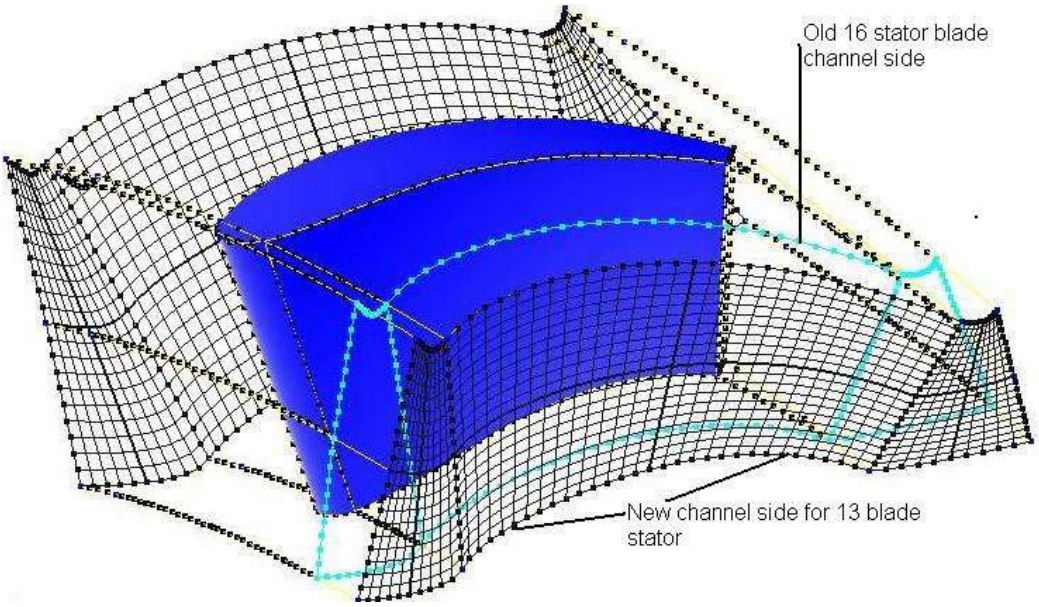

Figure 29 : 13─blade stator channel with one side extension.

Figure 28 shows the newly constructed channel side for 13 stator blade. The old 16 stator blade channel side was then deleted. Subsequently the same procedure was followed to get the other side of the channel for 13 stator blade. This time the new face was rotated, and the angle was 27.69 deg. The rotation was in the opposite direction. All the old faces were deleted and the new channel is shown in figure 30.

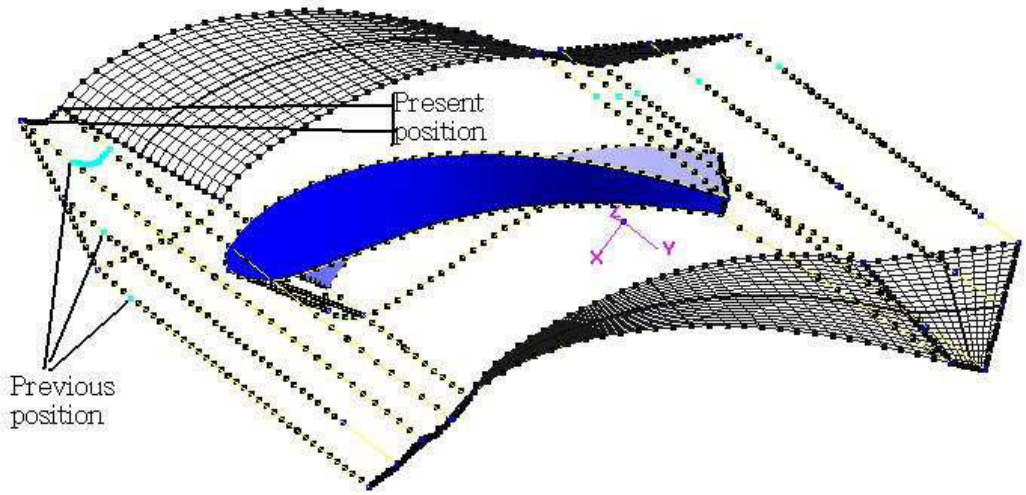

Figure 30 : 13─blade stator channel with the indication of increased dimension.

The grid for the channel was re structured, followed by the face creation and block creation, after the 13─blade channel formation. The reorientation of the

block was carried out at the end of the geometric structure creation. The virtual model for the 13─blade stator, visualising the position of the experimental channel setup in between the blades, is shown in figure 31:

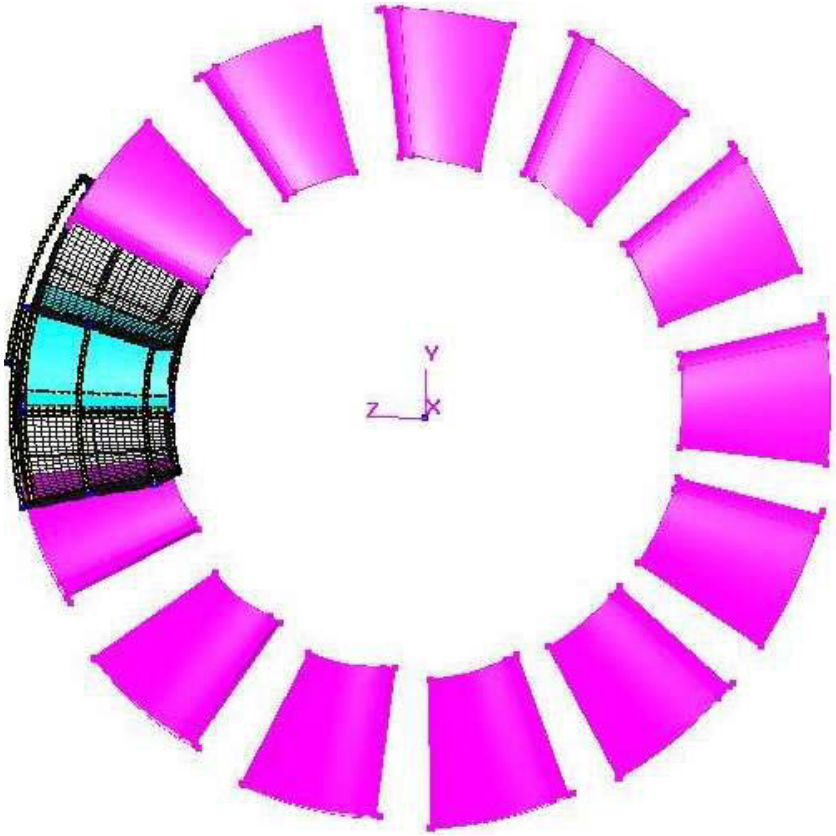

Figure 31 : Stator with 13 blades.

After the geometric construction, the file was ready for simulation and was saved as NAME.DTF file. The axis.dat file for the simulation was also stored in the same folder. After all the necessary data input the file was placed for simulation. Simulation results are provided in the following.

4.2.2 Performance comparison with the change of numbers of stator blades.

The tests were performed with a grid number 43×21×22 for the stator, and the remaining parts were kept as 38×21×22. The speed of the pump was set to 1000 rpm, and the turbine speed was changed to different speed ratios for different simulations.

Even if the value in the residual plotter did not drop significantly, the simulation didn't diverge. The highest residual drop was 1.0E-08 but the lowest drop was 1.0E-02. Generally a drop of 1.0E-03 or 1.0E-04 or more for the variables, indicates a good convergence. However as the simulation didn't diverge, it was considered to be a working torque converter. This would not, however, provide a very good result for fluid flow characteristics.

The performances of the torque converter with 13, 18 and 19 blades in the stator were compared with the performance of the torque converter with 16 blades at the same fluid temperature and at the same rpm.

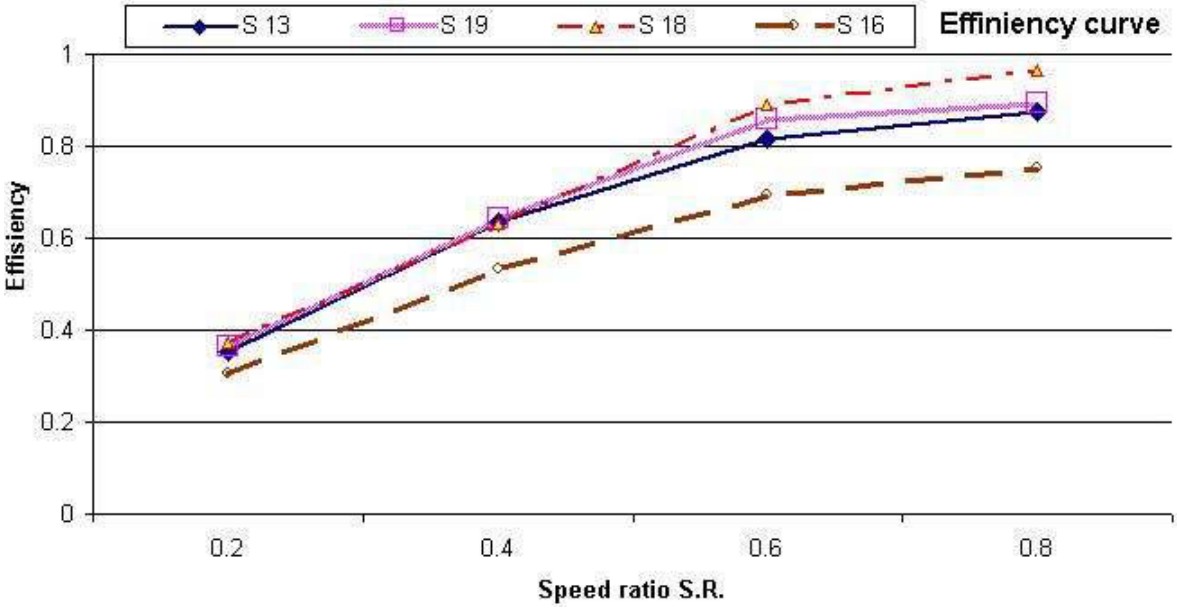

Figure 32: Efficiency comparison between the torque converters with 13, 18, 19 and 16 stator blades.

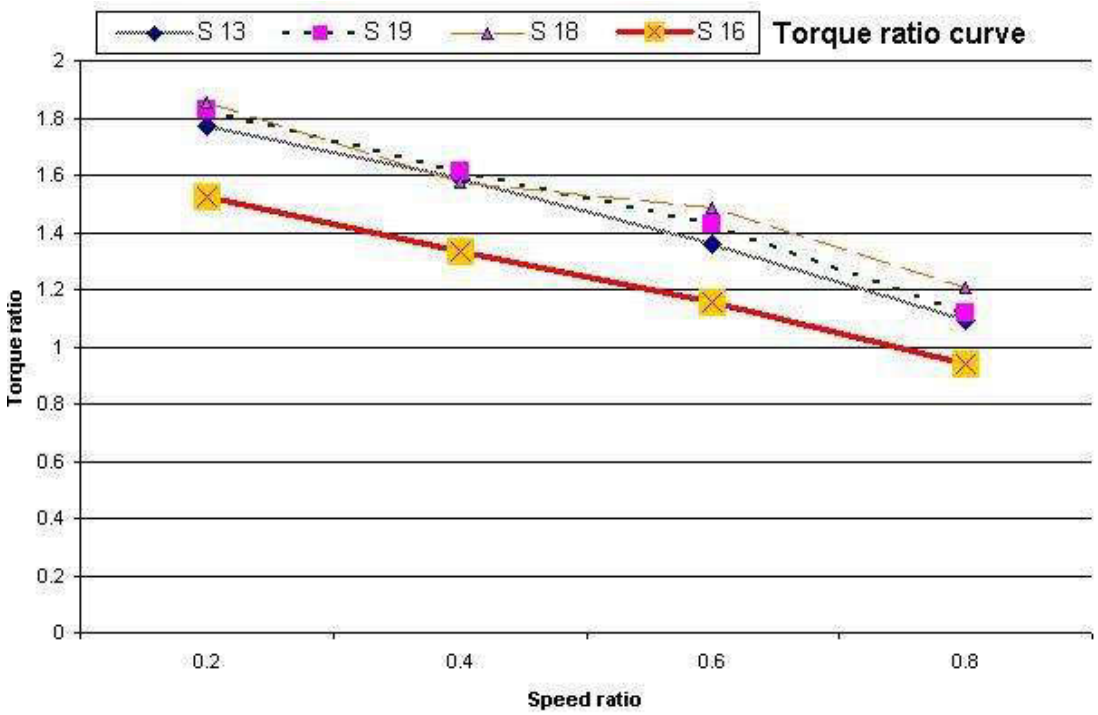

Figure 33: Torque Ratio comparison between the Torque Converters with 13, 18, 19 and 16 stator blades.

In the efficiency chart, the characteristic of the efficiency curves for the 13, 18, and 19-blade stator demonstrates a similarity in pattern with the 16-blade stator efficiency curve. Even in the speed ratio vs. torque ratio graph they showed similarity to each other with regard to the 16-stator blade, speed ratio. These indicate that the simulation was being performed correctly. However as it did not fulfil the criterion of a good converged simulation, It cannot be considered to be a perfect result.

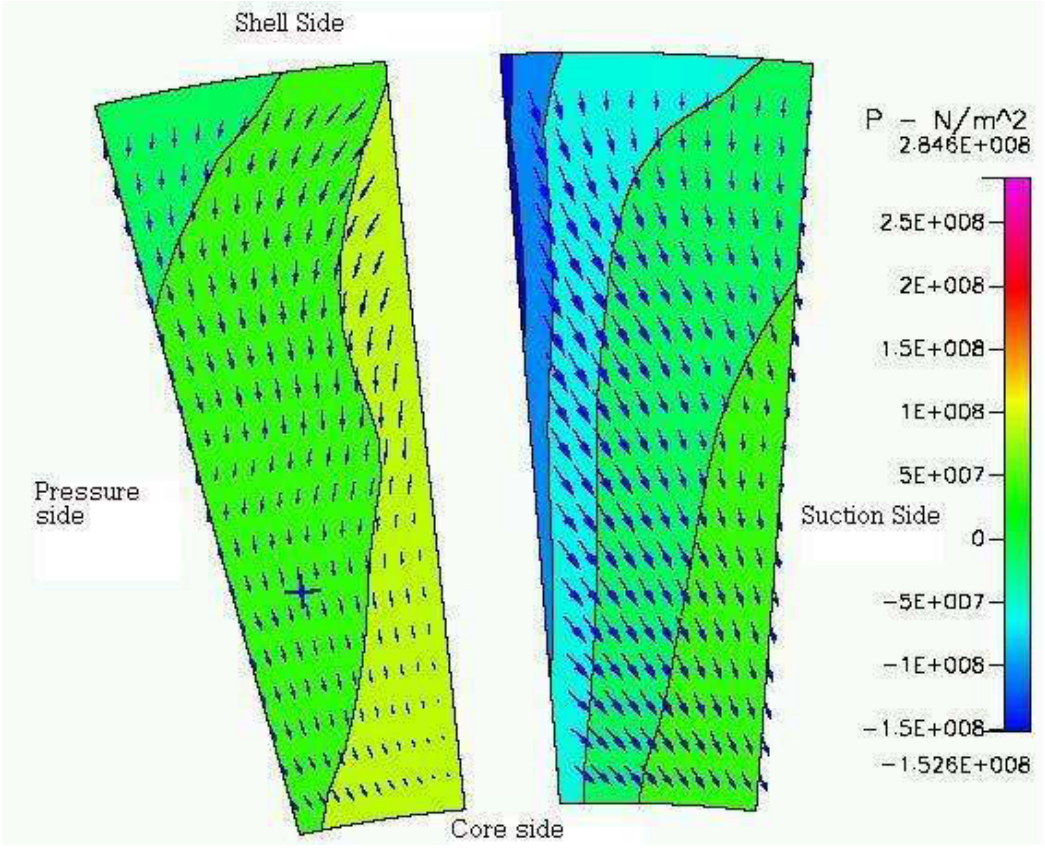

Figure 34 : Axial flow at the 19─blade stator inlet at 0.2 speed ratio with 1000 rpm pump speed.

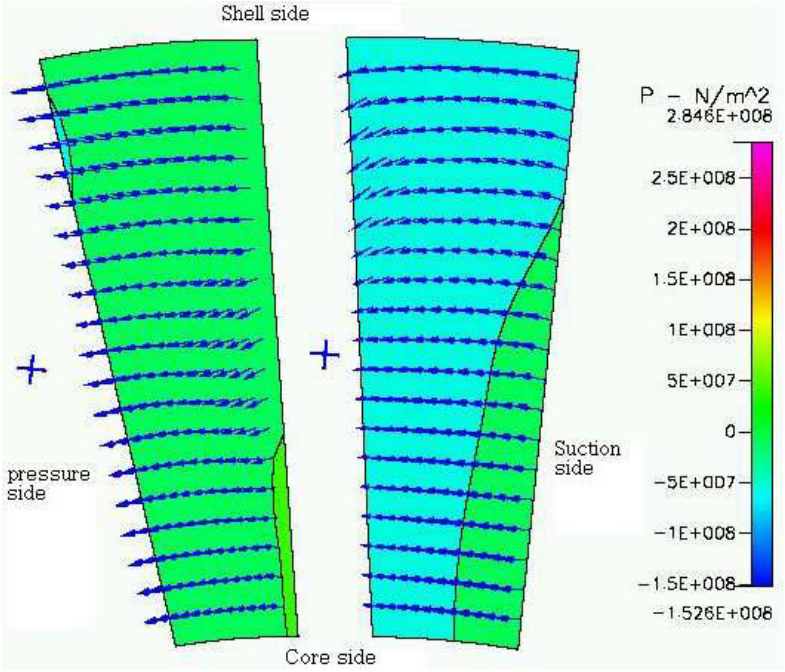

Figure 35 : Axial flow at the mid─plane of the 19─blade stator at 0.2 speed ratio with 1000 rpm pump speed.

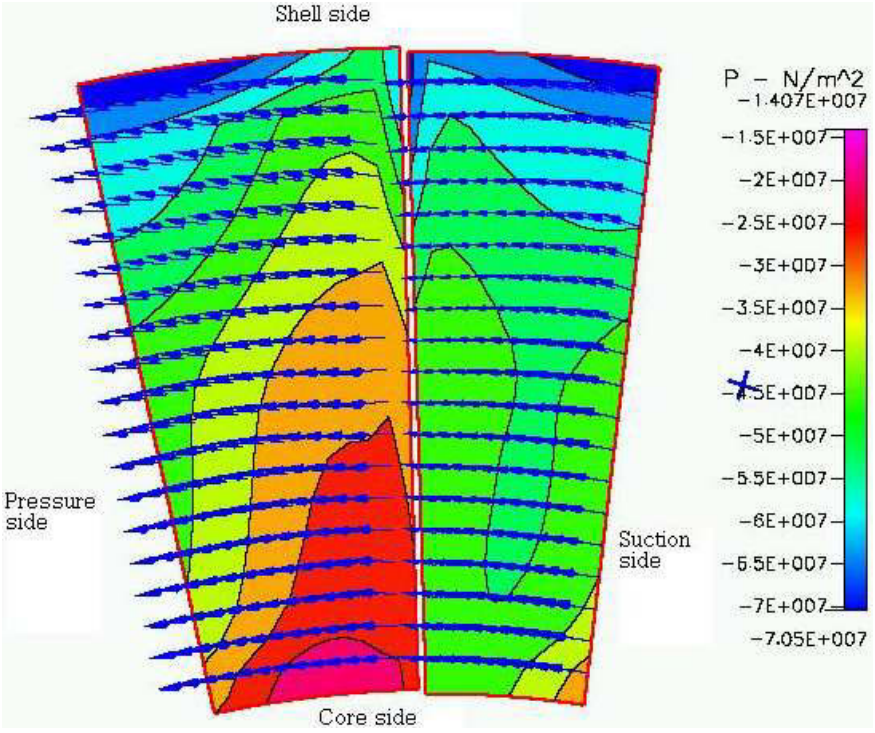

Figure 36 : Axial flow at the outlet of the 19─blade stator at 0.2 speed ratio with 1000 rpm pump speed.

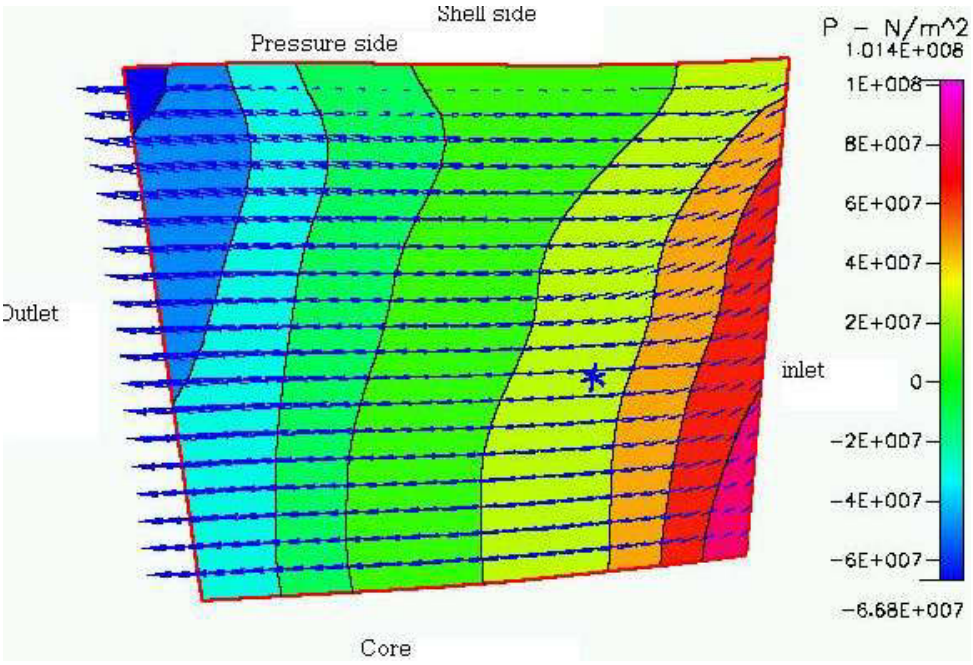

Figure 37 : Axial flow plotted with pressure contour at the pressure side of the 19─blade stator for 1000 rpm pump speed at 0.2 speed ratio.

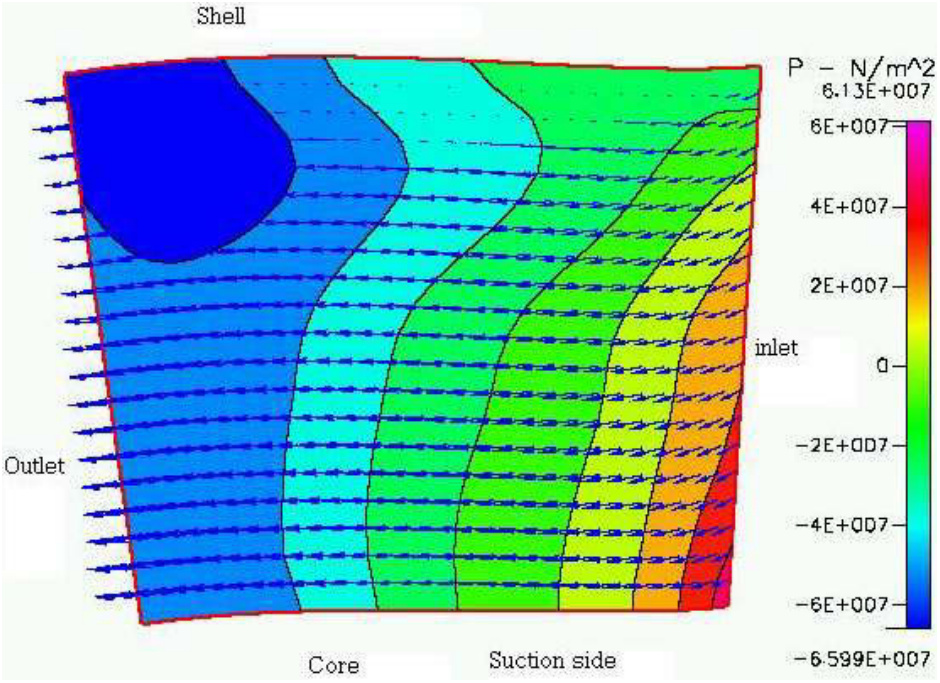

Figure 38 : Axial flow plotted with pressure contour at the suction side of the 19─blade stator for 1000 rpm pump speed at 0.2 speed ratio.

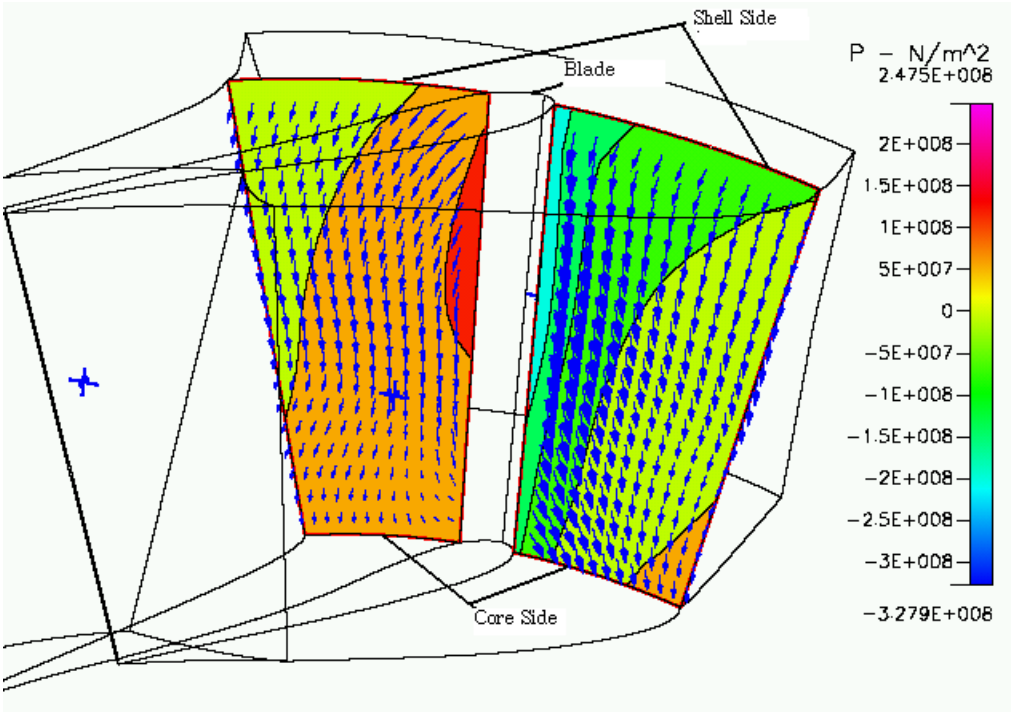

Figure 39 : Axial flow at the 13─blade stator inlet at 0.2 speed ratio with 1000 rpm pump speed.

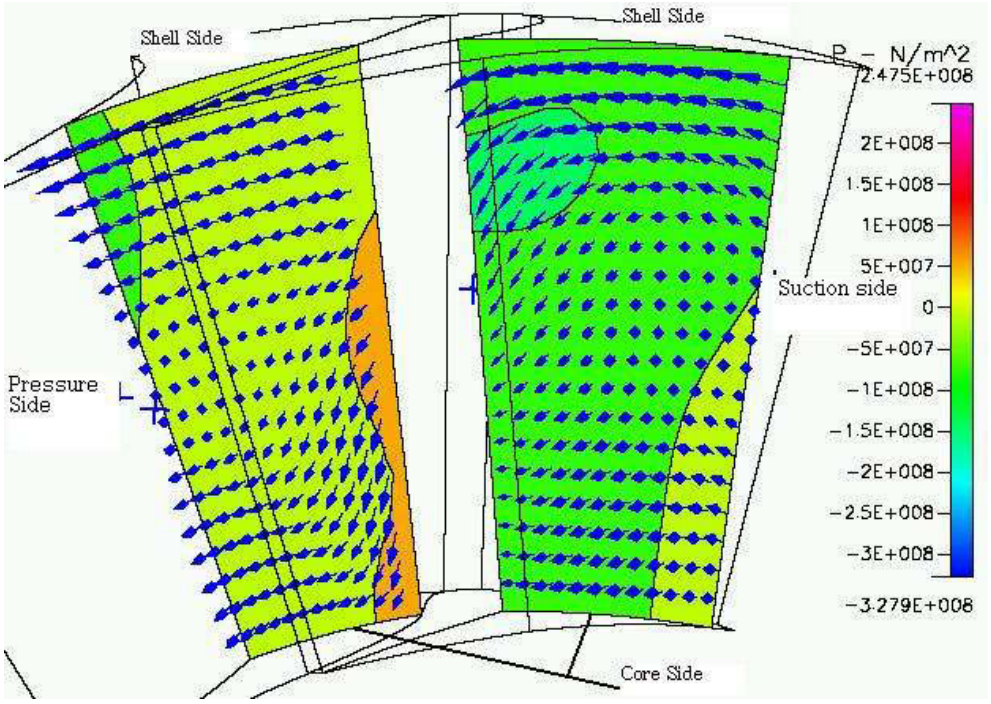

Figure 40 : Axial flow at the mid─plane of the 13─blade stator at 0.2 speed ratio with 1000 rpm pump speed.

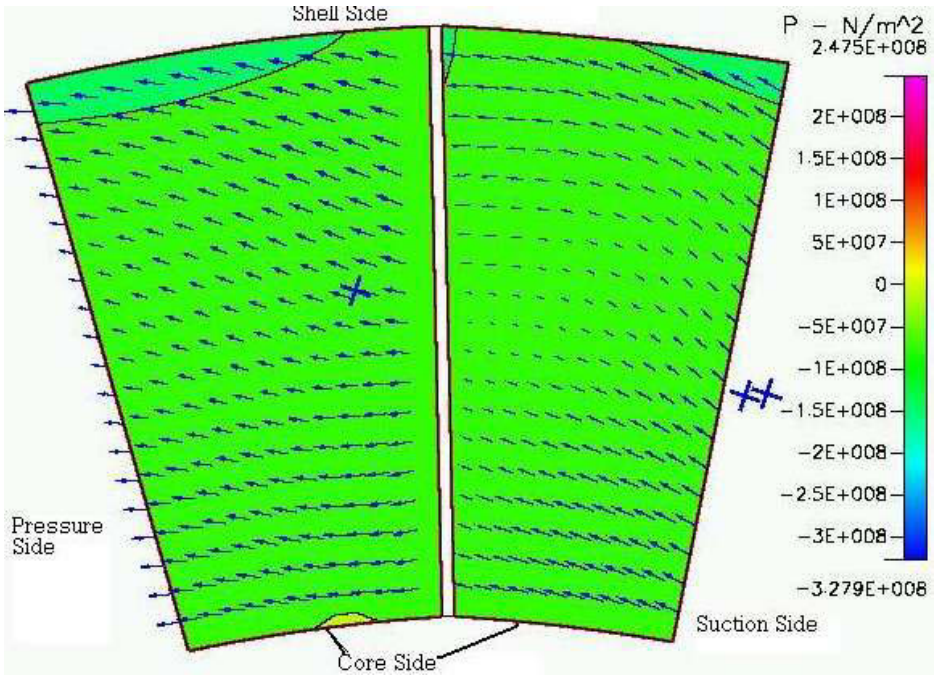

Figure 41 : Axial flow at the outlet of the 13─blade stator at 0.2 speed ratio with 1000 rpm pump speed.

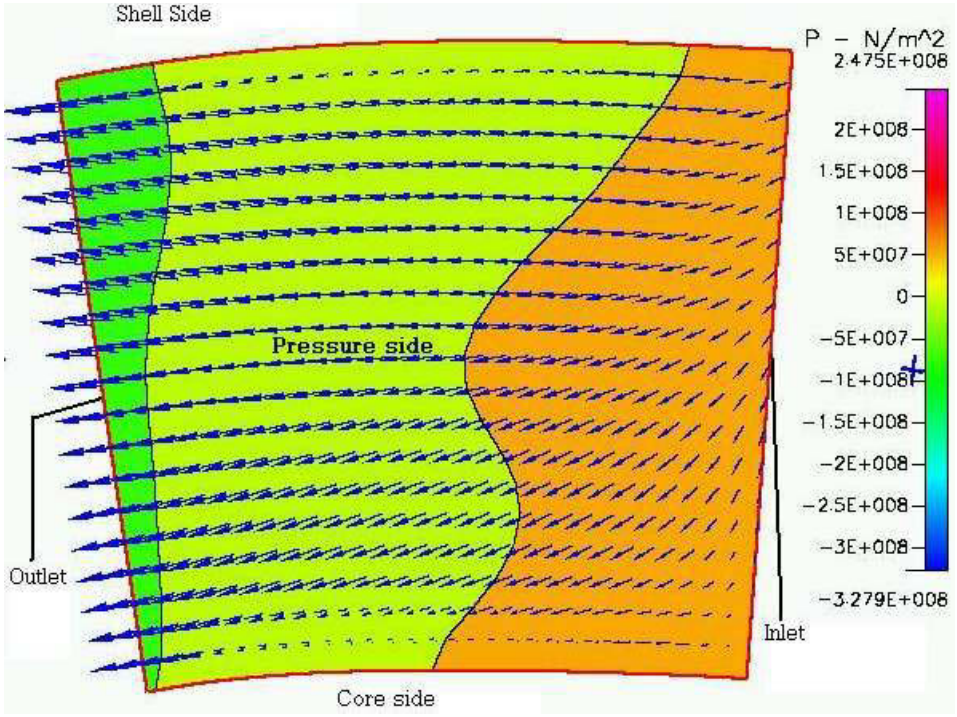

Figure 42 : Axial flow plotted with pressure contour at the pressure side of the blade, of the 13─blade stator for 1000 rpm pump speed at 0.2 speed ratio.

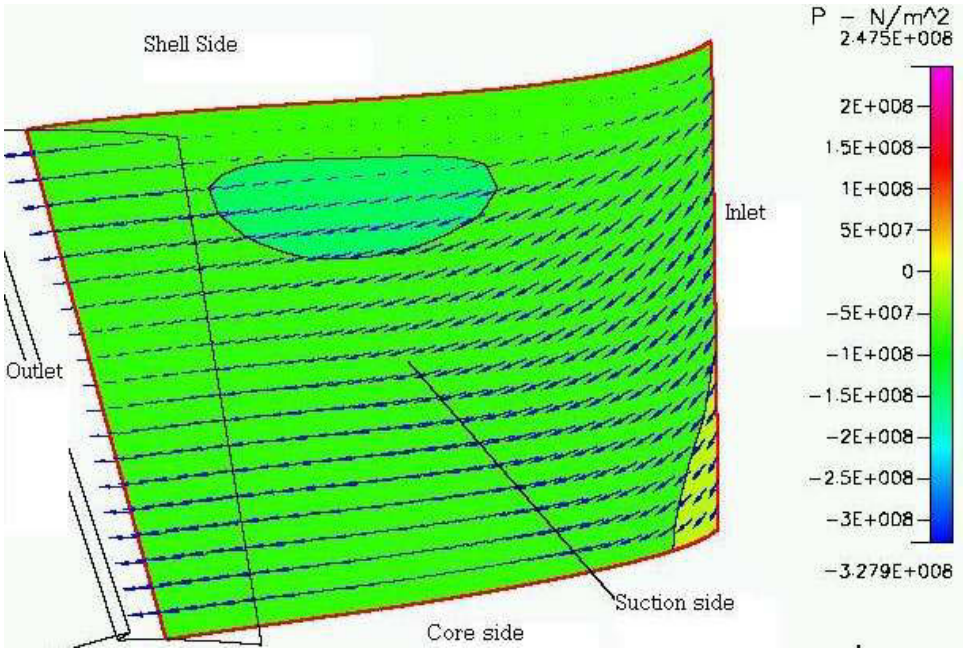

Figure 43 : Axial flow plotted with pressure contour at the suction side of the blade, of the 13─blade stator for 1000 rpm pump speed at 0.2 speed ratio.

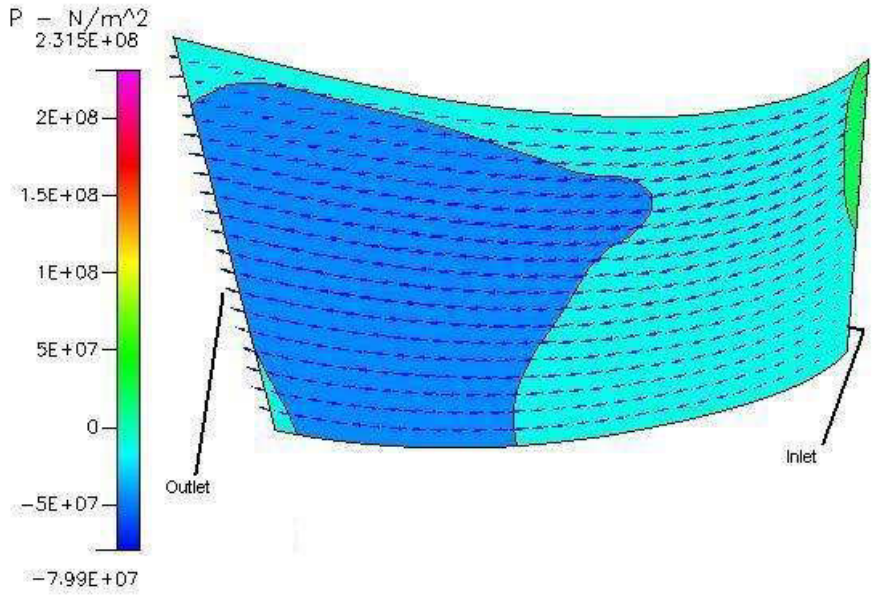

Figure 44: Pressure contour with axial flow, very close to the suction side of the 18─blade stator wall for 1000 rpm pump speed at 0.2 speed ratio.

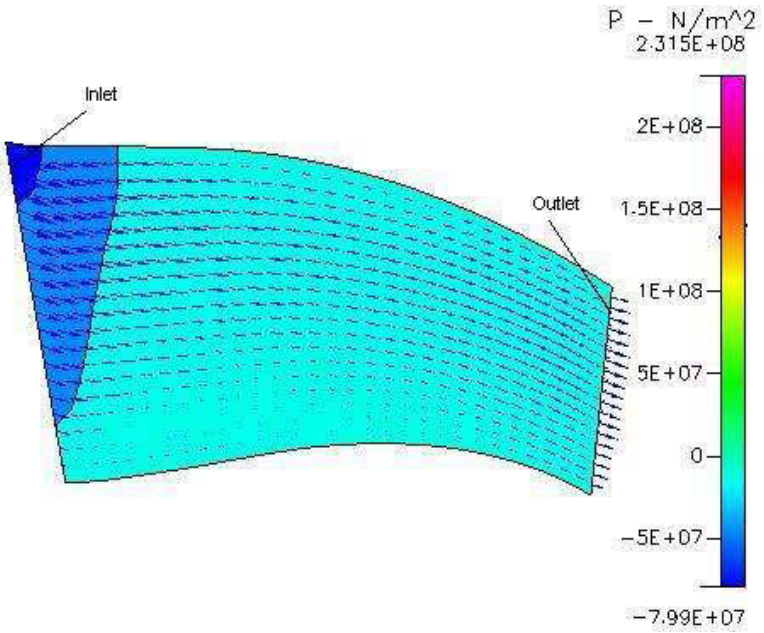

Figure 45 : Pressure contour with axial flow, very close to the pressure side of the 18─blade stator wall for 1000 rpm pump speed at 0.2 speed ratio.

Figure 32 shows the efficiency comparison chart between the torque converters with 13, 18, 19 and 16─blade stators. Efficiency for all the number of blades shows a similar profile, with efficiency increasing with speed ratio. Although the solutions did not show full convergence, the similarity in shape increases confidence in the results. The efficiency for blade numbers 13, 18 and 19 was generally around 1.2 times that for the original blade number 16, with the best improvement being for 18 blades, by a factor of 1.29 at 0.6 speed ratio factor and a factor of 1.26 at 0.8 speed ratios. At 0.8 speed ratio, the efficiency reached a very high 96% compared to 76% for 16 blades. This is a very significant improvement, especially as it at the high speed ratios that the torque converter normally operates, but the doubt concerning convergence must be admitted and so further corroboration is needed. There is also no obvious trend in the efficiency with blade number.

Figure 33 indicates the torque ratio comparison chart between the 18, 19 and 13─stator blades. Except for a slight dip in the 18 blade stator performance at 0.4 speed ratio, all of them showed the same pattern of behaviour, with torque ratio decreasing with speed ratio.

Figure 34 refers to the axial flow at the stator inlet for the 19─blade stator, simulated at 1000 rpm pump speed and 200 rpm turbine speed. Both the pressure side and suction side show the trace of flow mixing. Flow near the suction side of the blade is showing more deviation than near the pressure side.

Figure 35 shows the condition of the axial flow at the mid─plane of the stator. Flow near the stator blade suffers deviation. There is no sign of back flow visible at the mid─plane of the 19─blade stator for 1000 rpm pump speed at 0.2 speed ratio.

Figure 36 provides the axial flow at the outlet of the 19─blade stator for the same operating condition. The 19─blade stator exit shows smooth axial flow.

Figure 37 gives the pressure contour plot with axial flow for the 19─blade stator at 1000 rpm pump speed at 0.2 speed ratio, at the pressure side of the stator blade. The exit pressure of the stator is lower than the inlet pressure. At the inlet it shows some mixing of the flow but near the exit it shows smooth flow.

Figure 38 represents the suction side of the stator blade for the same operating condition of the 19─blade stator. Pressure contour was plotted against axial flow of the stator. The inlet shows some flow mixing but other than that everywhere shows smooth flow. There was no trace of back flow found.
Figure 39 stands for the axial flow at inlet for the 13─blade stator. The operating condition is 1000 rpm for the pump and 200 rpm for the turbine. The inlet indicates a mixing of the flow at the stator inlet.

Figure 40 represents the axial flow at the mid─plane of the 13─blade stator for 1000 rpm pump speed with 0.2 speed ratio. It demonstrates a strong mixing of flow at the middle of the channel. The mixing occurs near the blade side. For the pressure side, mixing occurs near the core side. For the suction side mixing of flow is strong near the shell side. The suction side shows comparatively lower pressure than that of pressure side. There was no sign of circulatory flow found. Back flow was also not visible in the representation.

Figure 41 is the picture of the exit of the 13─blade stator for the same operating condition. The mixing of flow still exists at the outlet. The shell side of the stator is showing the most mixing activities. There was no trace of circulatory flow observed at the outlet.

Figure 42 refers to the pressure side of the stator blade, of 13─blade stator. It was under the operating condition of 1000 rpm at 0.2 speed ratio. The pressure side of the stator blade shows flow deviation and mixing of flow at the inlet. For the pressure side, at the inlet and mid─plane, the mixing of flow near the core side is stronger than the shell side. However for the exit of the stator, the shell side is showing more noticeable mixing activities than the core side.

Figure 43 shows the axial flow plotted with pressure contour at the suction side of the 13─blade stator for the same operating condition. The inlet shows the mixing of flow stronger than the mid─plane and outlet. There was no sign of circulatory flow visible in this figure.
Figure 44 represents the pressure contour plotting with axial flow at the suction side of the 18─blade stator, at 0.2 speed ratio with pump speed of 1000 rpm. The pressure contour shows reasonably higher pressure at the stator inlet than at the exit at the suction side. The direction of the flow does not refer to any back flow or secondary flow at the stator.

Figure 45 shows the pressure side of the 18─blade stator at the same operating condition. At the inlet it shows some mixing of flow which is normal. However at the exit it does not refer to any mixing of flow or any circulatory flow.

According to the simulation result, the torque converter with 18 blades shows the best performance, subsequently followed by the 19, 13 and 16─blade stator, according to the efficiency and torque ratio graph mentioned above. The maximum drop of the residual plotter was 1.0E-08 but the minimum drop was 1.0E-02. Normally a drop of 1.0E-03 or 1.0E-04 or more for the other variables, indicates a fine convergence. However as the simulation did not diverge, the results can be considered to represent the complex three-dimensional flow, inside the torque converter. CFD is shown to be a useful method to use in experimenting with the performance of the torque converter for different blade numbers of the pump, turbine and stator. A wider range of studies is needed, with higher grid numbers in the structure.

4.3 Performance Investigation of a Torque Converter Using Non-Newtonian Fluids

With regard to viscosity, CFD─ ACE+ provides simulation for two types of fluids, Newtonian and Non-Newtonian. This section reports on the flow behaviour in the torque converter using Non-Newtonian fluids.

For a Newtonian fluid the viscosity is constant or, at most, temperature dependent, unaffected by shear stress. Thus the shearing stress is linearly related to the shearing strain (www.EngineeringToolBox.com).

Non-Newtonian fluids are categorised as purely viscous fluid and viscoelastic fluid. The purely viscous fluids are of two types, time dependent and time independent. this study investigated only shear thinning (Pseudoplastic) fluid and shear thickening (Dilatant) fluid under the time independent fluid section (The hand book of fluid dynamics, Edited by Richard W. Johnson; Chapter-22).The option for the fluid viscosity chosen from the volume condition control panel of the CFD─-ACE-GUI solver was 'power law' and the equation for that was:

$$\mu = K\mu_0 e^{(a_1 T - a_2 T^2)} [max(\dot{\gamma}, \dot{\gamma}_0)]^c$$

Where:

c= $n - 1 + a_3 \ln(\dot{\gamma}) + a_4 T$

μ_0 is the zero shear rate viscosity (kg/m-s)

n is the power law index

T is the local calculated temperature (k)

$\dot{\gamma}$ is the local calculated shear rate

$\dot{\gamma}_0$ is the cut-off shear rate

K, a_1, a_2, a_3, a_4 are fluid properties

(CFD user manual)

In this equation, the power law index determined whether the fluid would be shear thinning (Pseudoplastic) fluid or shear thickening (Dilatant) fluid. When $n>1$ then the fluid was shear thickening (Dilatant) fluid and when $n<1$, then it meant shear thinning (Pseudoplastic) fluid. When the value for $n=1$, then it is Newtonian fluid.

Both the shear thinning and shear thickening fluids were tried, in order to compare their flow pattern at both 313K and 373K and to compare the effect of each of them on the torque converter's performance. For the required fluid properties data, This study chose an automatic transmission oil called "Petromin Automatic transmission Fluid Dexron-III" as a trial. The product code for that particular oil was 3310. The simulation was performed at a pump speed of 1000 rpm, with speed ratios 0.2, 0.4, 0.6 and 0.8.

The findings of this part of the research was published in the 18th Australasian Fluid Mechanics Conference (AFMC) 2012. "Numerical Study of Performance of a Torque Converter Employing a Power-Law Fluid".

The simulation at speed ratio 0.2 was performed for power law index n= 0.5, 0.6, 0.7, 0.8, 0.9, 1.1, 1.2, 1.3, 1.4 and 1.5. At the speed ratio 0.4, 0.6, 0.8 this simulation has only been performed for n=0.5, 0.6, 0.7, 0.8 and 0.9. However, both of them were included in the same graph, so that a comparison could be made both of them from n=0.5 to n=0.9 at a glance and for n=1.1 to n=1.5 the behaviour of the torque converter could be observed for the change of power law index for a certain speed ratio.

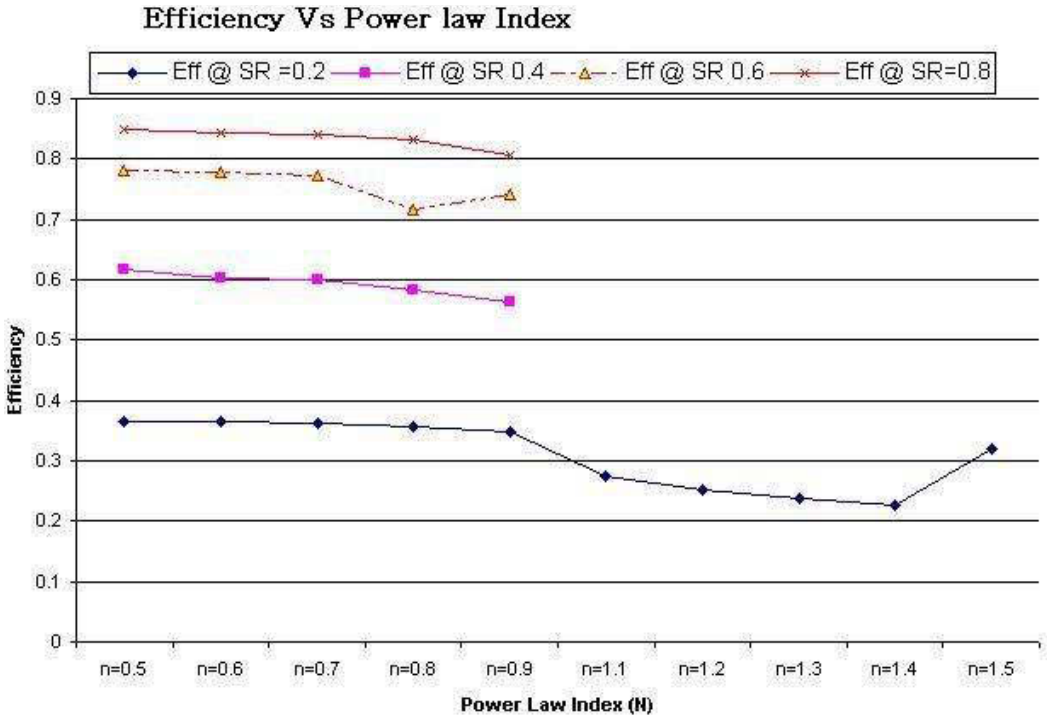

Figure 46: Turbine efficiency vs. power law index graph at 313K temperature.

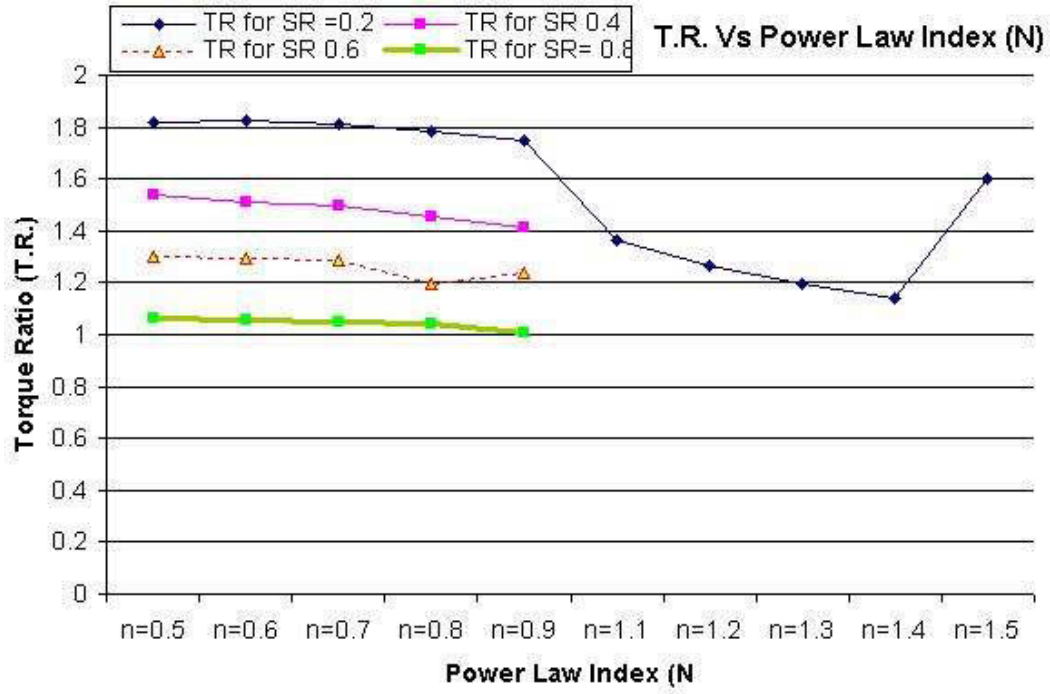

Figure 47: Turbine torque ratio vs. power law index graph at 313K temperature.

According to the graph shown above, almost all the speed ratios acted similarly except for S.R. =0.6. There could be some error for N=0.8 for S.R. =0.6 in particular. It seemed that the torque ratios, as well as the efficiency, decreased as the fluid moved from shear thinning to Newtonian fluid. For a speed ratio 0.2, the shear thickening fluid seemed to lose very little of its torque ratio and efficiency, as it approached Newtonian fluid. The efficiency and torque ratio suddenly dropped as it became shear thickening fluid from Newtonian fluid. This dilatant fluid suddenly recovered and crossed the torque ratio and efficiency of Newtonian fluid at N=1.5. Previous studies showed that for 1000 rpm pump speed at 0.2 speed ratio, Newtonian fluid demonstrated a torque ratio of 1.52 and efficiency of about 30%. Dilatant fluid at N=1.5 showed a torque ratio of 1.602 and efficiency 32.05% for 1000 rpm pump speed at 0.2 speed ratio.

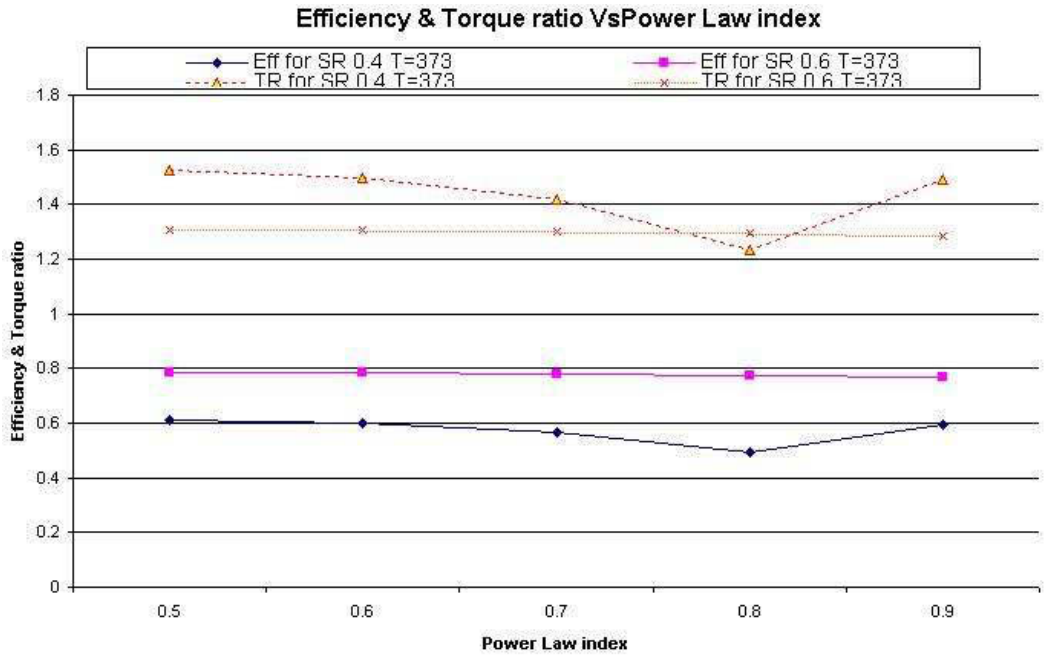

Figure 48: Turbine efficiency & torque ratio vs. power law index graph at 373K temperature.

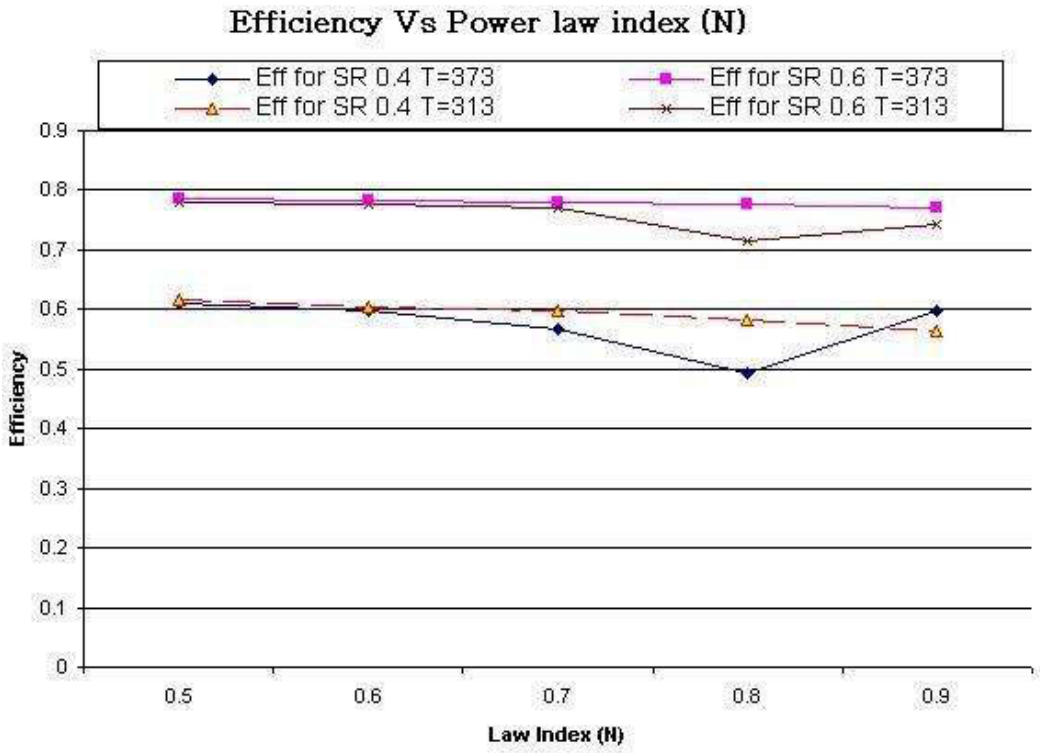

Figure 49: Efficiency curve comparison for temperature 313K and 373K.

The tested temperature seems to have very little effect on the torque ratio and efficiency of the torque converter. Except for the power law index 0.8, all of them behaved in almost the same way with a very minor difference in efficiency at power law index 0.9. The result for the power law index 0.8 is not well founded and behaved unusually compared to the other data in the same chart. But the efficiency data for the rest of the power law index (0.5, 0.6, 0.7 & 0.9) shows similarity in their pattern. So the data for power law index 0.8 is not taken under evaluation. The abovementioned chart for speed ratio 0.6 shows that, the efficiency increases when the temperature increases from 313 K to 373 K. However for the speed ratio 0.4, the efficiency does not increase until it reaches power law index 0.9.

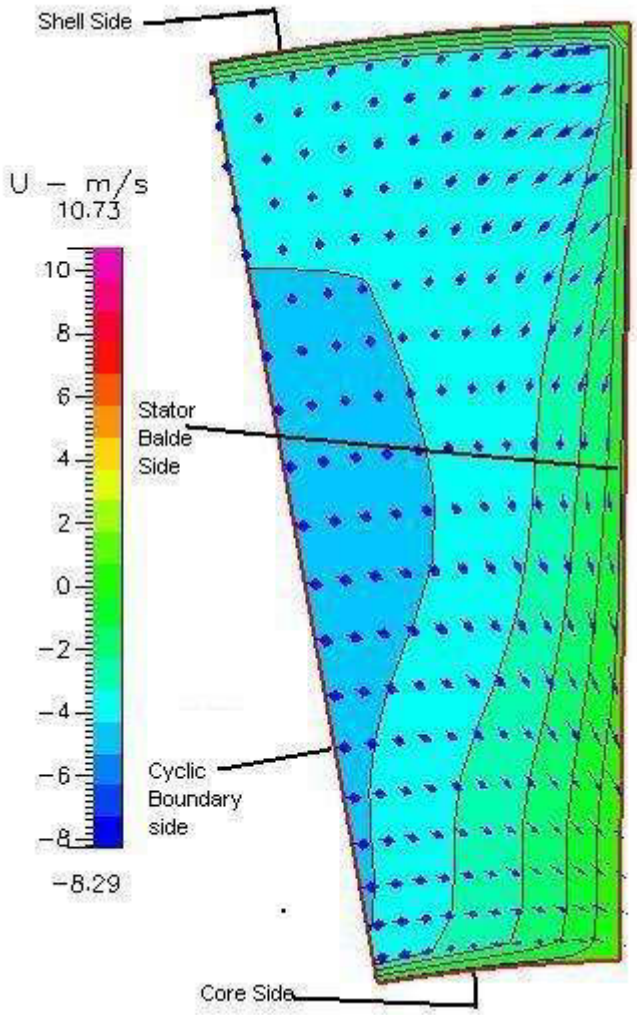

A slight deviation in the flow was observed in the inlet of the stator near the pressure side wall. This picture was taken at the inlet of the stator. The simulation was performed for pump speed 1000 at speed ratio 0.2 at temperature 313K. The fluid used for the simulation was shear thinning (Pseudoplastic) fluid and the value for the power law index was 0.6.

Figure 50: Fluid flow in the pressure side at the inlet plane of the stator at 313K.

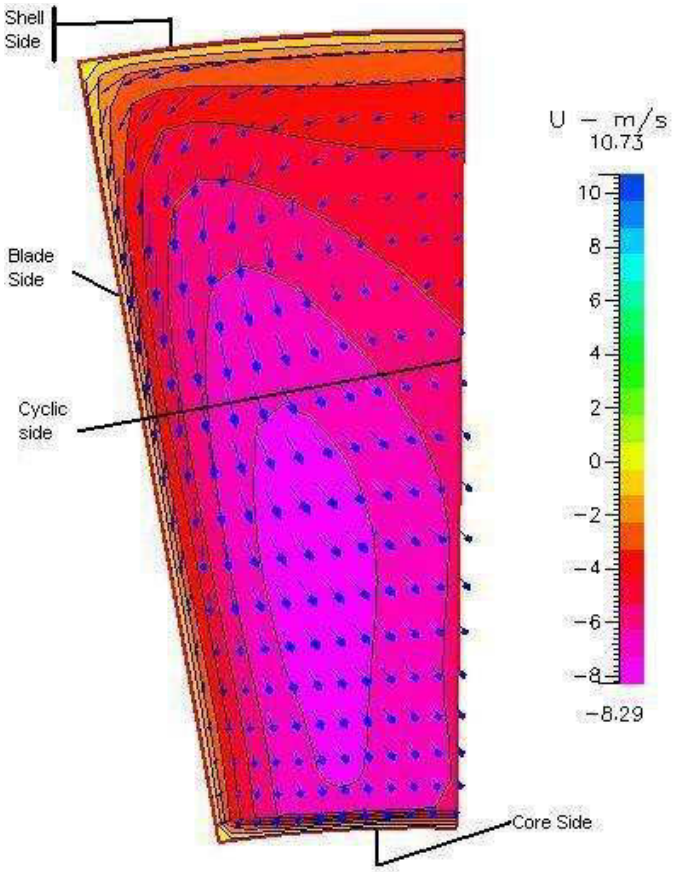

Figure 51: Flow in the suction side at the inlet plane of the stator at 313K.

The suction side flow for the same simulation seemed to have a higher variation than that of the pressure side at the inlet plane of the stator, as mentioned above. It took place near the stator blade wall. However, there was no circulating flow or any sign of flow separation observed in that particular simulation.

As the simulation was performed both at temperature 313K and 373K for the speed ratio 0.6 and power law index 0.6, it would be easier to compare the flow between them. For such a comparison the following figures are presented.

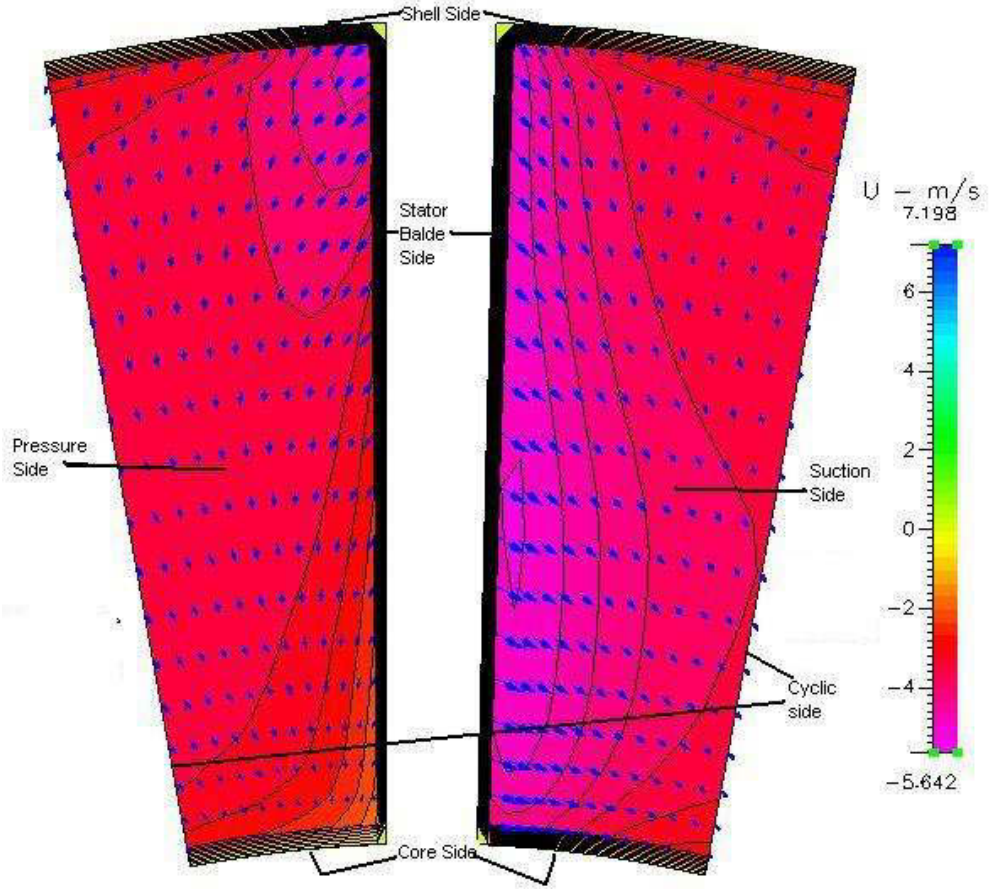

Figure 52: Velocity vectors with pressure contour in the pressure side and suction side at the inlet plane of the stator at 313K.

In the stator section of the torque converter, there was no back flow visible for the speed ratio 0.6 at pump speed 1000 and temperature 313k for n=0.6. In addition, no trace of circulating flow was found.

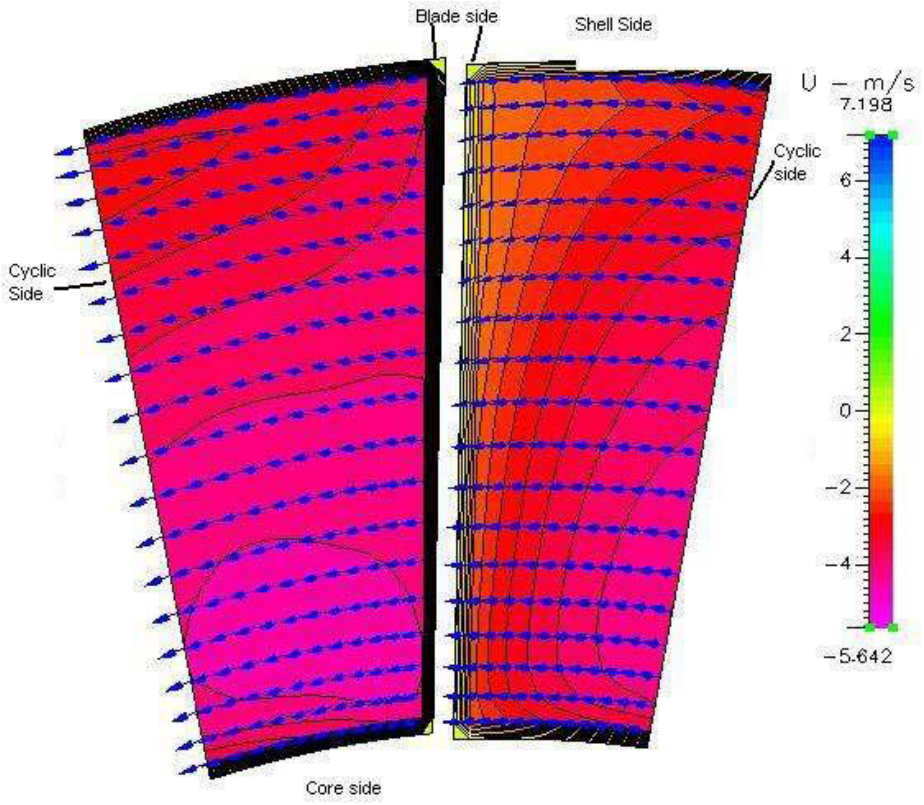

Figure 53: Fluid flow in the pressure side and suction side at the outlet plane of the stator at 313K.

No back flow was observed for this simulation with pump speed 1000 rpm at a speed ratio 0.6, with power law index value N=0.6, and at 313K of temperature at the outlet of the stator.

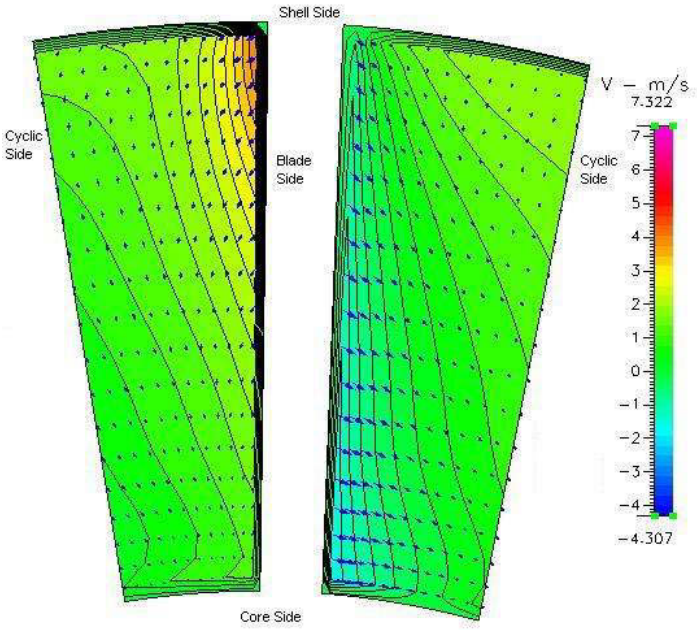

Figure 54: Fluid flow at the inlet of the stator for temperature 373K.

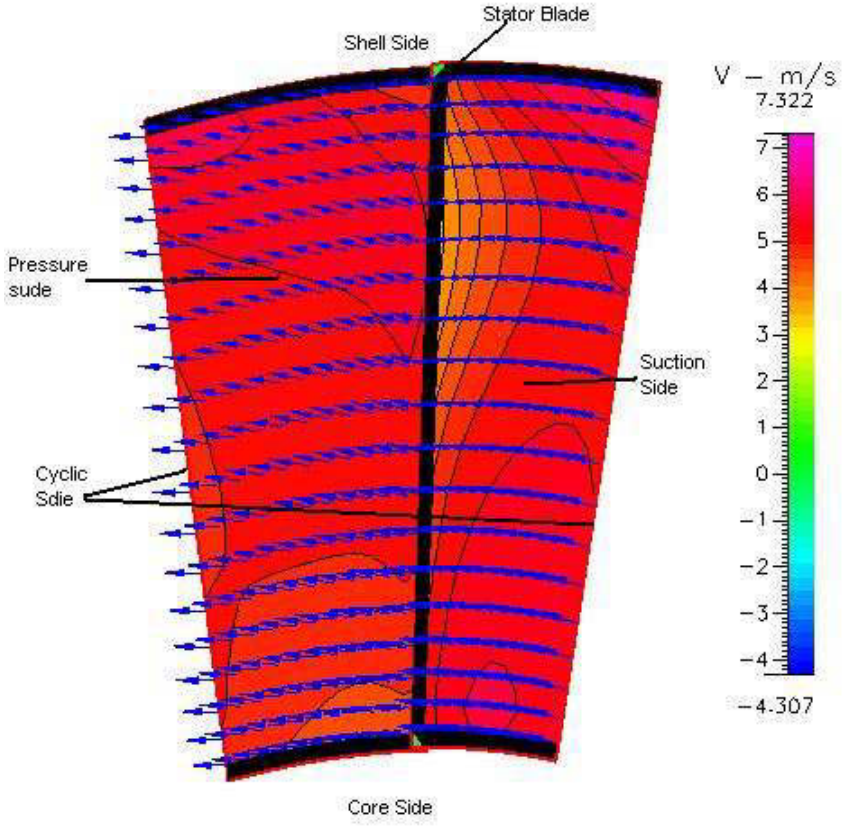

Figure 55: Fluid flow at the stator outlet for temperature 373K.

Both Figures 54 and 55 were taken from the simulation for pump speed 1000 at speed ratio 0.6, with power law index 0.6, and at temperature 373K. A very minor flow deviation was observed near the stator blade side at the inlet, and for the outlet the flow was fairly uniform.

A wider range of studies is needed to obtain a tangible assessment. However it showed a corridor for studying the effect of the Non-Newtonian fluid on the torque converter. According to this study the shear thickening fluid demonstrated lower efficiency than that of the shear thinning fluid for speed ratio 0.2 at a pump speed of 1000 rpm (figure 46). For the shear thinning fluid at the same pump speed, torque ratio and efficiency increases with the increase in the speed ratio (S.R.).

CHAPTER 5: CONCLUSIONS

Summary and Conclusions

The goal of this research was to investigate the fluid flow in a torque converter's stator using Computational Fluid Dynamics. The CFD─ACE software package of CFDRC and ESI group was used. Some technical difficulties with the software were encountered during the research. There was a bug in the software which did not allow the axis.dat to be operational. This external input file was very important and without this the mixing plane was not effective. This software problem affected the work of this study considerably over a substantial time period. It was eventually resolved when the software provider CFD Research Corporation supplied an updated version of the code, with this bug fixed.

The computer model used was very similar to the one which was used in Shin and Athavale's joint publication [SAE-1999-01-1056] and an attempt has been made to reproduce that paper's results. the results obtained were very close to their work. This validates the work in this study. During this research two papers in two different conferences have been published.

The research was conducted on the effect on the performance due to changing the torque converter's stator blade number. The findings of the research result were published in the ASME conference 2011. "IMECE2011-65078: Effects of Number of Stator Blades on the Performance of a Torque Converter".

The investigations were carried out with 43×21×22 mesh for the stator and the rest of the parts were kept unchanged as 38×21×22. The pump speed was kept at 1000 rpm, while the speed ratios were changed. According to the earlier mentioned efficiency comparison chart, between the torque converters with 13, 18, 19 and 16─blade stators obtained in this study, efficiency profiles for all the number of blades showed similarity in pattern. The results also demonstrated that the efficiency increased with speed ratio. For blade numbers 13, 18 and 19, the efficiency was generally around 1.2 times that of the original blade number 16. The results showed remarkable improvement of efficiency for 18 blades, by a factor of 1.29 at 0.6 speed ratio factor and a factor of 1.26 at 0.8 speed ratios. At 0.8 speed ratio, the torque converter showed a significant increase of efficiency. The efficiency climbed up to 96%, which is very high compared to 76% for 16 blades. This improvement was a very significant one. This improvement of efficiency was particularly significant as it occurred at the high speed ratio, higher than those the torque converter normally operates at. However the doubt regarding convergence has to be acknowledged and accordingly advanced verification is required. No apparent trend in the efficiency with blade number was observed.

the study observed fluid flow inside the stator, for different stator blade numbers. The trend of fluid flow inside the stator changed as the number of stator blades changed. The fluid flow inside the 18 blade stator channel showed most consistency while re-directing from the turbine exit to pump inlet, among all the 13, 16, 18 and 19 blade stator channel fluid flow. As the fluid flow inside the channel provided pressure moments and viscous moments to the blade, those moments played the central role in controlling the level of the efficiency. The data showed that the viscous moments were of very small magnitude compared to the pressure moments, in most of the cases. Consiquently it was possible that the adequate guidance of the flow could increase the performance of the stator and hence contribute to the efficiency significantly.

Even though the magnitude of the viscous moment was very small, it was not negligible. And too many blades may affect the performance due to an increase of frictional and viscous losses. This was possibly why the efficiency of the 19 stator blade torque converter decreased from the 18 blade stator blade torque converter.

The Numerical Study of Performance of a Torque Converter Employing a Power-Law Fluid was also performed. The tests were also performed with a grid number 43×21×22 for the stator, and the remaining parts were reserved as 38×21×22. The study was carried out at the speed ratio of 0.2 for power law index n= 0.5, 0.6, 0.7, 0.8, 0.9, 1.1, 1.2, 1.3, 1.4 and 1.5. At the speed ratio 0.4, 0.6, 0.8 the simulation was only performed for n=0.5, 0.6, 0.7, 0.8 and 0.9. Nevertheless, both of them were included in the same graph, so that both of them could be evaluated from n=0.5 to n=0.9 by a quick look and for n=1.1 to n=1.5 The behaviour of the torque converter could be monitored for the change of power law index for a certain speed ratio.
There was no indication of circulatory flows in the stator. Neither was any trace of flow separation in the stator observed. This research has made it evident that the use of a Power-Law fluid in a torque converter plays a significant role with speed ratio in its efficiency. The Pseudoplastic fluid demonstrated advanced efficiency and torque ratio using higher speed ratios at 1000 rpm pump speed and the same power index value. The aspects such as flow angles, shape and size of the channels also play important roles in the TC performance. This suggests directions for further investigation.

Other key conclusions, additional to those above, can be summarised as follows:

1. There was no sign of circulatory flows observed in the stator.

2. There was no trace of flow separation observed in the stator.

3. The efficiency and torque ratio of the torque converter increased for higher impeller speed at the same speed ratio.

4. The efficiency of the torque converter increased as the stator blade was increased from 16 to 18 blades.

5. The Pseudoplastic fluid showed higher efficiency and torque ratio for higher speed ratios at 1000 rpm pump speed and the same power index value.

These results and the methods developed in this thesis have the potential to lead to an improved efficiency in the torque converter.

CHAPTER 6: RECOMMENDATIONS FOR FUTURE WORK

The study of fluid flow in a torque converter's stator using Computational Fluid Dynamics can be facilitated by additional work and improvements and enhancements to the present work. the following are a number of recommendations for future work.

1. The grid construction could be increased in order to obtain an enhanced solution.
2. The change of number and shape of the stator blades and effect of these changes could be measured. These changes could be the blade thickness, stator blade chord length etc.
3. The effect of the change of blade inlet and exit angles could also be studied.
4. The torque converter size could be changed and investigation of the effect of the change on its performance could be undertaken.
5. The effect of different viscous fluids on the performance of the torque converter could be studied.
6. The effect of changing the axial length could be studied and compared with the existing experiments.

BIBLIOGRAPHY

Abe, K., Kondoh, T., Fukumura, K., and Kojima, M. (1991). "Three-Dimensional Simulation of the Flow in a Torque Converter" SAE Paper 910800.

Achtelik, C. and Eikelmann, J. (1996). "A High-Frequency-Response Pressure Probe for the Measurement of Unsteady Flow between Two Rotors in a Hydrodynamic Turbomachine." ASME 96-GT-412.

Bahr, H. M., Flack, R. D., By, R. R., and Zhang, J. J. (1990). "Laser Velocimeter Measurements in the Stator of a Torque Converter." SAE Paper 901769.

Bai, L., Kost, A., Mitra, N. K., and Fiebig, M. (1994). "Numerical Investigation of Unsteady Incompressible 3-D Turbulent Flow and Torque Transmission in Fluid Couplings." ASME 94-GT-69

Bellhouse, B. J., and Shultz, D.L., (1966), 'Determination of Mean and Dynamic Skin friction, Separation and Transition in a Low-Speed Flow With a Thin Filmed Heated Element." J. of Fluid Mechanics, Vol. 24, pp.370-400.

Benson, R. S. (1970) "A Review of Methods for Assessing Loss Coefficients in Radial Gas Turbines," Int. J. of Mech. Sci Vol. 12, pp.905-932

Browarzik, V. and Grahl, K. G. (1992). “Non Steady Flow Measurements Inside a Hydrodynamic Torque Converter by Hot-film Anemometry.” ASME Paper 92-GT-161.

Browarzik, V. (1994). “Experimental Investigation of Rotor/Rotor Interaction in a Hydrodynamic Torque Converter Using Hot-Film Anemometer.” ASME 94-GT-246

Brun, K. (1996) “Analysis of the Automotive Torque Converter Internal Flow Field.” Ph.D. Thesis, University of Virginia

Brun, K and Flack, R.D. (1997a). “Laser Velocimeter Measurements in the Turbine of an Automotive Torque Converter, Part I – Average Measurements,” J. of Turbomachinery, Vol. 119, No.3, pp.646-654.

Brun, K and Flack, R.D. (1997b). “Laser Velocimeter Measurements in the Turbine of an Automotive Torque Converter, Part II: Unsteady Measurements,” J. of Turbomachinery, Vol. 119, No.3, pp.655-662.

Brun, K and Flack, R.D., and Gruver, J. K. (1996). “Laser Velocimeter Measurements in the Turbine of an Automotive torque Converter Part II: Unsteady Measurements,” J. of Turbomachinery, Vol. 119, No.3, pp.562-577.

Bruningham, J. (1997) “ The Flow Field Within the Turbine of a GM 245 mm Torque Converter”, Master’s thesis, The Pennsylvania State University, University Park, PA.

By, R.R. and Lakshminarayana, B. (1991). “Static Pressure Measurement in a Torque Converter Stator.” SAE Paper 911934.

By, R.R. (1992). " An Investigation of Three Dimensional Flow Fields in the Automotive Torque Converter." PhD Thesis, The Pennsylvania State University, University Park, PA

By, R.R. and Lakshminarayana, B. (1995a). " Measurement and Analysis of Static Pressure Field in a Torque Converter Pump." J. Fluids Engineering Vol.117, No.2, pp. 109-115.

By, R.R., Kunz, R.F. and Lakshminarayana, B. (1995b). "Navier-Stroke Analysis of the Pump Flow field of an Automotive Torque Converter." J. Fluids Engineering Vol.117 ,No.2, pp. 116-122.

By, R.R. and Lakshminarayana, B. (1995c). " Measurement and Analysis of Static Pressure Field in a Torque Converter Turbine." J. Fluids Engineering Vol.117 ,No.3, pp. 473-478.

CFD─ACE, version: 2004.0.56 manual, CFDRC.

Cigarini, M. and Jonnavithula, S. (1995). Fluid Flow in a Automotive Torque Converter: Comparison of Numerical Results with Measurements. " SAE Paper, 950673.

Doebelin, E. O. (1966) " Measurement Systems : Application and Design" McGraw-Hill Book Company.

Dong, Y. and Lakshminarayana, B. (1994). " Assessment of the Stator Exit Flow for Various Pump-Turbine Configurations or 245 mm Torque Converter" Progress Report, PSU TURBO 9403.

Dong, Y. and Lakshminarayana, B., and Maddock, D. (1998a). " Steady and Unsteady Flow Field at Pump and Turbine Exit of a Torque Converter" J. Fluids Engineering. Vol.120 ,No.3, pp. 538-548.

Dong, Y. and Lakshminarayana, B., (1999). "Experimental Investigation of the Flow Field in an Automotive Torque Converter Stator" (FEDSM98-5127), J. Fluids Engineering. Vol.121 ,No.4, pp. 788-797.

Ejiri, E .and Kubo, M. (1999). "Performance Analysis of Torque Converter Elements" (FEDSM97-3219), J of Fluids Engineering, Vol 121, No.2 pp. 266-275.

Ejiri, E .and Kubo, M. (1998). " Influence of the Flatness Ratio of an Automotive Torque Converter on Hydrodynamic Performance" ASME Fluids Engineering Division Summer Meeting, FEDSM98-4866.

Fural, S. M., and Wasserbauer, C. A. (1965), " Off-Design Performance Prediction With Experimental Verification for a Radial Inflow Turbine," NASA TN D-2621.

Gandham, J. (1998) " CFD on Torque Converter: Validation of Computational Results," , 3rd Symposium of CFD on Torque Converter, General Motors.

Gruver, J. K., Flack, R. D., and Brun, K. (1996). " Laser velocimeter Measurement in the pump of a Torque Converter, Part1: Average Measurements." (ASME 94-GT-47), J. of turbomachinery Volume. 118, No.3, pp: 562-569.

Hodson, H. P., (1983), " The Development of Unsteady Boundary Layers on the Rotor of an Axial Flow Turbine," AGARD CP 351.

Hodson, H. P., (1985), " Boundary Layer Transition and Separation Near the Leading Edge of a High-Speed Turbine Blade ," J of Engineering for Gas Turbines and Power Vol. 107 pp:127-134.

Hodson, H. P., Huntsman, I., Nad Steele,A. B., (1994), "An Investigation of Boundary Layer Development in a Multistage LP Turbine," J. of turbomachinery Vol. 116 pp. 375-383.

"How Stuff Works" (2000), http://auto.howstuffworks.com/torque-converter2.htm, accessed on 17/11/04.

Kasser, J., Hascher, H., Novak, M., Lee,K. and Schock, H., "Tumble and Swirl Quantification Within a Motored Four-Valve SI Engine Cylinder Based on 3-D LDV Measurements," SAE Paper No. 970792, 1997.

Kost, A., Mitra, N. K., and Fiebig, M. (1994b). " Computation of Unsteady 3-D Flow and Torque Transmission in Hydrodynamic Couplings" ASME 94-GT-70.

Kubo, M. and Ejiri, E. (1998). "A Loss Analysis Design Approach to Improving Torque Converter Performance" ASME Paper 981100.

Lakshminarayana, B. (1996) "Fluid Dynamics and Heat Transfer of Turbomachinery" Wiley-Interscience Publication, John Wiley & Sons, Inc.

Lakshminarayana, B., and Horlock, J. H. (1973) "Generalized Secondary Vorticity Expressions Using Intrinsic Coordinates" J. of Fluid Mechanics, Vol. 59, Pt. 1, pp.97-115.

Lui, Y. (2001) " An Experimental Investigation on fluid Dynamics and Performance of an Automotive Torque Converter" Masters Thesis, The Pennsylvania State University, University Park, PA.

Maddock, D. (1991) " Design and Application of Automotive Torque Converters" A Report Prepared for Hydrodynamic Division of General Motors.

Marathe, B. V., Lakshminarayana, B., and Dong, Y. (1996). "Experimental and Numerical Investigation of Stator Exit Flow Field of an Automotive Torque Converter." (ASME 94-GT-32), J. of Turbomachinery, Vol. 118, No.3, pp 835-843.

Marathe, B. V., Lakshminarayana, B., and Maddock, D. G. (1997a). "Experimental Investigation of Steady and Unsteady Flow Field Downstream of Automotive Torque Converter Turbine and Inside the

Stator, Part I: Flow at the Exit of Turbine." (ASME 95-GT-231), J. of Turbomachinery, Vol119, No.3, pp: 624-633.

Marathe, B. V., Lakshminarayana, B., and Maddock, D. G. (1997b). "Experimental Investigation of Steady and Unsteady Flow Field Downstream of Automotive Torque Converter Turbine and Inside the Stator, Part II: Unsteady Pressure on the Stator Blade Surface." (ASME 95-GT-232). J. of Turbomachinery, Vol. 119, No.3, pp: 634-645.

Marathe, B. V. (1998) "Investigation of Three Dimensional Steady and Unsteady Flow Field Inside an Automotive Torque Converter." Ph.D. Thesis, The Pennsylvania State University, University Park, PA.

Numazawa, A., Ushijima, F., Kagenori, G. J., and Ishihara, T. (1983). "An Experimental Analysis of Fluid Flow in a Torque Converter." SAE Paper 830571. J. of Turbomachinery Vol.118, No.3, pp.578-589.

Sehyun Shin, Hyukjae Chang (Kyungpook National univ. Korea) and Mahesh Athavale Mahesh Athavale (CFD Research Corporation), "Numerical Investigation of the Pump Flow in an Automotive Torque Converter", SAE Technical Paper Series 1999-01-1056.

Senunghan Yan, Sehyun Shin and Incheol Bae (1999) "A Computer Integrated Design Strategy for Torque Converters Using Virtual Modelling and Computational Flow Analysis", SAE Technical paper Series: 1999-01-1046.

The hand book of fluid Dynamics, Edt by Richard W. Johnson; Chapter-22

Treaster, A. L. and Houtz, H. E. (1986) "Fabricating and Calibrating Five-Hole Probes" Proceedings of the ASME Fluid Measurements Symposium, May 1986, Atlanta, Georgia.

Treaster, A. L and Yocum, A.M. (1979) "The Calibration and Application of Five-hole Probes" ISA Transaction Vol.18, No.3 pp: 23-34.

Tsujita, H., and Mizuki, S. (1996). "Analysis of Flow Within Pump Impeller of Torque Converter." ASME 96-GT-404.

Von Backstrom, T. W., and Lakshminarayana, B. (1996). "Fluid Dynamics and Performance of Automotive Torque Converters: an Assessment." J. of Fluid Engineering, Vol.118, No.4, pp.665-676.

Watanabe, H., Tetsuo, K., and Kojima, M. (1997). “Flow Visualization and Measurements of Torque Converter Stator Blades Using a Laser Sheet Lighting Method and a Laser Doppler Velocimeter.” SAE Paper 970680, 1997.

Wasserbauer, C. A., and Glassman, A. J. (1975), “Fortran Program for Predicting the Off-Design Performance of Radial Inflow Turbines,” NASA TN-8063.

Schulz, H., Greim, R., and Volgmann, W. (1996). “ Calculation of Three Dimensional Viscous Flow in Hydrodynamic Torque Converter.” (ASME 94-GT-208),

“The Engineering Tool Box” (www.EngineeringToolBox.com), accessed on 19/01/2005.

My publications

The followings are two of the publications that were approved and published during this study

1. IMECE2011-65078: Effects of Number of Stator Blades on the Performance of a Torque Converter, which was published by the ASME conference 2011, held on November 11-17, 2011, Denver, Colorado, USA.

2. 18th AFMC-2012: Numerical Study of Performance of a Torque Converter Employing a Power-Law Fluid, which was published by the AFMC on its 18th conference, held on December 3-7, 2012, Launceston, Tasmania, Australia.

Proceedings of the ASME 2011 International Mechanical Engineering Congress & Exposition
IMECE2011
November 11-17, 2011, Denver, Colorado, USA

IMECE2011-65078

EFFECTS OF NUMBER OF STATOR BLADES ON THE PERFORMANCE OF A TORQUE CONVERTER

Shoab Ahmed Talukder
University of Technology, Sydney
Sydney, NSW, Australia

Dr. B. Phuoc Huynh
University of Technology, Sydney
Sydney, NSW, Australia

ABSTRACT

Torque converter (TC) is a totally enclosed hydrodynamic turbomachine, used most often in automobiles for the smooth transfer of power and speed change from the engine to the transmission, and torque magnification. A typical TC has 3 major components: a pump that is attached directly to the TC cover and connected to the engine shaft, a turbine connected to the transmission shaft, and a stator connected to the transmission housing via a one-way clutch and providing guidance for the fluid flow. In this work, effects of the number of stator blades on the performance of a TC are investigated numerically, using a commercial Computational Fluid Dynamics (CFD) software package. The standard k-epsilon turbulence model was used. A Newtonian fluid whose properties correspond to industrial oil was used for the working fluid. The range of speed ratio (between turbine's speed and pump's) of 0.2-0.8 was considered. It was found that as the stator blades' number increases (here from 13 to 19), the TC's efficiency and torque ratio vary significantly, passing through minimum and generally also reaching a maximum.

INTRODUCTION

The main focus of this study was to present the Effects of Number of Stator Blades on the Performance of a Torque Converter. This would help us to develop a more efficient torque converter, which would result in vehicles with better fuel economy. Fuel economy is important; both because the world's natural resources are limited and because environmental pollution has already reached at an unacceptable level. As numerous torque converters are being used every day all over the world, the slightest improvement in efficiency would result in a significant contribution. This would be an enhancement of the fuel economy, and would enable to decrease operating cost and pollution. A torque converter is a complex hydrodynamic turbo-machine. The closed-loop multi-component structure makes it complex.

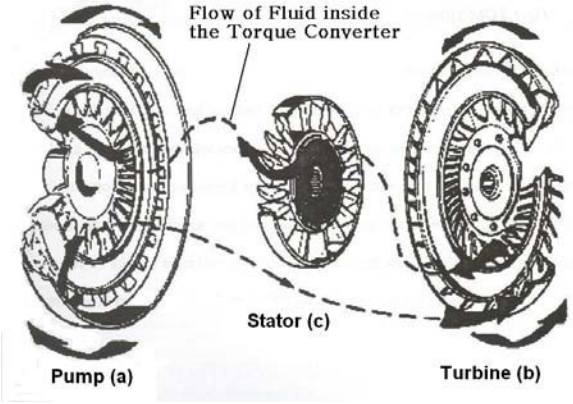

Figure1: Torque converter fluid flow path [1].

A typical torque converter has three major components (a) a pump, which is attached directly to the cover of the torque converter and connected to the engine shaft; (b) a turbine, which sits freely inside the casing and provides power to the transmission shaft; (c) a stator, which is attached to the transmission housing through a one-way clutch. The stator is placed in between the turbine exit and the inlet of the pump. Ideally the function of the stator is to redirect the fluid to obtain a zero flow incidence into the pump at a certain designed speed ratio. It also acts as a torque reactor at a low speed ratio, providing the torque amplification, thus differentiating the torque converter from the conventional fluid coupling. Different structural arrangements can cause variations to the fluid flow inside the torque converter. The structural arrangements could be on the basis of the blade numbers, blade angles, tip-bending, and size of the components of the torque converter or other governing factors. The long narrow passage

with curve and varying cross-sectional shape causes the fluid flow to be very complex in this turbo-machine.

This complex three-dimensional fluid flow is dominated by rotational speed, secondary flows, viscous effects and separation. The fluid flow is also dependent on the performance parameters, such as speed ratio, torque ratio, capacity factor, and k factor. In order to obtain a more efficient torque converter, a detailed understanding of the fluid flow is essential. To achieve that goal all these aspects must be taken in to consideration. A numerical analysis has been undertaken of the torque converters internal fluid flow using CFD (Computational Fluid Dynamics) software. Up on achieving this, the goal was to increase the efficiency of the torque converter by changing the number of the stator blades.

Due to these complexities and several of governing factors, the numerical studies became very complex and subsequently very few of them have been reported (SAE-1999-01-1056). Fujitani et. al. [2] computed the flow inside a torque converter with an assumption of inlet boundary condition for each element (pump, turbine and stator) was the same to the outlet boundary condition of the upstream-side element. Abe At al.[3] (1991) obtained a very strong three-dimensional and secondary flow by computing the internal flow field of a torque converter using a steady interaction technique and a third-order upwind scheme. Schulz, Greim and Volgmann [4] (1996) utilised a numerical method for the three-dimensional fluid flow-field in a torque converter, using steady and unsteady incompressible viscous flow to calculate the flow field. A vectorisable code was used to achieve an optimal performance on a modern vector computer. For a wide range of operational conditions, the flow at the stator outlet was reported to be uniform. The interaction of the stator with the pump and the turbine showed some unsteady behaviour, but it was reasonably negligible. By et al.[5] (1995b) computed the flow field in the pump of a torque converter using his modified Navier-Stokes code. They concluded that the inlet velocity profile strongly affects the total pressure loss and that the nature of the secondary flow field strongly depends on the pump rotation.

Marathe and Lakshminarayana[6] (1996) utilized a two-dimensional, steady, incompressible Navier-Stokes code to get the mid-span flow field of the stator. For the designed condition the, calculated midspan flow was accurate, but the off-design condition was not particularly accurate. Tsujita and Mizuki[7] (1996) experimented with a three-dimensional, incompressible, turbulent flow in the pump of an automotive torque converter. They tried at three different speed ratios: 0.02, 0.4 and 0.8 keeping the same inlet boundary condition. The K-ε model was used for turbulence. The computed result was satisfactory compared to the experimental results. In keeping with the growing use of CFD software, Cigarini and Jonnavihula[8] (1995) simulated a three-dimensional fluid flow for an automotive torque converter using the STAR-CD. They applied the steady interaction technique implemented in that fluid dynamic program. The computed performance characteristics agreed well with the experimental ones.

In order to improve the torque converters efficiency, Ejiri and Kubo[9,10] (1998, 1999) carried out a viscous calculation using STAR-CD, and modified the torque converter. The computational result was reasonably close to the actual flow pattern. Continuing with their research, they also concluded that for the maximum overall torque converter efficiency, there was an optimum value for turbine bias angle and the contraction ratio of the pump passage. Seunghan Yang, Sehyun Shin and Incheol Bae[11] (1999) carried out a computational flow analysis on a torque converter. They compared it with an experimental result and found their analysis to be satisfactory. In their paper they described the mixing-plane. The increasing pressure for pollution control and constant demand for higher fuel economic vehicle has lead Sehyun Shin, Hyukjae chang and Mahesh Athavale[12] (1999) to investigate the flow field in an automotive torque converter. In 1999 they have performed a numerical analysis, in order to achieve a detailed incompressible, three dimensional, turbulent and viscous flow field within the pump of an automotive torque converter. They have used a modified Navier-Stoke flow code for the computation of the torque converter flow along with mixing plane and K-ε turbulence models. Their numerical analysis showed remarkable similarity with the experimental performance data in terms of torque ratio, efficiency and input capacity factor. They relied on their numerical analysis more than the one-dimensional analysis to predict the performance of a torque converter.

In order to validate the computational result, it was required to be compared with existing experimental results. When computational results are validated, the achieved results can then be utilised in the design improvement process. Due to the complex three dimensional closed loop flow of the torque converter, a handful of obtainable internal flow data are available. Experimental data were gathered from different publications for pressure measurement [12-14] and velocity measurement [1, 14-15].

The global awareness of fuel efficient vehicle compels the drive to improve the torque converter efficiency. All the components (pump, turbine and stator) of the torque converter plays important role for its performance. The inlet and exit angle of the components govern the pattern of flow inside the torque converter significantly. The number of blades for each component also plays a vital role in the fluid flow inside the torque converter. The stator of a torque converter is responsible for redirecting the flow. Hence the number of blades for the stator plays an important role in the torque converters performance. This research concentrated on the effect of the stator blade number on the torque converters performance. In this process the numerical code was first validated against an existing experimental data. Then the effect of the optimised design for different number of blades for the stator was compared and overall torque converters performance was weighted.

PROBLEM DESCRIPTION AND COMPUTATIONAL METHOD

Torque Converter used in this computational study was about 230-mm of outer diameter. More specific dimensions are shown in the figure 2. The specifications for the Torque Converter's three elements are listed in table 1. The number of blades used in this torque converters pump, turbine and stator are 29, 31 and 16 respectively. The gap between the pump and the turbine was 3 mm at both shell side and core side. In between turbine and stator the gap was minimum 5 mm at the core side maximum 17 mm at the shell side. For stator and pump it was 5 mm at core side and 17.3 mm at shell side. Shell and core surface and the wall of the blade were given no slip wall boundary condition. In between the gap mixing plane were modelled for data transfer across the gap. The blades of pump and turbine are of uniform thickness and made out of metal sheet. As the stator has considerable variable thickness, slope and bend, it was made of casting. One of each component was included in the simulation for better understanding of the fluid flow.

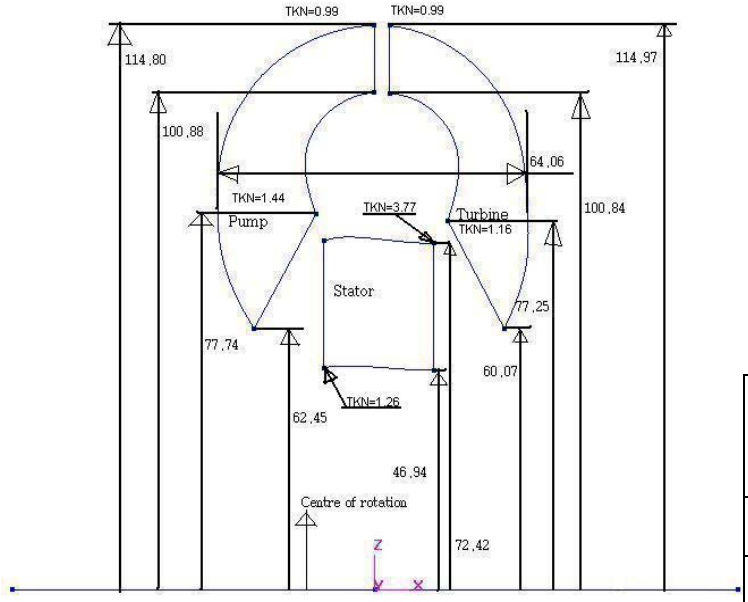

Figure 2: Dimensions of the Torque converter (in millimeters) (TKN=Thickness of the blade).

DETAILED COMPUTATIONAL MODEL

This complex three dimensional fluid flow was solved using the CFD package CFD-ACE developed by ESI Group. The goal of this study was to provide a better understanding of three dimensional fluid flow inside the stator and hence improve performance of the torque converter. In this work the standard k-epsilon turbulence model was used. For differencing scheme, upwind method was used for all parameters. The current study emphasis on the fluid flow inside the stator of a torque converter. Figure 3 reflects the three dimensional modeling of the stator. All the three elements of the torque converter were modeled in the similar fashion.

All the three components (pump, turbine and stator) were each given the same grid structure of 38 × 21 × 22 grid points. 38 points in the streamwise (inlet to exit) direction, 21 for pitchwise (suction to pressure) and another 22 in the spanwise (shell to core) direction. Simulation was carried out for 1000, 2000 and 2350 rpm of pump impeller speed with 0.1, 0.2, 0.4, 0.6 and 0.8 speed ratios for each of them. A convergence criterion of reduction of relative residuals by 3 to 4 orders of magnitude was used throughout. Difference between the results having 3 order of magnitude convergence and 4 order of magnitude convergence are insignificant.

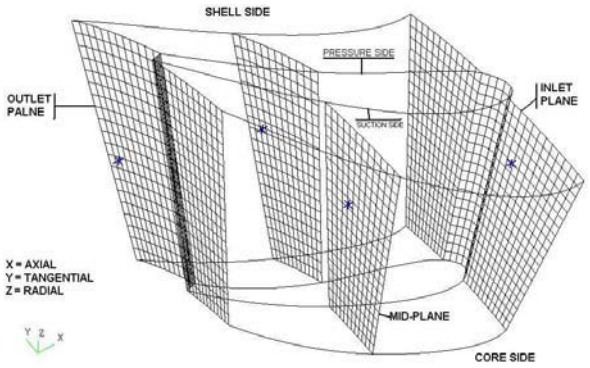

Figure3: Inlet, Mid-chord and Exit plane of a stator.

VALIDATION

The torque converter used for the validation simulation was about 230 mm in diameter. It has 16 stator blades, 29 pump blades and 31 turbine blades. All the specifications for the torque converter used in the simulation are provided below.

Element	Inlet angle Deg	Exit angle Deg	Number of blades
Pump	-16.30 ^{o}	-4.75 ^{o}	29
Turbine	33 ^{o}	-66.75 ^{o}	31
Stator	16.60 ^{o}	65.65 ^{o}	16

Table 1: Specifications of the elements for the simulating Torque Converter.

Element	Inlet angle	Exit angle	Number of blades
Pump	-16.5	-6.0	29
Turbine	49.5	-57.5	31
Stator	16.5	72.0	16

Table 2: Specifications of the TC used in SAE paper series 1999-01-1056, by Shin, Chang and Mahesh (1999-01-1056).

The graphical representation of comparison between this work's simulation and that of the SAE paper series 1999-01-1056 is given bellow in Figure 4 & 5.

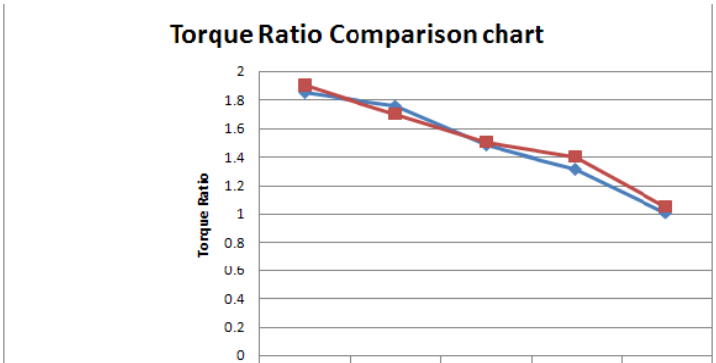

Speed Ratio	0.1	0.2	0.4	0.6	0.8
Torque ratio for 2350 rpm of pump speed [taken from our simulation]	1.85	1.76	1.48	1.31	1.01
Torque ratio (approx) [taken from Shin, Chang, Athavale (1999)]	1.9	1.7	1.5	1.4	1.05

Figure 4: T.R. comparison Chart

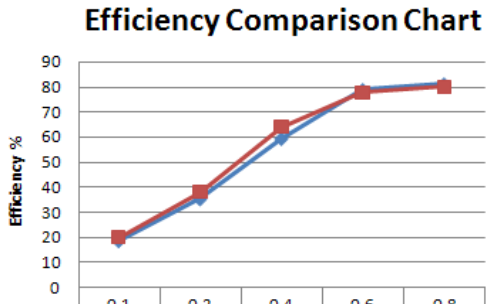

Speed Ratio	0.1	0.2	0.4	0.6	0.8
Efficiency (%) for 2350 rpm of pump speed [taken from our simulation]	18.5	35.23	59.35	78.88	81.11
Efficiency in (%) (Approx) for 2350 rpm [taken from Shin, Chang, Athavale (1999)]	20	38	64	78	80

Figure 5: Efficiency Comparison Chart.

The difference between my work and the Shin, Chang, Athavale (1999) was very little. This validated my simulation results against an existing research.

RESULTS & DISCUSSION.

The tests were performed with a grid number 43×21×22 for the stator, and the remaining parts were kept as 38×21×22. The speed of the pump was set to 1000 rpm, and the turbine speed was changed to different speed ratios for different simulations. The performances of the torque converter with 13, 18 and 19 blades were compared with the performance of the torque converter with 16 blades at the same fluid temperature and at the same rpm. These are shown in Figures 6 and 7.

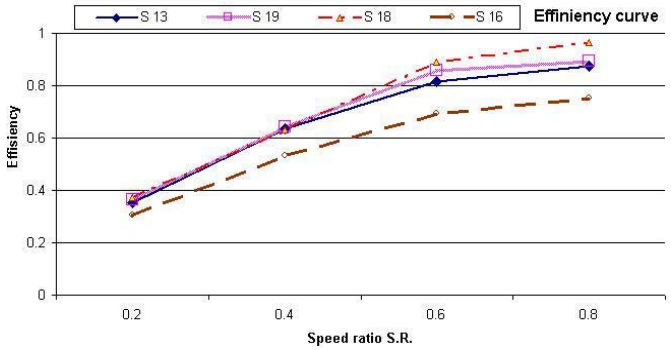

Figure 6: Efficiency comparison between the torque converters with 13, 18, 19 and 16 stator blades.

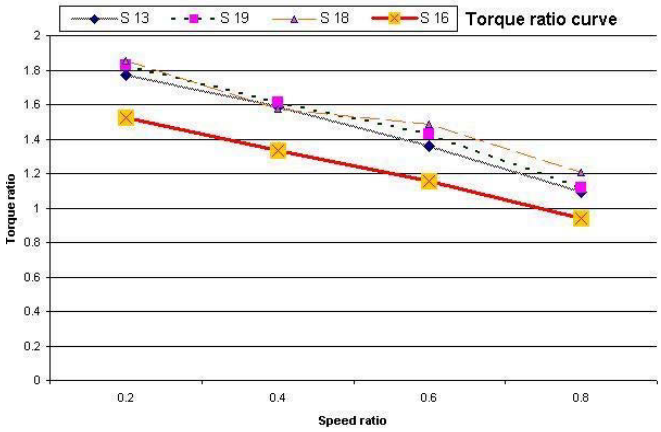

Figure 7: Torque Ratio comparison between the Torque Converters with 13, 18, 19 and 16 stator blades.

As number of blades increases from 13 through to 19, minimum efficiency occurs at 16 blades, while 18 blades give highest efficiency. Also, this was more pronounced at higher speed ratio. Similar pattern was observed in the torque ratio curve. There was no sign of circulatory flows observed in the stator neither was any trace of flow separation. It demonstrates that number of stator blades number has significant effect on efficiency of the TC. The balance between guidance verses friction has seems complex and requires further investigation.

CONCLUSION

There was no sign of circulatory flows observed in the stator. There was no trace of flow separation observed in the stator. My research evident that change of number of stator blade in a torque converter plays significant role in its efficiency. The factors like flow angles, shape and size of the channels also play important role over TC performance. This deserves further investigation.

ACKNOWLEDGMENTS

The computer model we used has been provided by Dr Mahesh Athavale, Manager, Advanced Research, CFD Research Corporation. I am also extremely grateful to my supervisor Dr. Phuoc Huynh for his support.

REFERENCES

1. Lui, Y. 2001," An Experimental Investigation on fluid Dynamics and Performance of an Automotive Torque Converter" Master's Thesis, The Pennsylvania State University, University Park, PA.

2. Fujitani, K.R.R. Himeno, and Takagi, M., 1988,"Computational study on flow through a torque converter," SAE paper **881746**.

3. Abe, K., Kondoh, T., Fukumura, K., and Kojima, M. 1991, "Three-Dimensional Simulation of the Flow in a Torque Converter" SAE Paper **910800**.

4. Schulz, H., Greim, R., and Volgmann, W. 1996, "Calculation of Three Dimensional Viscous Flow in Hydrodynamic Torque Converter." ASME Journal Turbomachinery, **118(3), pp. 578**.

5. By, R., 1993,"An Investigation of Three-Dimensional Flow Fields in the Automotive Torque Converter," Ph.D. thesis, Dept. of Aerospace Engineering, Pennsylvania State University.

6. By, R.R. and Lakshminarayana, B. (1995a). "Measurement and Analysis of Static Pressure Field in a Torque Converter Pump." J. Fluids Engineering., **117(2), pp. 109-115**.

7. Tsujita, H., and Mizuki, S. 1996, "Analysis of Flow Within Pump Impeller of Torque Converter." ASME **96-GT-444**.

8. Cigarini, M. and Jonnavithula, S. 1995, "Fluid Flow in an Automotive Torque Converter: Comparison of Numerical Results with Measurements." SAE Paper **950673**.

9. Ejiri, E .and Kubo, M. 1999, "Performance Analysis of Torque Converter Elements" (FEDSM97-3219), J of Fluids Engineering, **121(2) pp. 266-275**.

10. Ejiri, E .and Kubo, M. 1998, "Influence of the Flatness Ratio of an Automotive Torque Converter on Hydrodynamic Performance" ASME Fluids Engineering Division Summer Meeting, **FEDSM98-4866**.

11. Yan, S. Shin, S. and Bae, I. 1999, "A Computer Integrated Design Strategy for Torque Converters Using Virtual Modelling and Computational Flow Analysis," SAE paper **1999-01-1046**.

12. Shin, S. Chang, H. (Kyungpook National uni. Korea) and Athavale, M. (CFD Research Corporation), "Numerical Investigation of the Pump Flow in an Automotive Torque Converter," SAE Paper **1999-01-1056**.

13. Lakshminarayana, B. 1996, "Fluid Dynamics and Heat Transfer of Turbomachinery" Wiley-Interscience Publication, John Wiley & Sons, Inc. NY.

14. Lakshminarayana, B., and Horlock, J. H. 1973, "Generalized Secondary Vorticity Expressions Using Intrinsic Coordinates," J. of Fluid Mechanics, **59(1), pp.97-115**.

15. Shin, S., Chang, H. and Athavale, M. 1999, "Numerical Investigation of the Pump Flow in an Automotive Torque Converter," SAE Paper **1999-01-1056**.

18th Australasian Fluid Mechanics Conference
Launceston, Australia
3-7 December 2012

Numerical Study of Performance of a Torque Converter Employing a Power-Law Fluid

Shoab A. Talukder and B.P. Huynh
University of Technology, Sydney
Sydney, NSW, Australia

Abstract

Torque converter (TC) is a totally enclosed hydrodynamic turbomachine, used most often in automobiles for the smooth transmission of power and speed change from the engine to the transmission, and torque magnification. A typical TC has 3 major components: a pump that is attached directly to the TC cover and connected to the engine shaft, a turbine connected to the transmission shaft, and a stator connected to the transmission housing via a one-way clutch and providing guidance for the fluid flow. In this work, performance of a TC employing a power-law fluid is investigated numerically, using a commercial Computational Fluid Dynamics (CFD) software package. The standard k-epsilon turbulence model is used. A power-law fluid whose zero-shear properties correspond to an industrial oil is used for the working fluid. It is found that as the power-law index increases so that the fluid behaviour varies from being shear-thinning through Newtonian to shear-thickening, both efficiency and torque ratio decrease slightly. Also, the change is more pronounced at lower speed ratio.

Introduction

The main focus of this study is to present the effects of the power-law index on the performance of a torque converter employing a power-law fluid. This will help us to develop a more efficient torque converter, which will result in vehicles with better fuel economy. Fuel economy is important; both because the world's natural resources are limited and because environmental pollution has already reached unacceptable level. As billions of torque converters are used every day all over the world, the slightest improvement in efficiency will result in a significant contribution. This will be an enhancement of the fuel economy, and will enable to decrease operating cost and pollution.

A torque converter is a complex hydrodynamic turbo-machine; see figure 1 [9]. The closed-loop multi-component structure makes it complex. A typical torque converter has three major components (1) a pump, which is attached directly to the cover of the torque converter and connected to the engine shaft; (2) a turbine, which sits freely inside the casing and provides power to the transmission shaft; (3) a stator, which is attached to the transmission housing through a one-way clutch. The stator is placed in between the turbine exit and the inlet of the pump. The function of the stator ideally is to redirect the fluid to obtain a zero flow incidence into the pump at a certain designed speed ratio (turbine-speed/pump-speed). It also acts as a torque reactor at a low speed ratio, providing the torque amplification, thus differentiating the torque converter from the conventional fluid coupling. Different structural arrangements can cause variations to the fluid flow inside the torque converter. The structural arrangements could be on the basis of the blade numbers, blade angles, tip-bending, and size of the components of the torque converter, or other factors. The long narrow passages with curve and varying cross-sectional shapes cause the fluid flow to be very complex in this turbo-machine. This complex three-dimensional fluid flow is dominated by rotational speed, secondary flows, viscous effects and separation. The fluid flow is also dependent on the performance parameters, such as speed ratio, torque ratio (turbine-torque/pump-torque), capacity factor, and K factor. In order to obtain a more efficient torque converter, a detailed understanding of the fluid flow is essential.

Fujitani et. al. [6] computed the flow inside a torque converter with an assumption of inlet boundary condition for each element (pump, turbine and stator) being the same to the outlet boundary condition of the upstream-side element. Abe et al [1] obtained a very strong three-dimensional and secondary flow by computing the internal flow field of a torque converter using a steady interaction technique and a third-order upwind scheme. Schulz, Greim and Volgmann [11] utilised a numerical method for the three-dimensional fluid flow-field in a torque converter, using steady or unsteady incompressible viscous flow to calculate the flow field. By and Kunz [2] computed the flow field in the pump of a torque converter using a modified Navier-Stokes code. They concluded that the inlet velocity profile strongly affects the total pressure loss and that the nature of the secondary flow field strongly depends on the pump rotation. Marathe et al [10] utilized a two-dimensional, steady, incompressible Navier-Stokes code to get the mid-span flow field of the stator. For the designed condition, the calculated mid-span flow was accurate, but the off-design condition was not so.

Tsujita and Mizuki [14] experimented with a three-dimensional, incompressible, turbulent flow in the pump of an automotive torque converter. They tried at three different speed ratios (0.02, 0.4 and 0.8), while keeping the same inlet boundary condition. A k-ε model was used for turbulence. The computed result was satisfactory compared to the experimental data. In keeping with the growing use of CFD software, Cigarini and Jonnavihula [3] simulated a three-dimensional fluid flow for an automotive torque converter using the STAR-CD package. They applied the steady interaction technique implemented in that fluid dynamic program. The computed performance characteristics agreed well with the experimental ones. In order to improve the torque converters efficiency, Ejiri and Kubo [4, 5] also carried out a viscous calculation using STAR-CD, and modified the torque converter. The computational result was reasonably close to the actual flow pattern. Continuing with their research, they also concluded that for the maximum overall torque converter efficiency, there is an optimum value for a turbine angle and the contraction ratio of the pump passage.

Yang et al [15] carried out a computational flow analysis on a torque converter. They compared it with an experimental data and found their analysis to be satisfactory. In their paper they

described the mixing-plane. The increasing pressure for pollution control and constant demand for higher fuel economic vehicle has lead Shin, Chang and Athavale [12] to investigate the flow field in an automotive torque converter. In 1999 they performed a numerical analysis to achieve a detailed incompressible, three dimensional, turbulent flow field within the pump of an automotive torque converter. They have used a modified Navier-Stokes flow code for the computation of the torque converter flow along with mixing plane and a k-ε turbulence model. Their numerical analysis showed remarkable similarity with experimental performance data in terms of torque ratio, efficiency and input capacity factor. Experimental data have also been presented in references [7-10,12].

On the other hand, the working fluid in torque converters can deviate significantly from being Newtonian; but the non-Newtonian effects on their performance don't seem to have been considered. Thus in this work, performance of a torque converter is investigated when the working fluid is non-Newtonian of power-law type. Specifically, effects of the power-law index are considered.

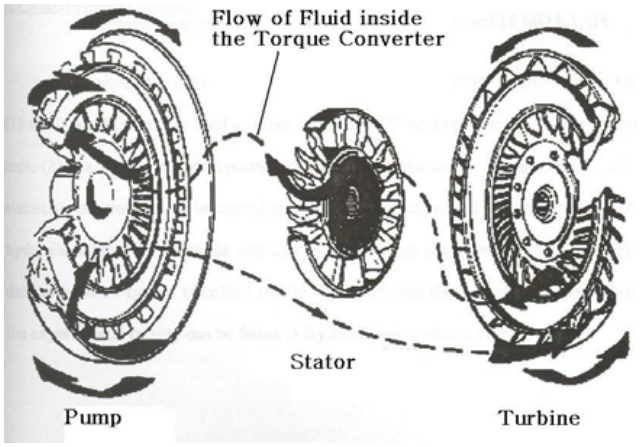

Figure 1. Torque converter fluid flow path [9].

Problem Description and Computational Method

Computation is conducted on a torque converter of about 230-mm of outer diameter. More specific dimensions are shown in the figure 2. The specifications for the torque converter's three elements are listed in table 1. The number of blades used in this torque converters' pump, turbine and stator are 29, 31 and 16 respectively. The gap between the pump and the turbine is 3 mm at both shell side and core side. In between turbine and stator, the gap is minimum 5 mm at the core side, and maximum 17 mm at the shell side. For stator and pump it is 5 mm at core side and 17.3 mm at shell side. Shell and core surface and the wall of the blade were given no slip wall boundary condition. In the gaps, mixing planes were modelled for data transfer across them. The blades of pump and turbine are of uniform thickness and made out of metal sheet. As the stator has considerable variable thickness, slope and bend, it is made of casting. One of each component was included in the simulation for better understanding of the fluid flow.

Detailed Computational Model

The complex three dimensional fluid flow was solved using the CFD package CFD-ACE of the ESI Group. The goal of this study is to provide a better understanding of three-dimensional fluid flow inside the stator (and other components) and hence improve performance of the torque converter. In this work the standard k-ε turbulence model is used. For differencing scheme, upwind method is used for all parameters. Figure 3 shows the three-dimensional model of the stator. The other elements of the torque converter (pump and turbine) were also modelled in similar fashion.

All the three components (pump, turbine and stator) were each given the same grid structure of 38 × 21 × 22 grid points, with 38 points in the streamwise (inlet to exit) direction, 21 in pitchwise (suction to pressure) and 22 in the spanwise (shell to core) direction. Simulation was carried out for 1000, 2000 and 2350 rpm of pump impeller speed with speed ratio (turbine-speed/pump-speed) in the range of 0.1 – 0.8 for each of them. A convergence criterion of reduction of relative residuals by 3 to 4 orders of magnitude is used throughout.

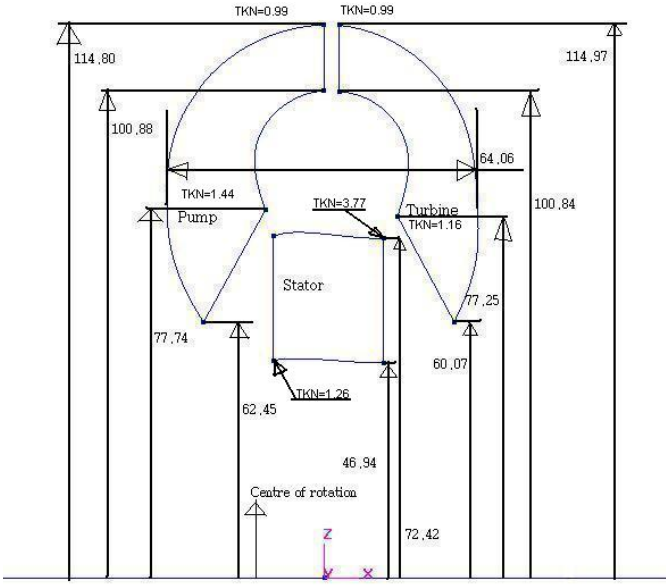

Figure 2. Dimensions (in millimeters) of the torque converter used in this work (TKN=Thickness of the blade).

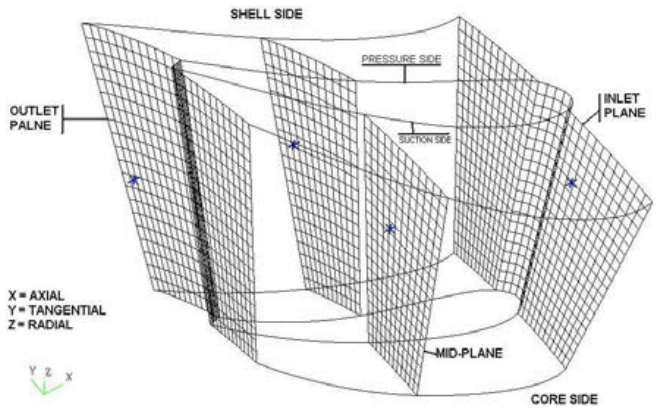

Figure 3. Inlet, Mid-chord and Exit plane of a stator.

Validation

Comparison is made between simulation results of this work and those of Shin et al [12]. Specifications for both torque converters (used in this work and in Shin et al's work) are shown in tables 1 and 2.

Comparison results are shown in figures 4 and 5. The difference is very small. Because Shin et al's work was shown to agree well with measurement data [12], confidence can thus also be accorded to this work's results.

Element	Inlet Angle – Degree	Exit Angle – Degree	Number of Blades
Pump	-16.3	– 4.75	29
Turbine	33.0	– 66.75	31
Stator	16.6	65.65	16

Table 1. Specifications of the torque-converter elements simulated in this work.

Element	Inlet Angle – Degree	Exit Angle – Degree	Number of Blades
Pump	-16.5	– 6.0	29
Turbine	49.5	– 57.5	31
Stator	16.5	72.0	16

Table 2. Specifications of the torque-converter elements used in Shin, Chang and Mahesh's SAE paper [12].

Results and Discussion

Simulation was performed at speed ratio of 0.2 for power-law index n in the range of 0.5 – 1.5. At the higher speed ratio 0.4 – 0.8 simulation was performed only with n = 0.5 – 0.9; difficulty with convergence was encountered at higher n values.

According to the figures 6 and 7, almost all results at different speed ratio (S.R.) show similar patterns of change, except for S.R. 0.6. This requires further investigation. It is evident that torque ratio (turbine-torque/pump-torque), as well as efficiency, decrease as the fluid property varies from being shear-thinning (n < 1) to Newtonian (n = 1); or, alternatively, torque converter's performance is enhanced with shear-thinning fluids.

On the other hand, with speed ratio 0.2, the shear-thinning fluid seemed to lose very little of its torque ratio and efficiency, as it approached being a Newtonian fluid. However, efficiency and torque ratio dropped substantially as the fluid becomes shear-thickening (n > 1). As power-law index increases further and the shear-thickening property becomes stronger, both torque ratio and efficiency decrease significantly further, before rising quickly as n approaches 1.5. A previous study [13] using Newtonian fluids showed that for 1000 rpm pump speed and 0.2 speed ratio, a torque ratio of 1.52 and efficiency of about 30% were obtained. In this work, at the same pump speed (1000 rpm) and speed ratio (0.2), a shear-thickening fluid with n = 1.5 results in torque ratio of 1.60 and efficiency 32.1%, a significant performance enhancement. Evidently, a lubricant whose viscosity increases quickly with higher shear (corresponding to n larger than about 1.4) alters strongly the flow field and the distribution of viscous forces, such that a reverse in the decreasing trend of torque ratio (and efficiency) occurs. To see how this happens requires detailed analysis of a complex flow; and this is a subject of further investigation.

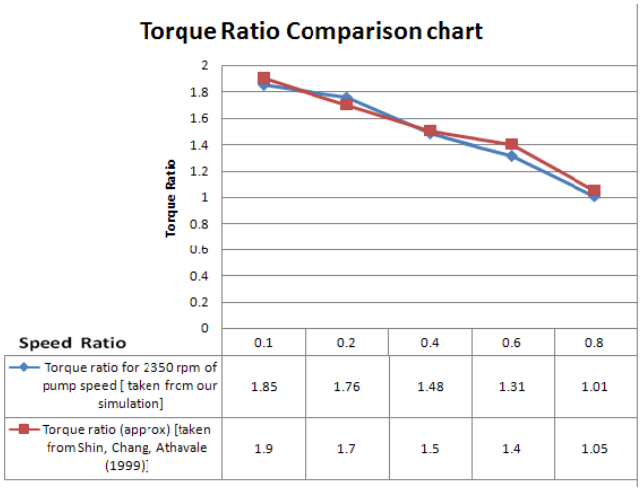

Speed Ratio	0.1	0.2	0.4	0.6	0.8
Torque ratio for 2350 rpm of pump speed [taken from our simulation]	1.85	1.76	1.48	1.31	1.01
Torque ratio (approx) [taken from Shin, Chang, Athavale (1999)]	1.9	1.7	1.5	1.4	1.05

Figure 4. Comparison of torque ratio between this work and Shin et al's.

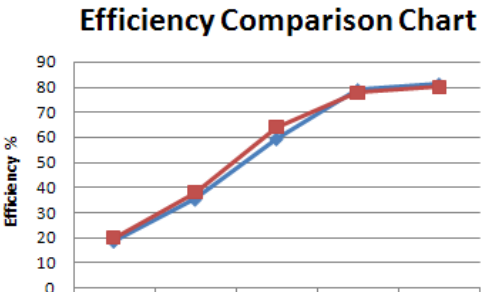

Speed Ratio	0.1	0.2	0.4	0.6	0.8
Efficiency (%) for 2350 rpm of pump speed [taken from our simulation]	18.5	35.23	59.35	78.88	81.11
Efficiency in (%) (Approx) for 2350 rpm [taken from Shin, Chang, Athavale (1999)]	20	38	64	78	80

Figure 5. Comparison of efficiency between this work and Shin et al's.

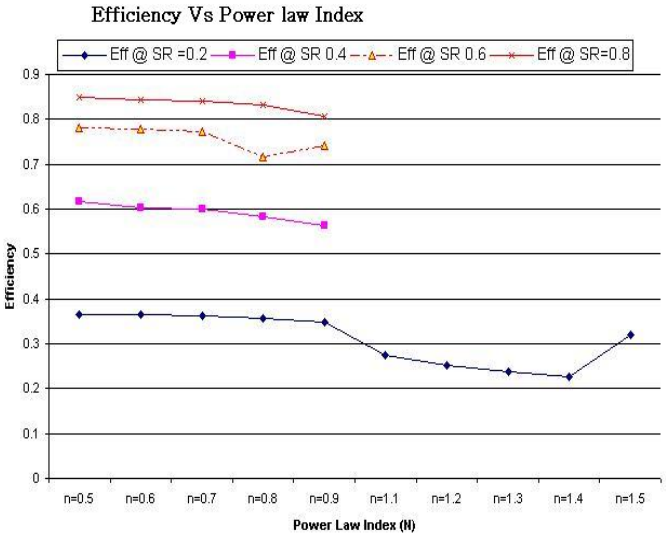

Figure 6. Torque-converter's efficiency vs. power-law index at different speed ratio.

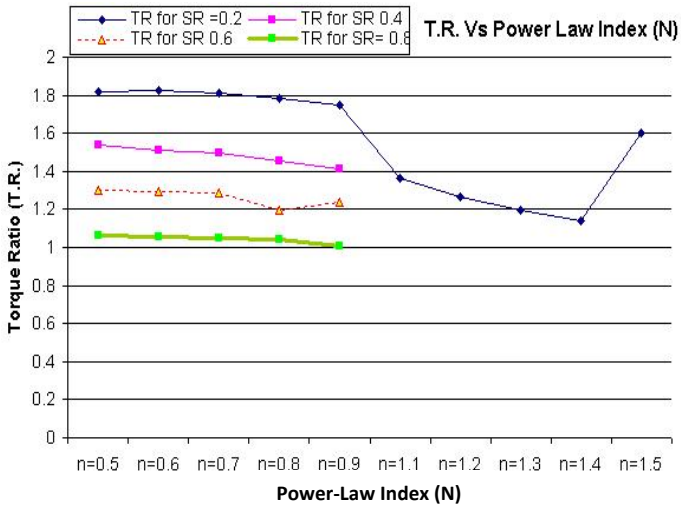

Figure 7. Torque-converter's torque ratio vs. power-law index at different speed ratio.

Conclusion

There was no sign of circulatory flows observed in the stator. There was no trace of flow separation observed in the stator. This research shows that the use of power-law fluids in a torque converter affects significantly the torque ratio (and efficiency). Torque-converter performance is enhanced using shear-thinning fluids; and as the power-law index n increases, both torque ratio and efficiency decrease. However, for the speed ratio of 0.2 when data are available, these decreasing trends revert to increasing with n when n is larger than about 1.4.

Acknowledgements

The computer model used in this work has been provided by Dr Mahesh Athavale, Manager, Advanced Research, CFD Research Corporation. The first author also wishes to thank Assoc. Prof. Peter Watterson for his valuable help and advice.

References

[1] Abe, K., Kondoh, T., Fukumura, K., and Kojima, M., 1991, Three-Dimensional Simulation of the Flow in a Torque Converter, *SAE Paper 910800*.

[2] By, R.R. and Kunz, R., 1995, Navier-Stokes Analysis of the Pump Flow Field of an Automotive Torque Converter, *J. of Fluids Engineering*, 117, pp. 116-122.

[3] Cigarini, M. and Jonnavithula, S., 1995, Fluid Flow in an Automotive Torque Converter: Comparison of Numerical Results with Measurements, *SAE Paper 950673*.

[4] Ejiri, E .and Kubo, M., 1998, Influence of the Flatness Ratio of an Automotive Torque Converter on Hydrodynamic Performance, *ASME Fluids Engineering Division Summer Meeting, FEDSM98-4866.*

[5] Ejiri, E .and Kubo, M., 1999, Performance Analysis of Torque Converter Elements, *J. of Fluids Engineering*, 121(2) pp. 266-275.

[6] Fujitani, K., Himeno, R. and Takagi, M., 1988, Computational study on flow through a torque converter, *SAE paper 881746.*

[7] Lakshminarayana, B., 1996, *Fluid Dynamics and Heat Transfer of Turbomachinery*, John Wiley & Sons, NY.

[8] Lakshminarayana, B., and Horlock, J. H., 1973, Generalized Secondary Vorticity Expressions Using Intrinsic Coordinates, *J. of Fluid Mechanics*, 59(1), pp. 97-115.

[9] Lui, Y., 2001, *An Experimental Investigation on fluid Dynamics and Performance of an Automotive Torque Converter*, Master's Thesis, The Pennsylvania State University, University Park, PA.

[10] Marathe, B.V., Lakshminarayana, B. and Dong, Y., 1996, Experimental and Numerical Investigation of Stator Exit Flow Field of an Automotive Torque Converter, *J. of Turbomachinery*, 118, pp. 835-843.

[11] Schulz, H., Greim, R., and Volgmann, W., 1996, Calculation of Three Dimensional Viscous Flow in Hydrodynamic Torque Converters, *J. of Turbomachinery*, 118, pp. 578-589.

[12] Shin, S., Chang, H. and Athavale, M., 1999, Numerical Investigation of the Pump Flow in an Automotive Torque Converter, *SAE Paper 1999-01-1056.*

[13] Talukder, S.A. and Huynh, B.P., 2011, Effects of Number of Stator Blades on the Performance of a Torque Converter, *Proceedings of the ASME 2011 International Mechanical Engineering Congress and Exposition*, Denver, Colorado, USA, 11-17 November

[14] Tsujita, H., and Mizuki, S., 1996, Analysis of Flow Within Pump Impeller of Torque Converter, *ASME 96-GT-444.*

[15] Yang, S., Shin, S. and Bae, I., 1999, A Computer Integrated Design Strategy for Torque Converters Using Virtual Modelling and Computational Flow Analysis, *SAE paper 1999-01-1046.*